UNIVERSITA' DEGLI STUDI DI MILANO-BICCOCA

DEPARTMENT OF BIOTECHNOLOGY AND BIOSCIENCES

Ph.D. course in Chemical science

XXIII cycle

"Design & Synthesis of relevant biomolecules for functionalization of biomaterials in tissue engineering"

Ph.D. Student: Nasrin Shaikh

Supervisor: Prof. Francesco Nicotra

Tutor: Prof. Laura Cipolla

Coordinator: Prof. Franca Morazzoni

Academic years 2008 – 2011

CONTENTS

CHAPTER 5   **Natriuretic peptides**

ACKNOWLEDGEMENTS

Abbreviations

$[\alpha]_D$	Optical rotary power
Ac	Acetyl
Aq.	Aqueous
ax	Axial
Bn	Benzyl
bs	broad singlet
Bu	butyl
c	concentration
COSY	correlation spectroscopy
CH_2Cl_2	Methylene chloride
$CHCl_3$	Chloroform
d	doublet
dd	double doublet
DCM	dichloromethane
DMF	*N,N*-dimethylformamide
ECM	extracellular matrix
eq	equatorial
equiv	equivalents
ESI	electrospray ionization
Et	ethyl
Et_2O	Diethyl ether
EtOAc	Ethyl acetate
EtOH	Ethyl alcohol

exp.	experiment
g	grams
h	Hours
HCl	Hydrochloric acid
HIV	human immunodeficiency virus
HPLC	high performance liquid chromatography
IR	infrared
KOH	Potassium hydroxide
m	multiplet
MCA	Monochloro acetate
Me	metyl
MeOH	Methyl alcohol
MGDG	monogalactosyl diacyl glycerol
min	Minutes
ml	Milliliter
mp	Melting point
MS	mass spectrometry
$NaHCO_3$	Sodium bicarbonate
NaOH	Sodium hydroxide
Na_2SO_4	Sodium sulfate
NMR	nuclear magnetic resonance
Pd/C	Palladium on activated charcoal
PE	petroleum ether
Ph	phenyl
Py	pyridine
quat	quaternary

r	relaxivity
r.t.	room temperature
s	singlet
t	triplet
*t*Bu	tert. Butyl
p- TSA	*p*-Toluene sulfonic acid
Ts	Tosyl
THF	tetrahydrofuran
TLC	thin layer chromatography
UV	ultraviolet
Y	yield
δ	chemical shift
HA/ HYA	Hyaluronic acid
NP	Natriuretic peptide
ANP	Atrial natriuretic peptide
BNP	B-type natriuretic peptide
CNP	C-type natriuretic peptide
TEMPO	2,2,6,6-Tetramethylpiperidine-1-oxyl
RHAMM	Receptor for Hyaluronan Mediated Motility

Chapter 1

General Introduction

1.1: INTRODUCTION

Tissue engineering has attracted many scientists and surgeons with a hope to treat patients in a minimally invasive way[1]. Tissue engineering involves the isolation of specific cells through a small biopsy from a patient, their growth on a three-dimensional biomimetic scaffold under precisely controlled culture conditions, the delivery of the construct to the desired site in the patient's body, and the stimulation of new tissue formation into the scaffold that can be degraded over time[2]. Tissue engineering also offers unique opportunities to investigate aspects of the structure-function relationship associated with new tissue formation in the laboratory and to predict the clinical outcome of the specific medical treatment. In order to achieve successful regeneration of damaged organs or tissues several critical elements should be considered including biomaterial scaffolds that serve as a mechanical support for cell growth, [3-8] progenitor cells that can be differentiated into specific cell types, and inductive growth factors that can modulate cellular activities[9-10]. The biomaterial plays an important role in most tissue engineering strategies [8, 11-12] For example, biomaterials can serve as a substrate on which cell populations can attach and migrate, being implanted with a combination of specific cell types as a cell delivery vehicle, or utilized as a drug carrier to activate specific cellular function in the localized region. Tissue engineering is an emerging biomedical technology addressed to the treatment of patients needed of tissues or organs. This interdisciplinary field of research involves different scientific approaches including cell biology, materials science, and bioengineering towards the development of biological substitutes that will restore normal cell function. Tissue engineering has an enormous potential for

reparative medicine, as this discipline uses materials and technology to restore or improve function of organs and tissues affected by disease, injury or deformation. Another application, not less interesting than that of the use of engineered tissues for implantation in regenerative medicine but probably less studied, is the use of these engineered tissue constructs for the study of physiology or pathophysiology *in vitro*. A functional *in vitro* tissue would be really useful to study the effects of drugs in that tissue (accelerating in this way the process of the application of new drugs), or the development of new therapies to treat some diseases.

The underlying concept for tissue engineering is the belief that cells can be isolated, expanded *in vitro* and seeded onto a carrier or scaffold prior to implantation. This scaffold usually needs to be a highly porous artificial extracellular matrix analog, capable to accommodate mammalian cells and guide their growth and tissue regeneration in three dimensions. Isolated cells cannot always build a new tissue by themselves. Most of the time, the surrounding microenvironment, which is also instructive, is crucial for tissue growth and function. The cellular microenvironment is basically comprised of: signaling molecules such as growth factors or hormones, the extracellular matrix (ECM) molecules, physical or mechanical factors, and the presence of other types of cells interacting with them by cell-cell contacts.

Therefore, the discovery and use of biomaterials capable to modulate cellular responses is a critical and limiting step in tissue engineering.

1.2: Biomaterials

Bone fracture is very common among the elderly as bones become more brittle as we age. Active young people also have a high risk of bone fracture through every day life and sporting activities. If a fracture is small, it can be filled with bone cement, such as Poly (methyl methacrylate). However, if the fracture is large, more durable metal

11

implants, such as titanium and titanium-based alloys, are used. The goal is to not only fill the fracture space with a strong material that can support the body's weight, but also to promote new bone growth to fully restore the bone's functions.

"Scientists have developed various methods to transform once inert implants into implants that can promote bone growth"

In the past, bone implants were made of inert materials, chosen because they didn't severely influence bodily functions or generate scar tissue, which is a thick, insensitive tissue layer that can form around an implant. But this simple design principle causes implants to loosen from the surrounding bone after around 10 to 15 years. Loosening becomes worse with time and can cause significant pain. As a result, patients often undergo additional surgery (called revision surgery) to remove the loose implant and insert a new one. Revision surgery is clearly undesirable as it is costly, painful and requires therapy all over again for the patient.

It is unsurprising that there has been an on-going effort to create implants that can integrate into the surrounding natural bone for the patient's lifetime. Using their understanding of bone composition and the bone-forming process, scientists have developed various methods to transform these once inert implants into implants that can promote bone growth.

One of the first approaches to make more proactive bone implants uses surface chemistry to encourage the implant to interact with osteoblasts (bone-forming cells). This method has resulted in a number of implant materials, such as bioactive glass, that show good bone formation. However, scientists often need to resort to trial and error processes to find an implant material that not only increases bone growth but also has good mechanical properties for use in cement less implants, such as the hip

implant. Such combinations are not always easy to find in one material or even a composite of materials.

"Significant promise can be drawn from recent advances in biomaterials research, especially where nanotechnology is involved. But discovering the perfect biomaterial that can last the lifetime of a patient is still a challenge."

Scientists have improved numerous implant materials, including titanium and titanium alloys, porous polymers, bone cements and hydroxyapatite, by placing nanoscale features on their surfaces. The bulk materials' properties remain unchanged, maintaining their desirable mechanical properties, but the surface changes enhance the interactions with proteins. This causes bone-forming cells to adhere to the implant and activates them to grow more bone.

Scientists are also creating 'smarter' implants that can sense what type of tissue is growing on them, communicate the information to a hand-held device and release drugs on demand to promote tissue growth. These implants are designed to help avoid complications frequently observed after bone implantation, such as infection, inflammation (or scar tissue growth), implant loosening and, in the case of bone cancer, cancer reoccurrence. Scientists have been investigating implants that have inherent mechanisms to protect the body from infection (such as silver and zinc) or inhibit cancer growth (such as selenium).

Significant promise can be drawn from recent advances in biomaterials research. But discovering the perfect biomaterial that can last the lifetime of a patient is still a challenge.

Biomaterials are those materials intended to interface with biological systems, to replace, reconstruct, enhance or support either tissues or tissue function. Biomaterials have typically been metalic, ceramic and polymeric. Metalic materials are being used

13

for long for prostheses; ceramics, specially hydroxyapatite (Hydroxyapatite, a calcium phosphate ceramic, which is a major component of bones and teeth. It is already used to make artificial bones and as a coating in hip replacement operations to encourage bone to grow onto the implant and help fix it in place) has been used for bone reconstruction, and polymeric materials have been found to present in numerable applications, from surgical sutures and surgical glues to contact lenses, heart valves, etc. For tissue engineering and regenerative medicine applications, a highly porous biomaterial or scaffold is usually needed to guide and accommodate the cells while promoting their function. The ideal scaffold for supporting cell attachment and growth should meet several criteria:

- Present building blocks derived from biomolecules

- Have basic units that are amenable to design and modification to achieve specific needs

- Present controlled rate of biodegradation and no cytotoxicity

- Promote cell-substrate interactions

- Elicit no immune responses and inflammation

- Be easy to produce, purify and process

- Be readily transportable

- Present chemical compatibility with aqueous solutions and physiological conditions,

- Be able to integrate with other materials etc.

Many different polymeric biomaterials are being used for tissue engineering, and they can be classified as naturally derived materials and synthetic polymers. *Natural polymers* such as collagens, hyaluronic acid, alginate and chitosan have been used as scaffolds to study the repair of nerves, skin, cartilage and bone. Collagen is one of the most abundant protein in mammals, it is normally obtained and purified from animal

and human tissues by an enzymatic treatment and salt/acid extraction. It is one of the most applied scaffolds for tissue engineering and it is used *in vitro* for the culture of many different types of cells. It also presents the advantage that is proteolitically degraded by cell-secreted proteases. The used of collagen has been approved by the United States Food and Drug Administration (FDA) for different medical applications such as the treatment of skin ulcers (Parenteau,), which is the case of Apligraf, approved in year 2000. Another collagen-based product InFuse Bone Graft is indicated for the treatment of degenerative disc disease or for the healing of bone fractures. (Nature designs tough collagen: Explaining the nanostructure of collagen fibrils P. Natl. Acad. Sci. USA, August 15, 2006)
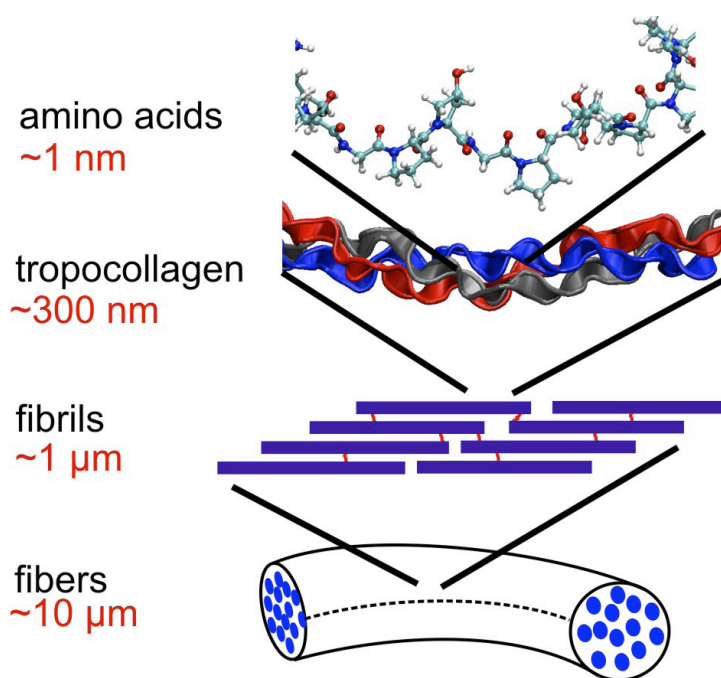
Fig-1: **The hierarchical design of collagen**. The structural features of collagen ranges from the amino acid sequence, tropocollagen molecules, collagen fibrils to collagen fibers. The new multi-scale model describes the mechanical properties of collagen fibrils using a hierarchical multi-scale scheme that starts from the atomistic level of amino acids.

Hyaluronic acid is a glycosaminoglycan found in nearly every mammalian tissue and

fluid. This material can be chemically cross-linked or combined with other materials in order to obtain the desired mechanical properties. It is degraded by cellular hyaluronidase, and it has been used in many different applications[13]. Hyaluronic acid has been approved by the FDA in cosmetics as wrinkle fillers (Restylan), or for the treatment of osteoarthritis (Nuflexxa).

Glucuronic acid   N-acetylglycosamine
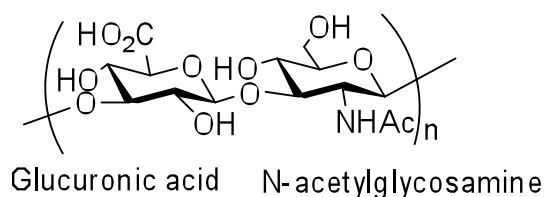
Fig-2: Structure of Hyaluronan

Alginate is an anionic polysaccharide distributed widely in the cell walls of brown algae, where it, through binding water, forms a viscous gum. In extracted form it absorbs water quickly; it is capable of absorbing 200-300 times its own weight in water[22]. Its colour ranges from white to yellowish-brown. It is obtained primarily form seaweed that has been used in a variety of medical applications including cell encapsulation and drug stabilization for delivery applications[13]. It can be chemically crosslinked to improve the mechanical properties, and it degradation occurs by hydrolysis. It has been approved by the FDA for the treatment of ulcers and severe burns (Phytacare), or in combination with collagen indicated for wound healing (Fibracol).
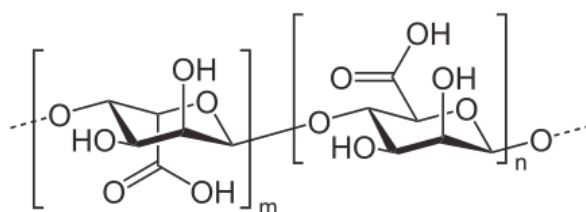
Fig-3: Structure of alginate

Chitosan is a naturally occurring polysaccharide which has a similar structure to

glycosaminoglycans. It is extracted from arthropod exoskeletons, and can be gelled in a wide array of conditions. It is enzymatically degradable by lysozyme and it has been used and modified to culture hepatocytes, neural tissue and bone [13].
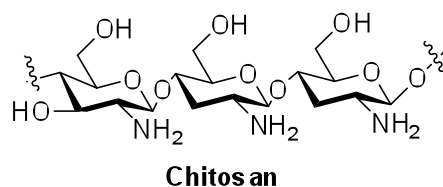
Fig-4: Structure of chitosan

1.2.1: Biomaterial functionalisation methods:-

The surface modification of biomaterials with bioactive molecules is a simple way to make smart materials. However, modification of metallic biomaterials used for orthopedic and dental implants is particularly challenging since they possess a paucity of reactive functional groups[14]. The use of superficial treatment, like plasma modification, is a strategy employed for immobilization of bioactive molecules on a ''bioinert'' material. One- and two-step carbodiimide strategies were used to immobilize lysozyme, a model biomolecule, and bone morphogenetic protein-4 (BMP-4), an osteoinductive protein, on the aminated surfaces by plasma of titanium alloy[15].

To date, different strategies can be used for the introduction of biomimetic elements into synthetic materials:

a) Physical adsorption (van der Waals, electrostatic, affinity, adsorbed and cross-linked),

b) Physical entrapment attachment (barrier system, hydrogel, dispersed matrix system)

17

c) Covalent surface immobilization, taking advantage of different natural or unnatural functional groups present both on the biomolecules and on the material surfaces (chemoselective ligation, via amino functionalities, heterobifunctional linkers, etc.).

The major methods of immobilizing a bioactive compound to a polymeric surface are adsorption via electrostatic interactions, ligand–receptor pairing (as in biotin–avidin), and covalent attachment (Figure 5). Non-covalent adsorption is sometimes desirable, as in certain drug delivery applications.
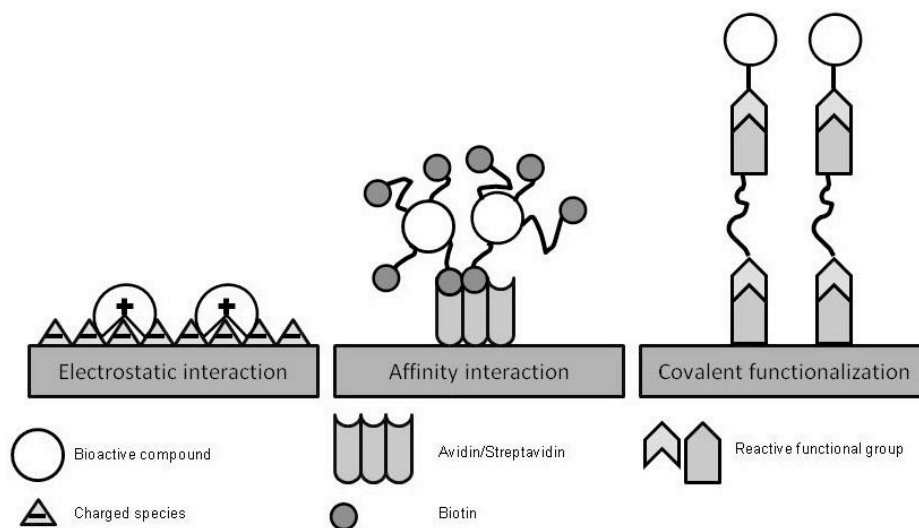
Fig-5: Different strategies for the introduction of biomimetic elements into synthetic materials:

Covalent immobilization offers several advantages by providing the most stable bond between the compound and the functionalized polymer surface. A covalent immobilization can be used to extend the half-life of a biomolecule, prevent its metabolism, or allow continued bioactivity of indwelling devices[16]. Bioactive molecules (growth factors, ECM proteins, etc.) that are free in solution, as opposed to immobilize to the matrix, may induce significantly different biological responses.

18

Growth factors are routinely added to cultures in vitro, and have been incorporated and released from polymeric systems with retention of bioactivity, which is exemplified by neurotrophins,[17] BMPs,[18-19] and VEGF[20]. *In vivo*, these soluble factors can be transported from the delivery site, where the design parameter for the delivery system is the duration over which therapeutic concentrations can be maintained. Alternatively, bioactive molecules immobilization can occur through reversible association with the scaffold, covalent binding to the polymer, or immobilized with release dependent upon degradation of a linking together or the matrix itself. For growth factor immobilization to fibrin, cell migration results in cell-activated plasmin degradation that can catalyze release of the factor. These scaffolds have been termed ''cell-responsive''[21] due to release of the factor upon cellular demand. Once released, these soluble factors can bind their receptors and initiate a signaling cascade.

Alternatively, immobilized biomolecules can ligate their receptors directly from the material surface; however, this type of interaction may not exactly replicate signaling through the soluble factor, as growth factor internalization can stimulate signaling pathways separate from those activated at the surface[22-23]. For example, NGF induces neurite outgrowth by signaling at the plasma membrane, yet promotes neuron survival when internalized [24-26]. Surface immobilization has been successfully used to attach several factors such as EGF[27], BMP-7[28], BMP-2[29], VEGF[20], NGF[30-32], and NT-3[33] to a variety of natural and synthetic biomaterials. Signaling by these immobilized or locally released bioactive ligands may be more potent than signaling by soluble versions added directly to culture media[34]. These studies also demonstrate that the immobilization strategy must consider protein structure and active region topology when designing suitable delivery systems in order to maximize bioactivity.

Ultimately, some factors may be best delivered in a sustained manner, while others benefit from direct attachment to the biomaterial substrate[35].

Different methods have been developed for covalent functionalization of biomolecules to diverse biomaterials. Many of these methods are illustrated in table[35].

For covalent functionalization to an inert solid polymer, the surface must first be chemically modified to provide reactive groups ($-OH$, $-NH_2$, $COOH$, $-SH$) for a second functionalization step. When the material does not contain reactive groups, functional groups for biomolecules immobilization can be generated by chemical and physical modification, on the polymer surfaces in order to permit covalent attachment of biomolecules. With this goal, a wide number of surface modification techniques have been developed, including plasma, ionic radiation graft polymerization, photochemical grafting, chemical modification and chemical derivatization[37].

For example peptides can react via the N-terminus with different groups on polymers (Figure 2). This is usually done by reacting an activated carboxylic acid group with nucleophilic N-terminus of peptides. The carboxylic group can be activated with different peptide coupling reagent, e.g. 1-ethyl-3-(3-dimethylaminopropyl)-carbodiimide (EDC, also referred to as water soluble carbodiimide, WSC), dicyclohexyl-carbodiimide (DCC) or carbonyl diimidazole (CDI).
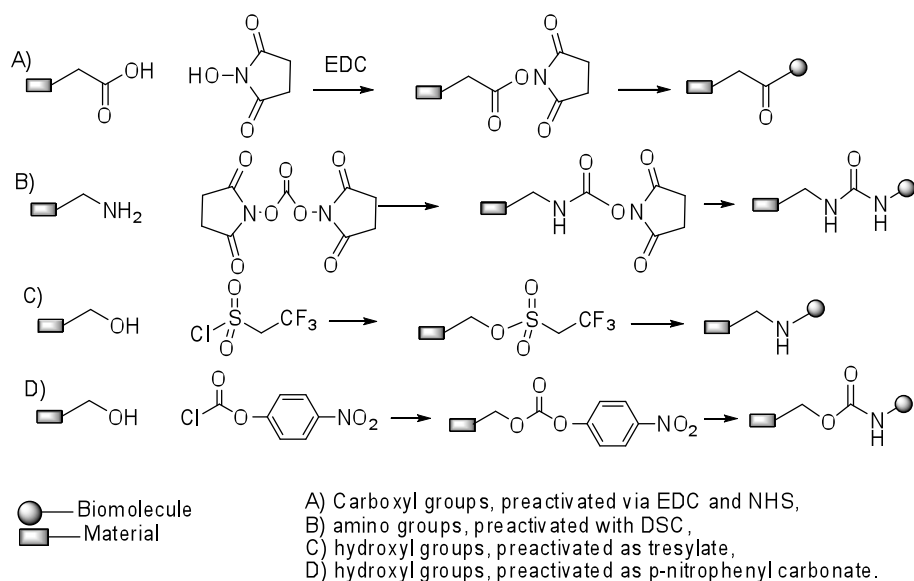
Fig-6: Coupling methods to different groups on materials.

In a more recent approach named chemoselective ligation (Figure 3), selected pairs of functional groups are used to form stable bonds without the need of an activating agent and without interfering with other functionalities usually encountered in biomolecules [38-40]. Chemoselective ligation proceeds usually under mild conditions and results in good yields.
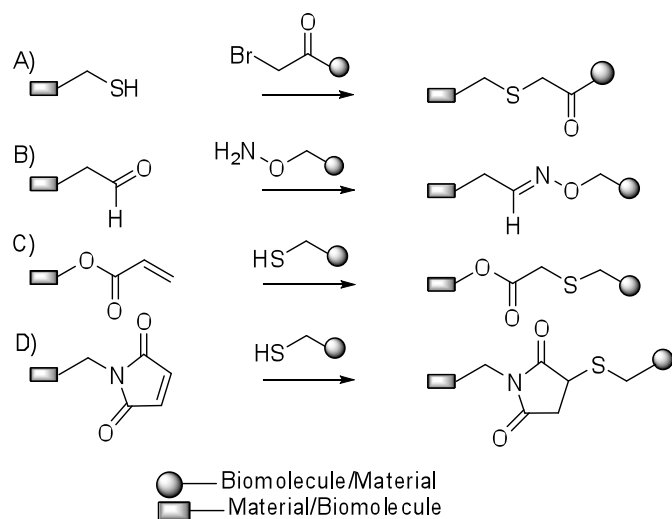
A) Thiol and bromoacetyl-biomolecule
B) Aldehyde and aminooxy-biomolecule
C) Acrylate and aminoxy-biomolecule
D) Maleinimde and thiol biomolecule

Fig-7. Chemoselective ligation methods.

A biomolecule may also be attached, with these coupling methods, via a spacer group, in order to give better access to the target receptor. One example of spacer is PEG that has been differently functionalized at two extremities[41]. Metal or ceramic surface may also be silane chemistry, exploiting functionalized triethoxysilanes [42-43].

1.2.2: Biomolecules for biomaterials design:

Sugars have been known to humankind since prehistoric times, with Stone Age rock paintings recording the harvesting of honey (a mixture mainly of glucose, fructose and the disaccharide sucrose), and ancient Egyptian hieroglyphics depicting various features of its processing. Likewise, the use of honey in India is reported as far back as records go, and in biblical references, in Old Testament times, Palestine was a land flowing with milk and honey[44]. Carbohydrates were considered to be solely of use for energy storage, and as skeletal components.
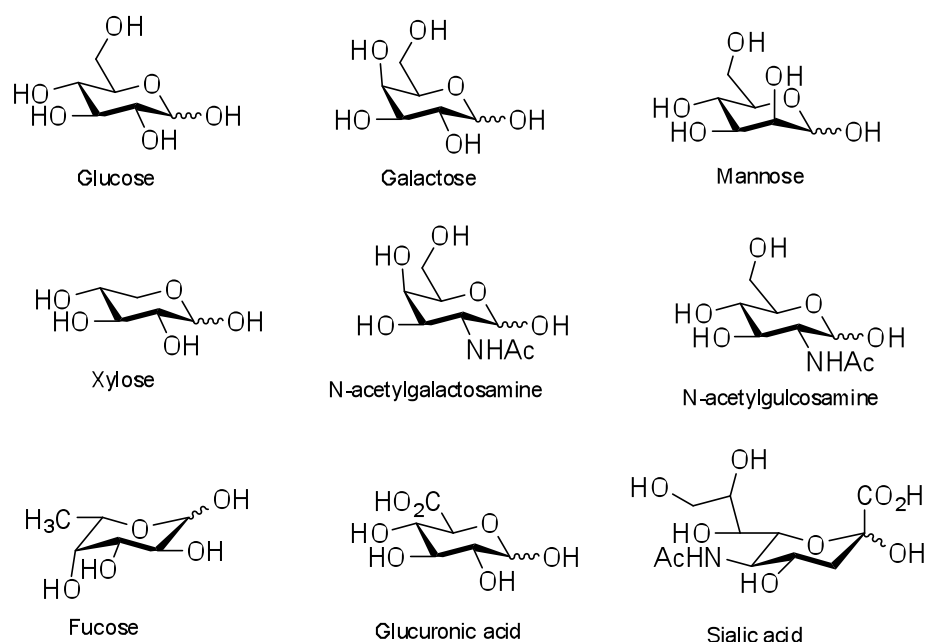
Fig-8: Common monosaccharides in mammalian cells.
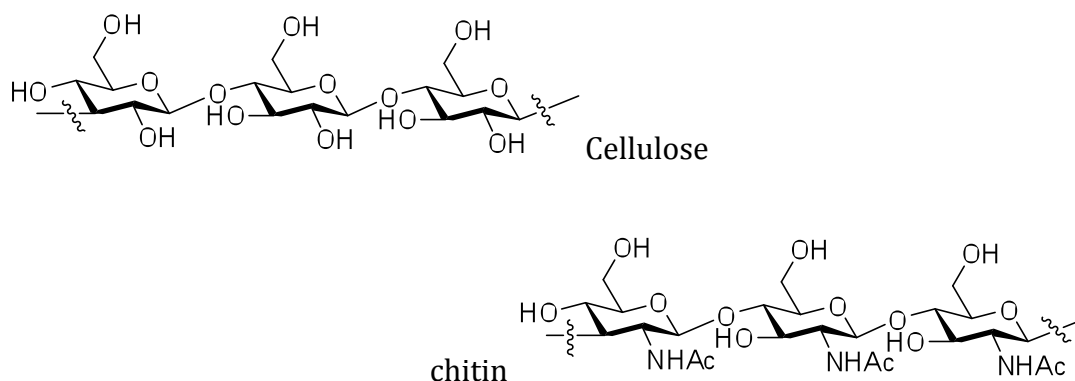
Cellulose

chitin

Fig-9 : Chemical structure of a) cellulose and b) chitine.

Carbohydrates are synthesized in plants from CO_2 and H_2O via a multistep biochemical process, (Equation 1)

$$CO_2 + H_2O \rightarrow C_6H_{12}O_6 + O_2 \qquad (1)$$
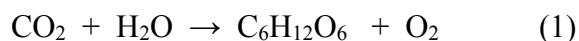
Mammals also convert D-Glucose into a polymeric form, glycogen (Fig. 10), which is stored primarily in muscle tissue and in the liver to be metabolised when it is needed.
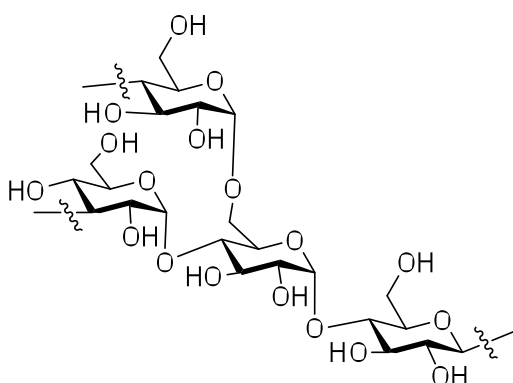
Fig-10: Structure of glycogen.

The abundance of carbohydrates in nature and their diverse roles in biological systems make them attractive as subjects both for chemical and biological research[44]. However, this hypothesis was challenged in 1963 when a protein was isolated from *Canavalia ensiformis* that demonstrated ability to bind to carbohydrates on erythrocytes. In 1982 the first animal carbohydrate binding protein was identified, and this sparked interest in the wider roles of carbohydrates whitin biological systems.

23

The traditional view of carbohydrate polymers as energy source (starch and glycogen) and structural materials (cellulose, collagen, and proteoglycans) has expanded. Today, carbohydrates are known to have a wide variety of biological functions. For example, the sulfated polysaccharide, **heparin**, plays an essential role in blood coagulation[46].
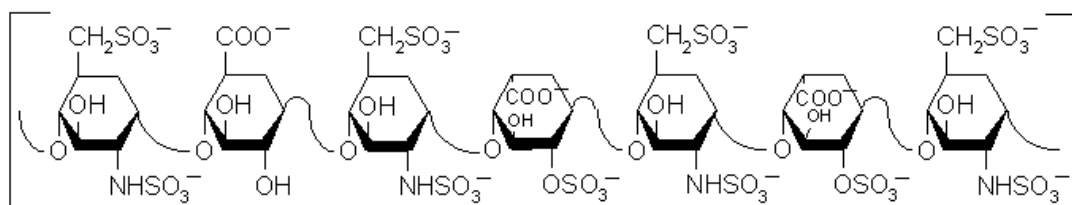
Fig-11: Structure of Heparin

Another related polysaccharide, **hyaluronan,** which acts as a lubricant in joints, has been used to protect the corneal endothelium during ophthalmologic surgery[47]. In addition to hyaluronan's lubricating and cushioning properties, polysaccharide and glycoprotein participate in a number of recognising processes. Synthetic carbohydrate based polymers are increasingly being explored as biodegradable, biocompatible and biorenewable materials for use as water absorbent, chromatographic supports and medical devices. Moreover synthetic polymers bearing sugar residues also offer a good surface for cell attachement and might thus be applied to cell recognising events in tissue engineering. Different types of synthetic polymers bearing sugar residues are known[48]. Linear polymers, comb polymers, dendrimers, and cross-linking hydrogels represent the four major classes (Figure 12). One of the most relevant glycidic structures for biomaterial applications is hyaluronic acid.
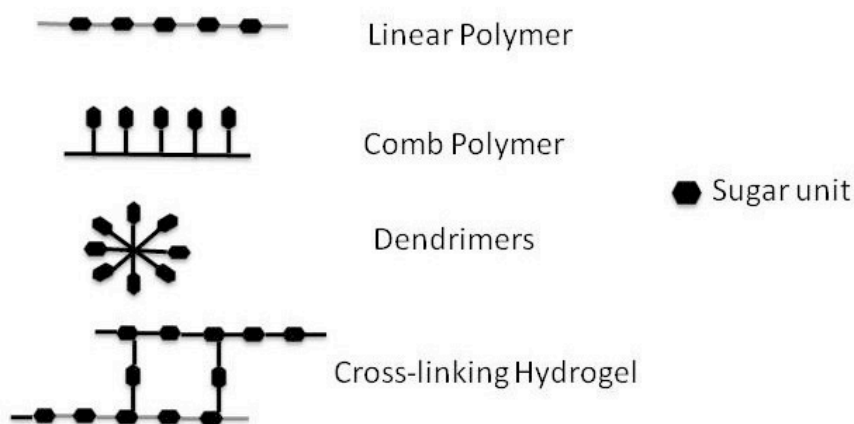
Fig-12: Major classes of synthetic sugars containing polymers.

It is well known that the glycidic part of glycolipids and glycoproteins strongly interact with lectins present at cell surfaces[49]. In particular, it is known that β-galactose residues are recognized by asialoglycoprotein receptors on the surfaces of hepatocytes [49-50] and promote hepatocyte attachment[51-56]. Therefore, it is expected that the β-galactose residues incorporated into silk fibroin may act as an efficient ligand for hepatocyte attachment to silk fibroin scaffolds.

Oligosaccharides were covalently coupled to silk fibroin using cyanuric chloride generating the glycoconjugate described in Figure 5, in which the sugar is linked to the tyrosine and cystine residues via a cyanuric chloride linker [57-58].
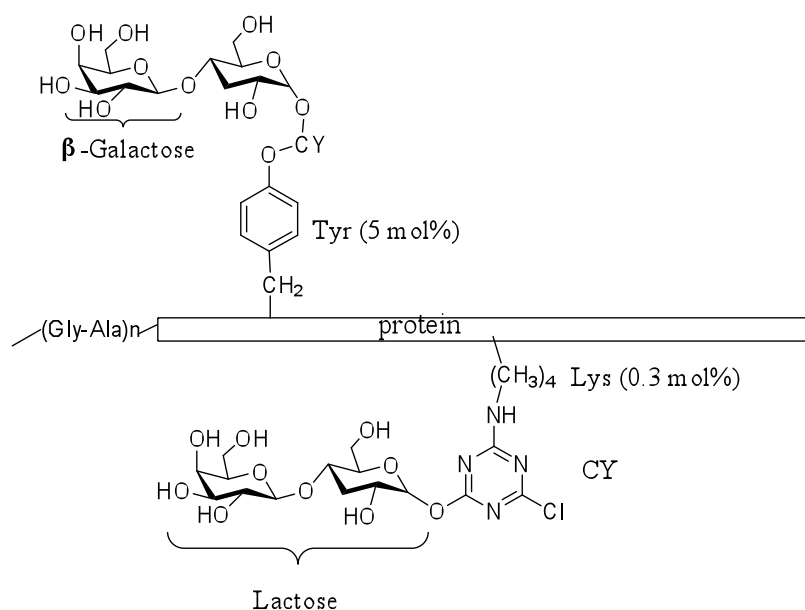
Fig-13: Covalent linking of lactose to silk fibroin.

Although hepatocyte attachment on silk fibroin-coated dishes was lower than that on uncoated polystyrene dishes, the attachment on the dishes coated with 0.1%(w/v) and 1%(w/v) solutions of lactose-cyanuric chloride-silk fibroin (Lac–CY–SF) was comparable to that on collagen-coated dishes. After 2 days of culture, hepatocytes on the conjugate-coated dishes showed a small amount of dispersion compared to those on collagen-coated dishes. These results support the concept that the Lac–CY–SF glycoconjugates can serve as a scaffold for hepatocyte attachment.

Hajime Sato et al. exploited the anionic polysaccharide heparin to extend the scope of micropatterned carbohydrate displays by applying electrostatic interaction. They also used micropatterned carbohydrate displays on silicon substrates by a combination of photolithography and self-assembly[59]. This technique has intresting potential applications in tisuue engineering. Top-down photolithography and bottom-up molecular self-assembly are the two main approaches to biomacromolecular micro patterning. Photolithography has been widely used in electronic devices and most practically applied for precise micropatterning of proteins for cell cultivation[60].

26

Heparin is a glycosaminoglycan polysaccharide with a variable number of sulfate groups and its binding to basic fibroblast growth factor (bFGF) is known to modulate cell proliferation and differentiation.

The interaction of heparin with bFGF induces the dimerization of bFGF, which is required for binding of bFGF to FGF receptor (FGF-R) on cell surfaces[61-62], as illustrated below.
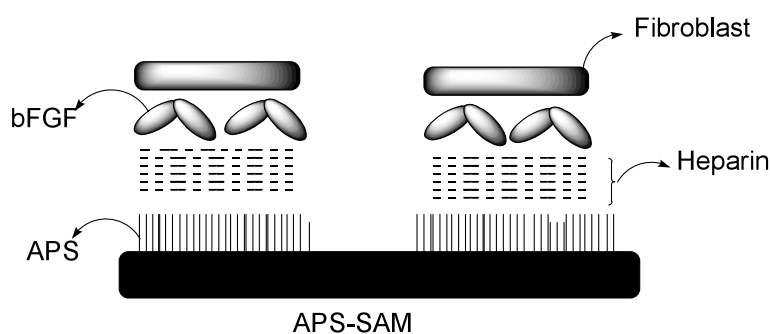
Fig-14: Adhesion of fibroblast cell.

The self-assembled monolayer (SAM) of 3-aminopropyl-trimethoxysilane (APS) as ammonium-terminated template was prepared on silicon and glass substrates, and micropat terned by photolithography. Self-assembling of heparin onto the APS-SAM through electrostatic interaction and then molecular recognition of bFGF to heparin and of fibroblast cells to bFGF has been achieved[63].

Adsorption of heparin was not observed on a silicon substrate without APS-SAM. Heparin adsorbed on APS- SAM remained on the substrate after rinsing with PBS buffer. The electrostatic interaction was essential for anchoring heparin on APS-SAM. The time-course of heparin adsorption to APS-SAM does not fit with a simple Langmuir model, suggesting that, in addition to electrostatic interaction, some other interaction such as hydrogen bonding may contribute a little to the adsorption of heparin to APS-SAM[64-65].

The above carbohydrate display using heparin has an attractive potential for tissue engineering, since it allows a facile and effective strategy for bio-macromolecular patterning with significant bioactive molecules.

Chapter-2
Aim of work

2:Introduction

Carbohydrates, glycoconjugates, and oligosaccharides are critical components of living systems and mediate a vast number of fundamental biological processes from complex cellular operations required to initiate and sustain life, to recognition events that are responsible for autoimmune diseases, organ rejection, and inflammation. This functional diversity is reflected in the diversity of carbohydrate structures. There is an increasing demand for efficient access to oligosaccharides and glycoconjugates to deepen our understanding of glycobiology and to expedite the development of therapeutic agents.

Biomaterials science brings together researchers from diverse academic backgrounds. They must communicate clearly. Some disciplines that intersect in the development, study and application of biomaterials include: bioengineer, chemist, chemical engineer, electrical engineer, mechanical engineer, materials scientist, biologist, microbiologist, physician, veterinarian, ethicist, nurse, lawyer, regulatory specialist and venture capitalist. Bone tissue engineering has become a significant area of research, and as a result of emerging activity in this field, a new class of drugs has been introduced with excellent potential to stimulate bone formation and to induce new bone regeneration. Biodegradable scaffolds should ideally provide the initial strength required to resist blood flow, and then gradually degrade to leave a graft composed solely of host tissue. During my Ph.D work the project was divided into three main parts,
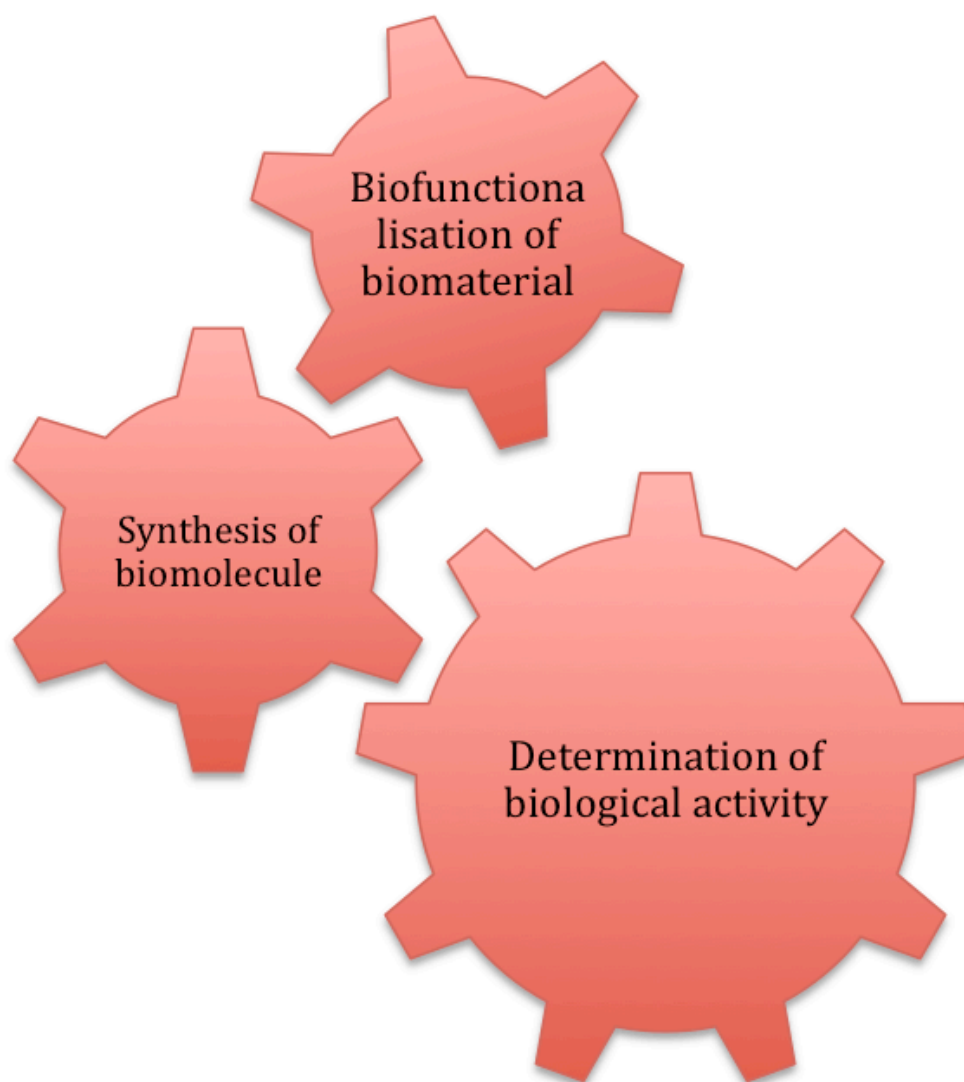
2.1: **Synthesis of biomolecule**: Living systems are composed of networks of interacting biopolymers, ions and metabolites. To understand complex cellular processes requires the ability to track molecules within their native enviroments. In recent years, an alternative strategy for tagging biomolecules has emerged involving the incorporation of unique chemical functionality—a bioorthogonal chemical reporter into a target biomolecule using the cell's own biosynthetic machinery. Bioorthogonal chemical reporters are non-native, non-perturbing chemical handles that can be modified in living systems through highly selective reactions with exogenously delivered probes. We are using organic synthesis to construct new

bioactive compounds, new chemicals to cross-link proteins and new probes of biological function. We can design and synthesize analogues with improved selectivity or with other valuable properties.

2.2: **Biofunctionalisation of biomaterial** : The ECM performs two main functions: i) structural support for the cell environment; ii) signalling, in order to elicit specific biological responses. The bioactive molecules for material functionalisation should mimic these two roles of ECM in tissue. it's really a hard task to design a biomaterials possessing both structural and signaling features. In the field of osseous substitution, the possibilities being offered to the surgeons prove sometimes difficult to apply in particular in the case of great losses of osseous substance. For these reasons, it is necessary to develop innovative techniques to satisfy the request increasing for substitutes and to see appearing on the market solutions combining availability, perenniality and biosecurity of the implants. In order to improve the tissue integration and subsequently the long-term maintenance, the implant surface can be modified by mechanical, physical, chemical or biological functionalization. In this way, the surface becomes biologically active by further grafting of biomolecules. The goal in biomaterial surface modification is to retain a material's bulk properties while modifying only its surface to possess desired recognition and specificity. Two principal concepts are considered for materials functionalization. (i) The Drug Delivery Systems (DDS) where the bioactive molecules goes to the target. (ii) The grafting of the bioactive compounds on small strongly bound spacer molecules. In this system, the target goes to the bioactive molecules.

2.3: **Determination of biological activity**: The functionalized biomateriale have been studied by using SEM/TEM and some are also in process..

Chapter-3

Synthesis of Ultrasonic assisted Fischer glycosylation

3.1. Introduction:

Biological information storage and transfer have been classically associated with two types of biomolecules: nucleic acids and proteins. Sugar molecules have been almost exclusively assigned as biochemical fuels in energy metabolism or building blocks of polymers with structural functions in the cell wall (e.g., cellulose and chitin). Only recently, with the advent of modern glycobiology, have carbohydrates become important molecules to consider in relation to the life of a cell, and new light has been shed on the role of sugars in the transmission of biological information[66–69]. The main reason why the role of sugars and oligosaccharides in the life code has remained unnoticed for such a long time is simple: glycoconjugates are much more complex, variegated and difficult to study than proteins or nucleic acids. As a result of the new vision of sugars in modern glycobiology, great efforts are currently being devoted to unraveling the 'hardware of the sugar code'; that is, to understand how oligosaccharides, with their unique structural variability, generate compact units with explicit information properties. The level of diversity introduced in the oligosaccharide structures by the occurrence of the two anomeric variants at each glycosidic linkage and the presence of five potential attachment points (hydroxyls) per sugar is much higher than that in oligonucleotides or peptides with the same number of monomers.

Carbohydrates make up a substantial portion of the biomass on earth, mostly in the form of structural polysaccharides such as cellulose from plants and chitin from arthropods and fungi. All known living organisms also display an array of free or covalently linked carbohydrates collectively known as glycans[70]. The glycans, constituting the sugar code of a cell, protrude from its surface and are covalently anchored to membrane proteins or lipids. Cell surface proteins are present as a set of

34

glycoforms that differ in their sugar part and the population of sugars in glycoforms changes under a variety of conditions, including diseases[71–73]. Protein glycosylation is highly sensitive to alteration in cellular function and abnormal glycosylation is diagnostic for a number of disease states, including cancer[74-75], autoimmune diseases [69,76-77] and genetic diseases[78]. This is why several glycol-processing enzymes have been recognized as important targets for therapeutic intervention[79]. This concept inspired the development of important classes of therapeutics, such as the anti-influenza drugs zanamivir (licensed by GlaxoSmithKline as Relenza®)[80] and oseltamivir (licensed by Roche as Tamiflu®)[81], both inhibitors of the viral neuraminidase; the antidiabetic and antiobesity compound miglitol[84], a glucosidase inhibitor licensed by Bayer as Glyset® or Miglustat® and a similar glucosidase inhibitor developed by Actelion, Zavesca®, primarily used to treat Type 1 Gaucher disease **(Figure 1)**[82].
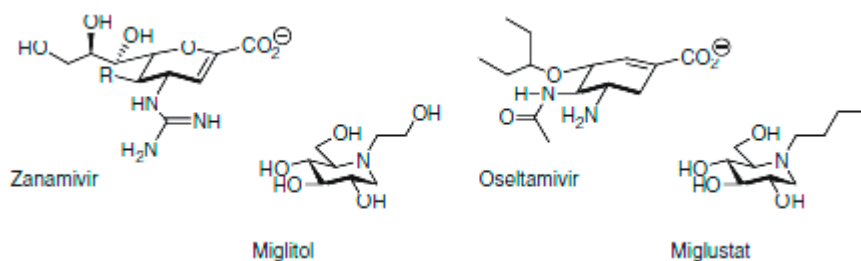
Fig-1: Examples pf glycomimetic drug

Glycosidase inhibitors are also under investigation as antiviral and anti-tumor agents, mimetics of sialyl–Lewis X as anti-inflammatory agents and Lipid A antagonists for sepsis treatment. Also, specific oligosaccharidic fragments linked to immunogens generate synthetic vaccines and fragments structurally related to heparin, exert not only anticoagulant and anti-thrombotic properties, but are also under investigation as

anti-atherosclerosis, anti-inflammatory, anti-angiogenetic, anticancer, antiviral and even anti-Alzheimer agents.

The potentialities of glycocompounds as therapeutics are therefore wide[83] and attention is mainly concentrated on carbohydrate mimics, in which proper modifications allow a stronger interaction with the target protein, higher stability and better pharmacokinetic properties. For example, in the case of zanamivir and oseltamivir, both compounds mimic the oxonium-ion intermediate of the enzymatic reaction and, therefore, act as inhibitors **(Figure 2)**, but the latter has better pharmacokinetic properties. Another original opportunity to exploit carbohydrates for the development of new drugs comes from their unique structural feature; the conformational rigidity combined with multifunctionality. This feature, widely exploited in living organisms for molecular recognition, makes sugars ideal scaffolds that can be decorated with different pharmacophores in order to generate libraries of bioactive compounds following a rational-design or combinatorial approach.
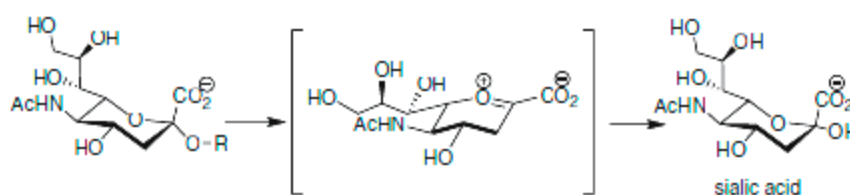
Fig-2: Mechanism of sialidases

3.2: General synthetic discussion

The reasons why synthetic chemists have modified carbohydrates, generating compounds generally defined 'carbohydrate mimetics' are various:

- To increase the metabolic and chemical stability

- To insert a functional group that improves the interaction with receptors/enzymes (a proper pharmacophore)

- To allow a chemoselective ligation to another chemical entity, such as a sugar, protein, solid support or nanoparticle.

The most common modifications performed on the structure of carbohydrates are summarized in **Figure 3**.

X=O, Y=C, C-Glycoside

X=O, Y=N, N-Glycoside

X=C, Y=O or C , Carbasugar

X=O, Y=P, P-Glycoside

X=N, Y=H or C, Iminosugars

X=S, Y=O, Thiosugars

X=O, Y=C, C-Glycoside

X=P, Y=O, Phosphasugar
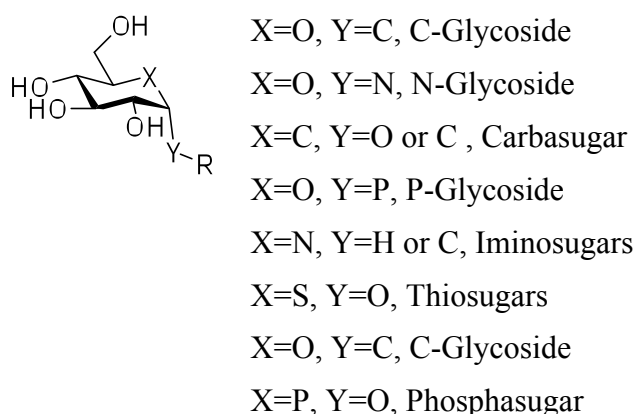
Fig:3 Different Classes of glycomimetics

Huisgen and Krebs were largely academic teaching tools until they experienced a renaissance in the form of the copper-catalyzed azide–alkyne cycloaddition, often referred to as ''click'' chemistry.[85–87] Click reactions are defined more broadly as those that meet the necessary criteria of being selective, high yielding, and having good reaction kinetics. A subclass of click reactions whose components are inert to the surrounding biological milieu is termed bioorthogonal[88]. This goes one step beyond the typical definition of a click reaction because of the added complications of biocompatibility. Bioorthogonal reactions that are cycloadditions lacking exogenous metal catalysts, the so-called Cu-free click reactions. Exogenous metals can have mild to severe cytotoxic effects and can thus disturb the delicate metabolic balance of the

systems being studied[89]. One of the most popular bioorthogonal functional groups is the azide. The small size, coupled with its inert nature towards endogenous biological functionalities, sets the azide apart. Additionally the azide has unique chemistries with other bioorthogonal functionalities, most notably phosphines and alkynes. Indeed the reaction of azides with triarylphosphines equipped with an ester a process termed the Staudinger ligation—was the first bioorthogonal reaction ever performed in living systems[90]. However, the relatively slow kinetics of the Staudinger ligation limited its use in probing fast biological processes.
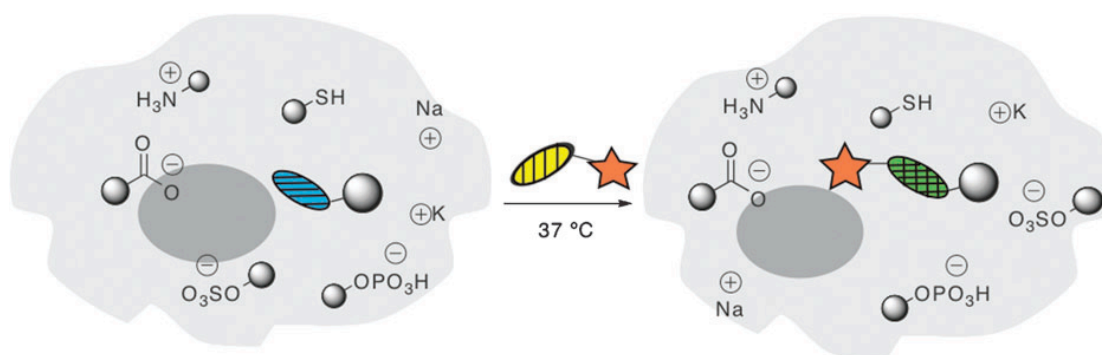
Fig 4: A general bioorthogonal reaction. The bioorthogonal functionality, oval with horizontal lines, reacts with its counterpart, oval with vertical lines, to label a biomolecule in live cells or organisms.

Cycloadditions were viewed as ideal reactions because of tunable electronics and their intrinsic selectivity[91]. Huisgen developed the [3+2] cycloaddition between an azide and an acyclic alkyne[92], but this reaction required a good deal of heat to overcome the activation barrier of deforming the alkyne's bond angle to form the triazole (Fig. 2A). Sharpless and co-workers and Meldal and co-workers developed a Cu-catalyzed rendition of this reaction using terminal alkynes as substrates, but the metal's cytotoxicity limits its use in living systems. The first cyclooctyne that we evaluated, compound 1 (''OCT,'' Fig. 2C), was shown to undergo cycloaddition with azides to

give triazole 2 and although its reaction kinetics were vastly accelerated compared to the linear alkynes, there was room for improvement[93]. Postulating that the reaction involved the lowest unoccupied molecular orbital (LUMO) of the alkyne and the highest occupied molecular orbital (HOMO) of the azide we sought to lower the LUMO of the alkyne by withdrawing electron density from the bond[94]. Adding one fluorine atom to the ring system (3) increased the reaction rate constant by 3-fold[95]. With the addition of a second fluorine atom to the ring, to create a compound bertozzi et al call DIFO (4), they observed a marked increase in rate constant, making the reaction 60 times faster than the parent compound, 1[96].
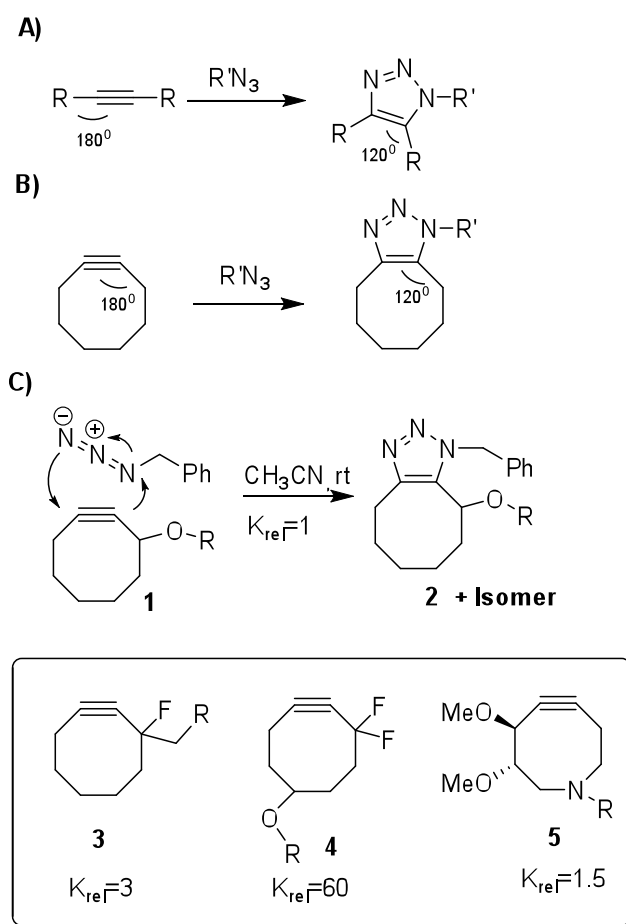
Scheme-1: The Cu-free reaction of azides and alkynes. (A) A comparison of bond angles between linear alkynes and triazoles. (B) A comparison of bond angles between a strained cyclooctyne and its corresponding triazole product. (C)

Comparison of second-order rate constants of cyclooctynes in a model reaction with benzyl azide.

Rutjes and co-workers developed an alkyne surrogate that forms a similar product (Scheme 2)[97].
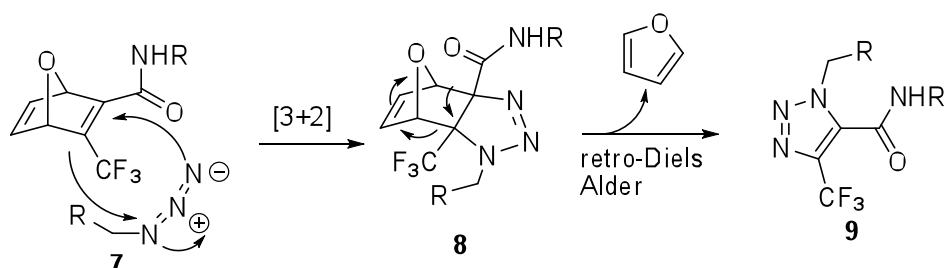
Scheme-2: The two-step reaction of oxanorbornadienes with azides forms triazoles.

An activated oxanorbornadiene (7) first reacts with an azide in a [3+2]-cycloaddition to give 8. This is followed immediately by a retro-Diels–Alder reaction to give a stable 1,2,3-triazole, 9. They found that further activation of the strained double bond in 7 with trifluoromethyl groups gives acceptable rate constants for the click reaction. The Fox group explored the use of the inverse-electron demand Structure 7,8,9 Diels–Alder reaction to attach a trans-cyclooctene (10, Scheme 3A) to a bipyridyltetrazine-tethered probe (11)[98].
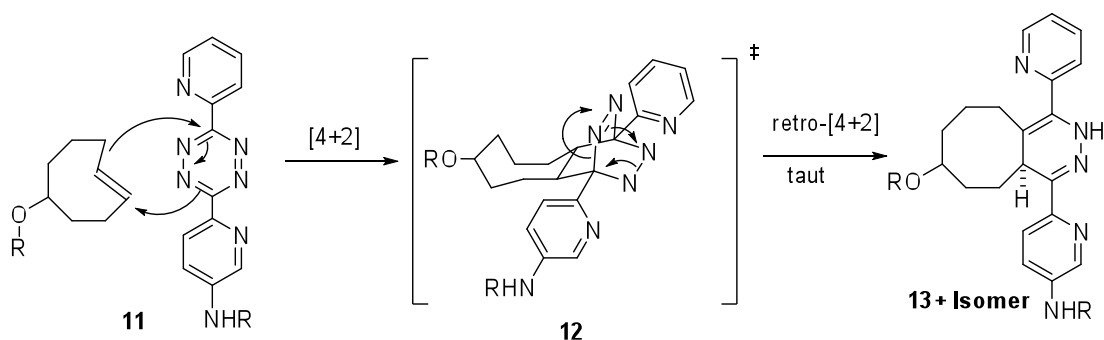
Scheme-3: Inverse-electron-demand Diels–Alder reactions of strained alkenes: the reaction between trans-cyclooctene 10, with biaryltetrazine 11.

While cis-cyclooctenes are relatively inert, the trans isomer is highly strained and thus

remarkably reactive. The reaction produces intermediate 12, which rapidly decomposes to extrude nitrogen and to form 13 upon tautomerization. The reaction rates for these systems are orders of magnitude higher than for any other Cu-free click reaction. These alkenes are useful, but photoisomerization is always a concern when dealing with strained alkenes.

Shortly after Fox's report, Hilderbrand and co-workers presented their work with monoaryltetrazines (14, Scheme 4)[99]. They used norbornene (15) in place of the trans-cyclooctene to give 16. Norbornene is more stable than trans-cyclooctene, but the reaction rates are not as high. Similarly, the monoaryltetrazine is not as reactive as the biaryltetrazine, but it is more stable in a biological setting. In yet another independent effort, Pipkorn and co-workers used tetrazine chemistry to assemble late-stage synthetic intermediates for cancer treatment[100].

Scheme-4: Inverse-electron-demand Diels–Alder reactions of strained alkenes: The reaction between norbornene 15 with aryltetrazine14.

Their system took advantage of a highly strained cyclobutene-containing molecule (17, Scheme 3C) with a biaryltetrazine (18) to give 19. A head-to-head comparison of the reactions of these various alkenes and tetrazines has not been reported, but combining the best feature of each approach could add valuable tools to the field.
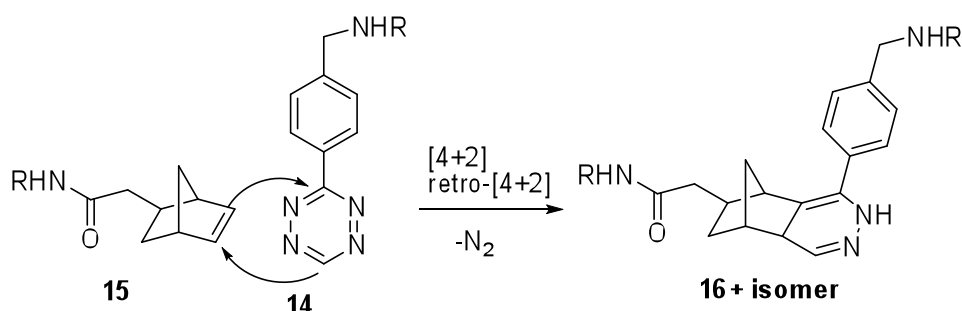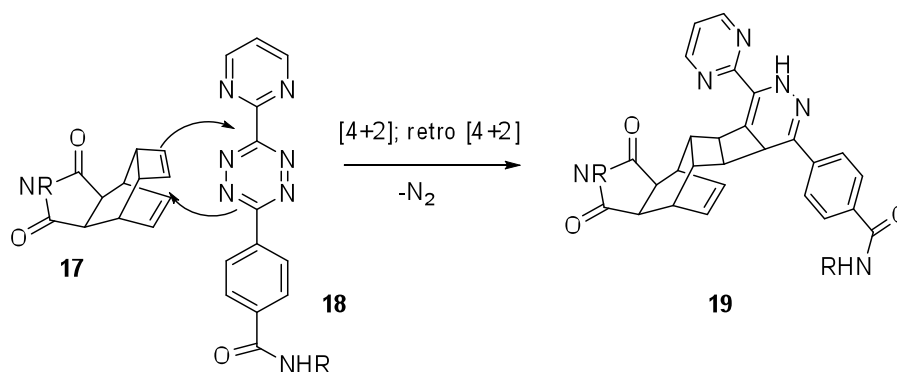
Scheme-5: Inverse-electron-demand Diels–Alder reactions of strained alkenes, the reaction between cyclobutene 17 with biaryltetrazine 18.

The penultimate copper-free click reaction that we will examine is another gem from Huisgen that had long been overlooked, the photoinducible dipolar cycloaddition between a nitrile imine (20) and an alkene (21, Scheme 6)[101].
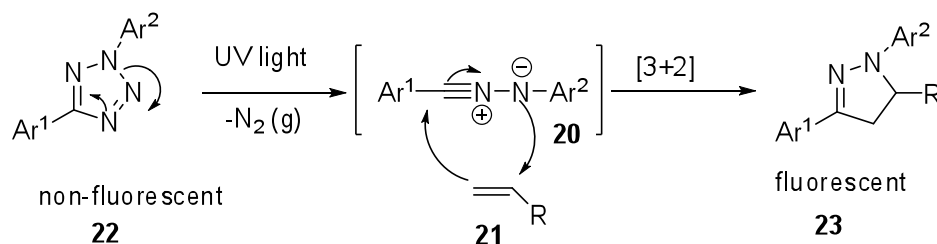
Scheme-6: In situ generated dipoles as bioorthogonal reagents.The photo-click reaction.

Lin and co-workers recently utilized this transformation as a bioorthogonal reaction, dubbing it the ''photo-click'' reaction[102]. Terminal alkenes are quite small and, when not in conjugation with a carbonyl group, unreactive. Tetrazoles (22) are activated using relatively low energy UV-light, releasing nitrogen to produce nitrile imines, which serve as active 1,3-dipoles in cycloadditions. Nitrile imines react with alkenes to make pyrazoline cycloadducts (23). The rate of nitrogen extrusion is high so that cells need not be exposed to the potentially damaging UV-light for prolonged times. The reaction between the nitrile imine and alkene is slower, but it outcompetes

degradation of the unstable nitrile imine in the presence of water. Additionally, while the starting materials are not fluorescent, the pyrazoline product is fluorescent, making the system fluorogenic, an attractive characteristic rarely seen in bioorthogonal reactions[103-104]. Carell and co-workers[105] took advantage of yet another Huisgen discovery[106] in their recent work with the reaction between nitrile oxides (24) and norbornenes (25, Scheme 7).
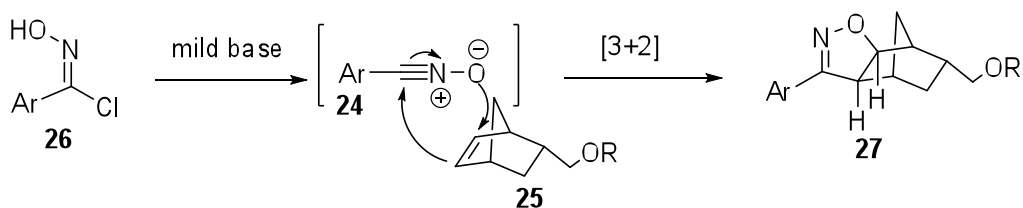
Scheme-7: In situ generated dipoles as bioorthogonal reagents, the generation and reaction of the nitrile-oxide.

Nitrile oxides are generated by the deprotonation of the relatively stable arylchlorooximes (26) by a weak base. Upon generation, the dipoles readily react with alkenes, and the added strain of the norbornene allows the reaction to proceed rapidly to give the isoxazoline product, 27.

Despite, the utility of the Staudinger ligation, the phosphine reagents have certain liabilities. They are susceptible to oxidation by molecular oxygen, for example, which limits their shelf-life and may also provide a pathway for rapid liver metabolism (12). Moreover, the Staudinger ligation has a relatively sluggish reaction rate, compromising its ability to monitor rapid biological processes in vivo (9). In the context of mouse models, rapid kinetics are important so that the reaction can occur on a faster time scale than metabolic clearance of the probe. Bertozzi et al shows that bioorthogonal reaction modeled on the Huisgen 1,3-dipolar cycloaddition of azides and alkynes, which forms triazole products (13). Modifies to the classic reaction

included situation of the alkyne within a strained cyclooctyne ring (14) as well as the addition of propargylic fluorine atoms (15, 16), two features that significantly accelerated the reaction rate. Another strategy for accelerating the reaction of azides and terminal alkynes involves the use of a Cu catalyst (17, 18), now widely referred to as "click chemistry," but the toxicity of the metal precludes its use in the presence of live cells or organisms. Because cyclooctyne reagents react with azides at rates approaching that of the metal-catalyzed transformation, we refer to these cycloadditions with the term "Cu-free click chemistry." Various cyclooctyne reagents have recently been used to probe glycans on cultured cells (16, 19) and in developing zebrafish (20), as well as protein and phospholipid dynamics in live cells (21, 22).

They evaluate Cu-free click chemistry for its performance in mice with the goal of identifying new reagents that are suitable for bioorthogonal ligations in vivo. They have delivered azides to cell-surface sialoglycoconjugates by injecting mice with the metabolic precursor peracetylated N-azidoacetylmannosamine ($Ac_4ManNAz$) (Fig 4 A) (11, 23).
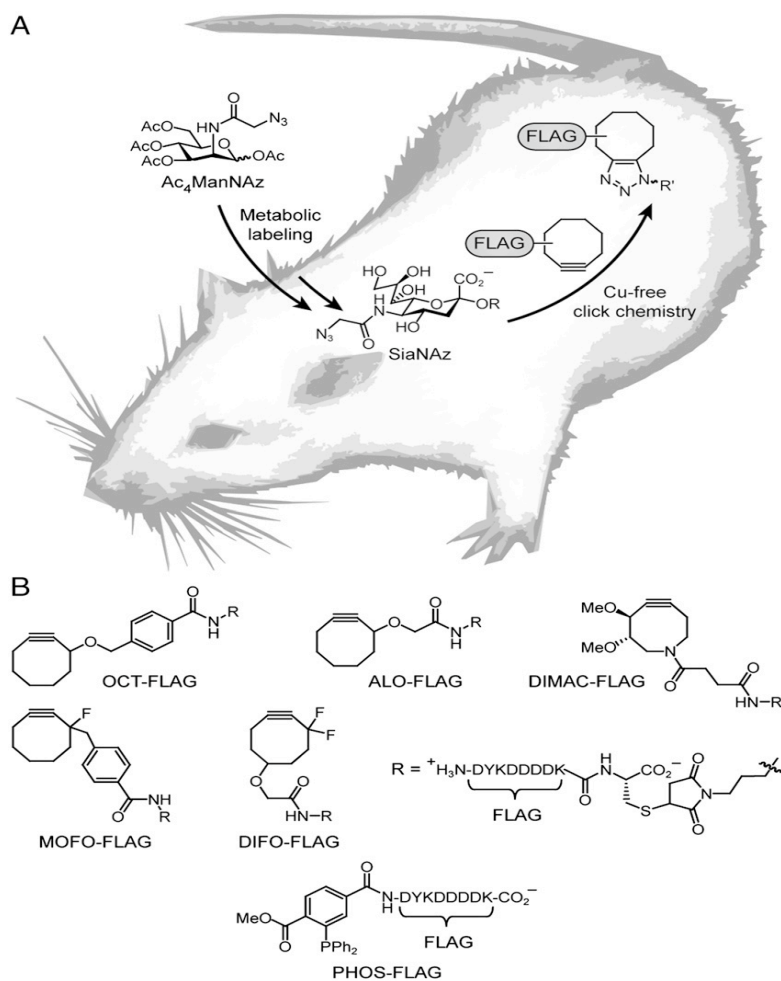
Fig. 4. Cu-free click chemistry in mice. (A)Mice were injected with Ac4ManNAz once daily for 1 wk to allow for metabolic labeling of glycans with SiaNAz. The mice were then injected with a cyclooctyne-FLAG conjugate for in vivo covalent labeling of azido glycans. (B) Panel of FLAG conjugates used in this study (Chem. Soc. Rev., 2010, 39, 1272–1279).

Then labeled glycoconjugates bearing the corresponding azido sialic acid, SiaNAz, by covalent reaction in vivo with a panel of cyclooctyne-FLAG peptide conjugates (Fig 4B). The labeled biomolecules were probed by ex vivo analysis of cells and tissue lysates. The relative amounts of ligation products observed with different cyclooctynes suggest that both intrinsic reaction kinetics and other properties such as solubility and tissue access govern the efficiency of Cu-free click chemistry in mice. More broadly, Cu-free click chemistry appears to possess the requisite

bioorthogonality to achieve specific biomolecule labeling in this important model organism. Oligosaccharide structures present a high level of diversity introduced by the occurrence of the two anomeric variants at each glycosidic linkage and by the presence of five potential attachment points (hydroxyls) per sugar unit, affording highly complex linear or branched different glycan structures, mediating a great deal of biological information (glycocode). Despite the increasing knowledge about natural glycan diversity, the deciphering of information content for the glycocode is still challenging. Glycotechnology still needs the development of simplified and sound synthetic methods in order to facilitate not only analysis of proteins for carbohydrate-binding activities but also elucidation of their ligands, for example with the use of glycoarrays[107].

Glycoconjugation exploiting the click chemistry requires the functionalization of carbohydrates with alkynes or an azido group. The simplest method to do that is the glycosylation of unprotected sugars with propargyl or azidoalkyl alcohol. Hence improved and simplified methods for the synthesis of azido or alkynyl carbohydrate derivatives are highly desirable.

3.3: AIM OF WORK: -

Simple alkyl and aryl glycosides of free sugars are extremely useful for both synthetic and biological studies. Fischer glycosylation is the best choice for preparing these simple alkyl or aryl glycosides from free sugars. However, this procedure suffers from some serious drawbacks such as the use of a large quantity of alcohol (critical for expensive alcohols) and strong mineral acids at reflux conditions for long reaction times[108]. Thus neutralization and purification of the final product becomes an issue for these transformations.

The typical synthesis of each propargyl/azido alkyl sugar derivative is thus lengthy requires four to five steps including protection of hydroxyl, activation of sugar, glycosylation with the alcohol, displacement of leaving group by the azide and deprotection. Typical overall yields for these reactions ranges from 27-55%.

In our on going efforts to prepare oligosaccharide mimics to develop drug-like molecules, we often required glycosides as synthons. In the search for an alternative procedure for Fischer type glycosylation, we envisioned sulfuric acid immobilized on silica (H_2SO_4–silica)[109] is an efficient alternative for the required transformation using a lower quantity of alcohol and shorter reaction time. Moreover, purification would only require filtration. Here in, we have shown our results on H_2SO_4–silica catalyzed Fischer type glycosylations with various alcohols and free sugars.

3.3.1: Results and Discussion:

Most common methods for the synthesis of glycosides involve the reaction of a glycosyl donor, that is a fully protected saccharide with a leaving group at the anomeric position (i.e. peracetates glycosyl halides or trichloroactemidates), and a glycosyl acceptor frequently containing only one free hydroxyl group promoted by suitable activators[110]. The synthetic sequence is then followed by final deprotection steps to the desired glycoside. A valuable alternative is glycosylation on unprotected sugars. Fischer glycosylation has been used for decades for the synthesis of simple alkyl (methyl, ethyl, allyl) and aryl glycosides from free sugars[111-115]. The reaction is usually catalysed by acid and refluxed the alcohol acceptor as solvent. This procedure for Fischer glycosylation has a few disadvantages, including the use of strong mineral acids, a large excess of alcohol and high temperature/long reaction times, which often lead to by-product formation. Plusquellec and co-workers[116] proposed the direct O-glycosylation of reducing sugars in the presence of ferric chloride affording furanosides with organic co-solvents such as THF or dioxane in good yields. In the presence of $BF_3.Et_2O$ alkyl a-pyranosides were obtained but with moderate yield.

In our on going efforts to develop one step reaction for the synthesis of glycoside using resin-catalyzed glycosylation. Resin-catalyzed glycosylation has been known in the literature for decades, though its use has mostly been limited to the preparation of methyl glycoside. But Maha et al reported a resin-catalyzed glycosylation was used as a methodology for the synthesis of glycoside. In all cases yields were ranging from 33-56%. Which were comparable to or better than yield obtained using previously described multi-step methodology.

We have tried a resin-catalyzed glycosylation by using a resin Dowex-50. In general reaction was carried out by mixing the free sugar with anhydrous Dowex-50 (120mg/mmol of substrate) in a neat alcohol (4ml/mmol) at temp ranging from 80-90^{0}C. But In our cases with all sugar the reaction don't go for completion at the glysosylation step and a portion of starting material remain unreacted. It was initially thought that the starting material contain moisture, causing the reaction not to proceed to completion. However, drying the starting material, using increasing amount of catalyst (resin), an increased excess of alcohol, and prolonged reaction time did not significantly increased glycoside formation. Furthermore increasing the temp did not lead to product formation. Instead we observed destruction of resin with prolonged stirring at high temp (above 100^{0}C). Attempts to pull out water out of reaction mixture using vaccum distillation resulted in loss of alcohol.
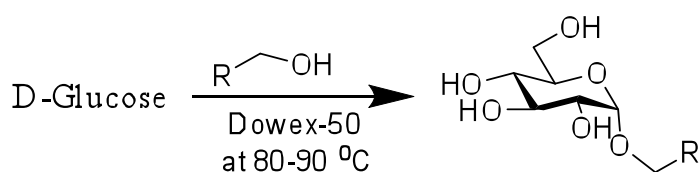
Scheme-8: Resin catalyzed glycosylation

While searching for alternative procedure for improving yields of glycoside formation we came across the method by Balaram et al. They used a sulphuric acid immobilized on silica as a catalyst for the preparation of glycoside from free sugars.In all sugar derivatives they have got good to excellent yield.Sulfuric acid immobilized on silica (H_2SO_4-silica) as an efficient alternative for required transformation using a lower quantity of alcohol and shorter reaction time. Moreever, purification would only required filteration.The general procedure for glycoylation, D-glucose (180 mg, 1 mmol) was suspended in propargyl alcohol (290µl, 5 mmol) and stirred at 65 ^{0}C.

H$_2$SO$_4$–silica (5 mg) was added and stirring was continued until all the solids had dissolved (~2.5 h). At this point, TLC (CH$_2$Cl$_2$–MeOH; 5:1) showed complete conversion of the starting D-glucose to a faster running component. After cooling to room temperature, the reaction mixture was transferred to a short (4 cm : 1 cm) silica gel column and the excess propargyl alcohol was eluted with CH$_2$Cl$_2$ (20 mL) followed by elution of the product glycoside with CH$_2$Cl$_2$–MeOH (15:1) to afford the desired propargyl glycoside in 75% yield. For detailed characterization, the product was per-O-acetylated using Ac$_2$O (4 equiv) and catalytic H$_2$SO$_4$–silica. ^{1}H and ^{13}C NMR spectroscopy of the per-O-acetylated product revealed formation of the desired glycoside in a 6:1 (α/β) ratio. The anomeric mixture was separated by flash chromatography. Although formation of furanoside and acyclic acetals in small quantities is common with this type of reaction, no such by-product was evident here.
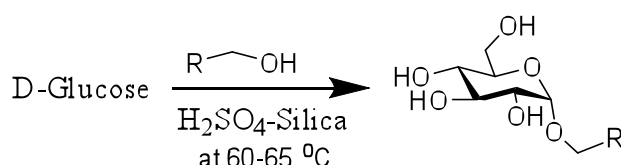
Scheme-9: H$_2$SO$_4$-Silica, at 60-65^{0}C Glycosylation

A similar reaction was performed except on this occasion the reaction mixture was allowed to stir at room temperature for 12 h after complete dissolution of the starting sugar. The product was processed in a similar way and then per-O-acetylated. After purification of the acetate, NMR showed a significant improvement in anomeric selectivity (10:1, α/β) due to the slow shifting of the equilibrium towards the thermodynamic product. The same result was obtained when the reaction was allowed to continue under heating for an additional 3 h.

Comparisons between the anomeric selectivity of propargyl glycoside prepared under

different conditions are illustrated in Table-1 below.

Table-1: comparison between anomeric selectivity obtained by different method.
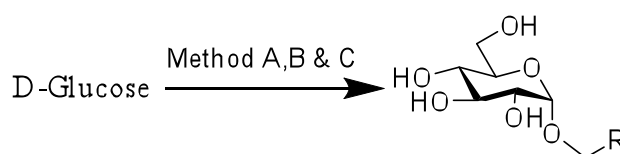
Method	α/β	Yield%
Method A: 2.5h stirring at 65 ^{0}C (until complete dissolution of starting material	6:1	75
Method B: After 2.5 h heating at 65 0C, the mixture was allowed to stir at room temp for 12 h	10:1	81
Method C: Stirring continued at 65 0C for an additional 3h after complete dissolution.	10:1	80

As a control, when the glycosylation reaction was performed without H_2SO_4–silica, no product formation was evident even after heating for 12 h at 60 ^{0}C. This confirms the utility of H_2SO_4–silica as a catalyst for the reaction.

Recently, glycosides having 2'-azidoalkyl and propargyl aglycons [117-119] have become synthetic intermediates of increased importance in chemoselective ligation reactions, hence their synthesis should require be simple and rapid.
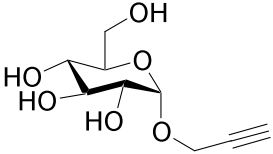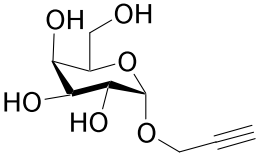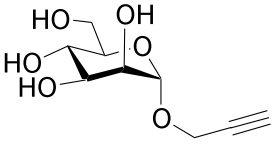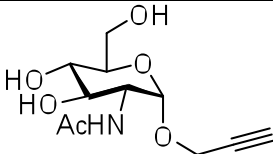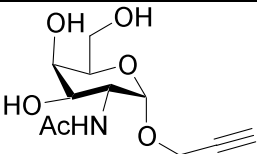
In this thesis I have propose an improved procedure for Fischer glycosylation towards propargyl and 2'-azidoethyl glycosides using H_2SO_4–silica as catalyst[118] plus ultrasounds, as illustrated in Scheme 1. This procedure is exemplified with most biologically relevant 2-acetamido-2-deoxy-monosaccharides, such as *N*-acetylglucosamine, *N*-acetylgalactosamine and *N*-acetylmannosamine. In order to show high applicability of the procedure, the glycosylation was tested also on a sample disaccharide, such as lactose.

Scheme-10: H_2SO_4-Silica catalyzed glycosylation of free sugars

Ultrasound-assisted Fischer glycosylation has been already proposed [116, 120] but to the best of our knowledge this methodology has not been used in combination with silica supported H_2SO_4 as the catalyst. In these conditions the glycosylation reaction proceeds in short times (15 min-30 min) depending on the substrates, with the only exception of lactose, which requires 12 h, while D-galactose requires the shortest reaction time (15 min). Longer reaction times observed for lactose are in agreement with other reported procedures, and are probably due to lower solubility product of the disaccharide in the acceptor alcohol. In this last case, we didn't get much improvements on reaction times, compared to already reported procedures [117-118] but we observed better yields. Results are summarised in Tables I and II.

Table –I: Propargyl glycosides from free sugar

Product	Reaction time	Yield	Ratio α/β	Literature data
1	30 min	85%	10:1	Ref.118
2	15 min	80%	10:1	Ref.118
3	30 min	90%	1:0	Ref.118
4	30 min	90%	1:0	Ref.290
5	30 min,	85%	1:0	-
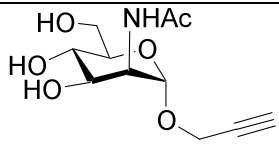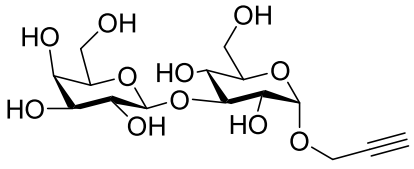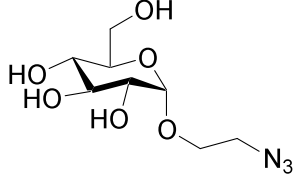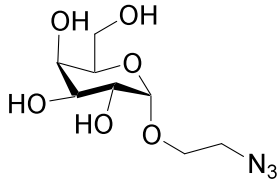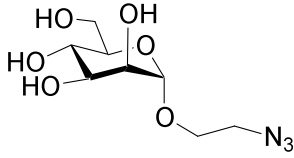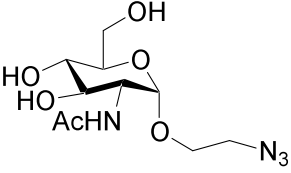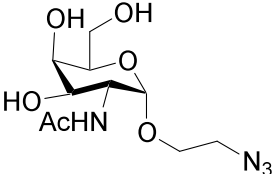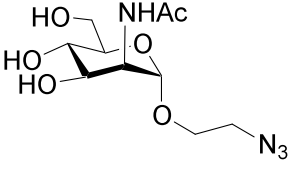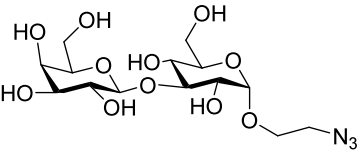
Product	Reaction time	Yield	Ratio (α/β)	Literature Data
6	30 min,	80%	1:0	-
7	12hrs	98%	1:0	-

Table-**II: 2'-Azidoethyl glycosides from free sugar**

Product	Reaction time	Yield	Ratio (α/β)	Literature Data
8	30 mins	90%	20:1	Ref.117
9	30 mins	70%	10:1	Ref. 117
10	30 mins	80%	1:0	Ref. 117

11	30 mins	75%	1:0	Ref. 117
12	30 mins	78%	1:0	Ref. 117
13	30 mins	85%	1:0	–
14	12hrs	75%	1:0	Ref. 117

In all tested cases the reaction proceeds with production of the α-glycoside as the dominant product, corresponding to the most thermodynamically stable anomer; total consumption of the starting material (except for lactose) and no significant by-products were observed, thus the yields were usually high.

Glycosides **1-4**, **8-12** and **14** have been previously characterised and NMR data are in perfect agreement with those already reported. Compounds **5, 6, 7** and **13** were unknown in the literature and full characterisation as their peracetylated derivatives is given in the experimental.

Ultrasound assisted glycosylation

Silca gel H_2SO_4 was prepared according to ref. 44. The starting material (1 mmol) was suspended in the acceptor alcohol (5 mmol) and stirred at 40 °C in ultrasound bath for 30 min. After this time, the free sugar is almost completely dissolved; at this point H_2SO_4–silica (60 mg activated silica/mmol sugar) was added. Ultrasonication was continued till the disappearance of the starting material (15-30 min), checked by TLC. The reaction mixture was recovered by filtration on a silica pad, washing with ethanol. The filtrated were evaporated and the residue (glycoside) was washed twice with diethyl ether in order to remove the unreacted acceptor (propargyl alcohol or 2-azidoethanol). Only glycosylation of lactose required longer times (12 h) and 15 mmol of alcohol acceptor per mmol of disaccharide.
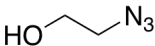
3.3.2:Experimental procedures:

Reactions were carried out using commercially available starting materials and solvents without further purification. All solvents were dried over molecular sieves, for at least 24 h prior to use. Thin-layer chromatography (TLC) was performed on Silica Gel 60 F_{254} plates (Merck) charring with a solution containing conc. H_2SO_4/EtOH/H_2O in a ratio of 5:45:45 or with an oxidant mixture composed of $(NH_4)Mo_7O_{24}$ (21 g), $Ce(SO_4)_2$ (1 g), conc. H_2SO_4 (31 ml) in water (500 ml). Flash column chromatography was performed on silica gel 230–400 mesh (Merck). NMR spectra were recorded at 400 MHz (^{1}H) 100.57 MHz (^{13}C) on a Varian Mercury instrument. Chemical shifts are reported in ppm downfield from TMS as an internal standard; J values are given in Hertz. All compounds have been characterized by NMR spectroscopy as their peracetylated derivatives. Glycosides **1-4**, **8-12** and **14** have been previously characterised and NMR data are in perfect agreement with those already reported (references to literature are reported in Tables I and II, next section). Key data are given for unknown compounds.

Preparation of H_2SO_4–silica:

 To a slurry of silica gel (10 g, 200–400 mesh) in dry diethyl ether (50 mL) was added commercially available conc. H_2SO_4 (3 mL) with shaking for 5 min. The solvent was evaporated under reduced pressure resulting in free flowing H_2SO_4–silica which was then dried at 110 ^{0}C for 3 h.

Synthesis of Azidoethanol:-

2-bromo-1-ethanol (5g, 36 mmol) and sodium azide (3.83 g, 59 mmol) were dissolved in a mixture of acetone (60 mL) and water

(10 mL) and the resulting solution was refluxed overnight. Acetone was then removed under reduced pressure, 50 mL of water were added and the mixture was extracted with diethyl ether (3 x 50 mL). The organic layers collected were dried over MgSO4 and, after removal of the solvent under reduced pressure, 2-azido-1-ethanol was isolated as colourless oil (2.82 g, 77%). ∂H(300 MHz, CDCl$_3$)1.68 (1H, s, CH$_2$-OH), 3.38 (2H, t, J 6.6, CH$_2$-N$_3$), 3.67 (2H, t, J 6.3, CH$_2$-OH). ∂C(300 MHz, CDCl$_3$) 31.32 (CH$_2$-CH$_2$), 48.27 (CH$_2$- N$_3$), 59.48 (CH$_2$-OH). max/cm-1 3331, 2945, 2881, 2087, 1455, 1258, 1044, 955, 900.

Propargyl 2-acetamido-3,4,6-tri-*O*-acetyl-2-deoxy-α-D-galactoside (5) :
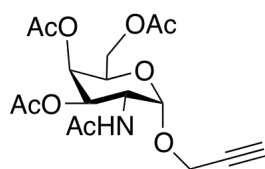
In a commercially available 2-acetyl-galactoseamine (308.4 mg, 1 mmol) added propargyl alcohol (290µl, 5 mmol) at rt and kept in ultrasonic for agitation for 5 min till all starting get dissolve then added a catalyst H$_2$SO$_4$-Silica (5mg). After 15 min TLC (MeOH: CH$_2$Cl$_2$, 2:5) shows a completion of reaction with higher running compound. The reaction is quenche with sodium bicarbonate (Na$_2$CO$_3$) and then was washed with diethyl ether (3 x 50 mL) to remove unreacted reagent. Propargyl 2-acetamido-2-deoxy-α-D-galactoside was isolated as white solid (295mg, 85%). The product was dissolved in dry pyridine and Ac$_2$O (1.1 equiv/ OH) was added. After complete consumption of the starting material, the mixture was diluted with EtOAc, then extracted twice with 5% Acq. HCl. The organic layers were collected, dried over dry Na$_2$SO$_4$, filtered and concentrated to dryness. The residue was purified by flash chromatography using EP/EtOAc mixtures as eluent to obtained **5.** ^{1}H NMR (CDCl$_3$, 400 MHz) δ: 4.53 (d, 1H, J 9.3 Hz, NH), 5.44. (t, 1H, J 9.5Hz, *H-3*), 4.73 (t, 1H, J 9.5 Hz, *H-4*), 4.76 (d, 1H, J 8.7 Hz, *H-1*), 4.44 (dt, 1H, J 9.5 Hz, 8.7 Hz, *H-2*), 4.40 (dd,

1H, J -11.5 Hz, 9.9 Hz, *H-6a*), 4.06 (dd, 1H, J 1.5 Hz, -11.5 Hz, *H-6b*), 4.34 (m, 1H, J

11.0 Hz, 9.9 Hz, *H-5*), 4.36 (m, 2H, CH_2-C≡CH), 2.75 (t, 1H, CH$_2$-C≡C*H*), 2.03,

2.02, 2.01 (s, 9H, 3 · COCH_3) 2.07 (s, 3H, NHCOCH$_3$). ^{13}C NMR (CDCl$_3$, 101 MHz)

δ: 171.7 (NH*CO*CH$_3$), 100.3 (*C-1*), 79.8 (CH$_2$-*C*≡CH,), 75.8 (CH$_2$-C≡*CH*), 59.5

(*CH$_2$*-C≡CH), 62.6 (*C-6*), 53.9 (*C-2*), 69.2(C-4), 70.4 (C-3), 71.1(C-5), 21.8

(NHCOCH_3), 21.8, 20.3, 19.7 (3 XCOCH_3). Exact mass: Calcd for C$_{11}$H$_{17}$O$_6$N:

259.26; found m/z (M + H) 260.25.

Propargyl 2-acetamido-3,4,6-tri-*O*-acetyl-2-deoxy-α-D-mannoside (6)

In a commercially available 2-acetyl-mannoseamine (308.4

mg, 1mmol) added propargyl alcohol (290µl, 5 mmol) at rt

and kept in ultrasonic for agitation for 5 min till all starting get

dissolve then added a catalyst H$_2$SO$_4$-Silica (5mg). After 30 min TLC (MeOH:

CH$_2$Cl$_2$, 2:5) shows a completion of reaction with higher running compound. The

reaction is quenche with sodium bicarbonate (Na$_2$CO$_3$) and then was washed with

diethyl ether (3 x 50 mL) to remove unreacted reagent. Propargyl 2-acetamido-2-

deoxy-α-D-mannoside was isolated as white solid (279mg, 80%). The product was

dissolved in dry pyridine and Ac$_2$O (1.1 equiv/ OH) was added. After complete

consumption of the starting material, the mixture was diluted with EtOAc, then

extracted twice with 5% Acq. HCl. The organic layers were collected, dried over dry

Na$_2$SO$_4$, filtered and concentrated to dryness. The residue was purified by flash

chromatography using EP/EtOAc mixtures as eluent to obtained **6**.^{1}H NMR (CDCl$_3$,

400 MHz) δ: 6.92 (d, 1H, *NH*), 5.40. (t, 1H, J 11.0Hz, *H-3*), 4.91 (t, 1H, J 11.0 Hz, *H-

4*), 4.82 (d, 1H, J 0.5 Hz, *H-1*), 4.44 (dt, 1H, J 5.7 Hz, 0.53 Hz, *H-2*), 4.45 (dd, 1H, J

9.7 Hz, -11.5 Hz, *H-6a*), 4..08 (dd, 1H, J 1.50 Hz, -11.5 Hz, *H-6b*), 4.41 (m, 1H, J

10.3 Hz, 9.7 Hz, *H-5*), 4.44 (m, 2H, C*H₂*-C≡CH), 2.71 (t, 1H, CH₂-C≡C*H*), 2.03, 2.02, 2.4 (s, 9H, 3 COC*H₃*) 2.09 (s, 3H, NHCOC*H₃*).^{13}C NMR (CDCl₃, 101 MHz) δ: 172.3 (NH*C*OCH₃), 100.3 (*C*-1), 79.8 (CH₂-*C*≡CH), 75.8 (CH₂-C≡*C*H) 59.5 (*C*H₂-C≡CH), 62.6 (*C*-6), 53.8 (*C*-2), 69.3 (C-4), 70.4 (C-3), 71.0 (C-5),   19.8 (NHCO*C*H₃), 20.3, 20.3, 20.8 (3 XCO*C*H₃). Exact mass- Calcd for C₁₁H₁₇O₆N : 259.26; found m/z (M + H)-260.30.
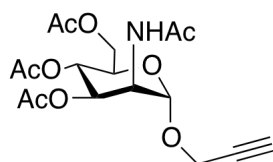
2'-Azidoethyl 2-acetamido-3,4,6-tri-*O*-acetyl-2-deoxy-α-ᴅ-mannoside (13)
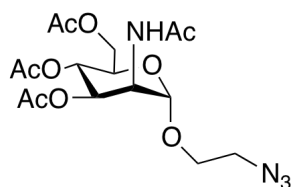
In a commercially available 2-acetyl-mannoseamine (308.4 mg, 1mmol) added azidoethanol (440 μl, 5 mmol) at rt and kept in ultrasonic for agitation for 5 min till all starting get dissolve then added a catalyst H₂SO₄-Silica (5mg). After 30 min TLC (MeOH: CH₂Cl₂, 2:5) shows a completion of reaction with higher running compound. The reaction is quench with sodium bicarbonate (Na₂CO₃) and then was washed with diethyl ether (3 x 50 mL) to remove unreacted reagent. 2'-Azidoethyl 2-acetamido -2-deoxy-α-ᴅ-mannoside was isolated as off white solid (248mg, 85%). The product was dissolved in dry pyridine and Ac₂O (1.1 equiv/ OH) was added. After complete consumption of the starting material, the mixture was diluted with EtOAc, then extracted twice with 5% Acq. HCl. The organic layers were collected, dried over dry Na₂SO₄, filtered and concentrated to dryness. The residue was purified by flash chromatography using EP/EtOAc mixtures as eluent to obtained **13**.^{1}H NMR (CDCl₃, 400 MHz) δ: 5.70 (d, 1H, N*H*), 5.53. (t, 1H, J 8.0 Hz, *H-3*), 4.94 (t, 1H, J 8.0 3.0,Hz, *H-4*), 6.02 (d, 1H, J 1.9 Hz, *H*-1), 4.44 (dt, 1H, J 3.7 Hz, 1.9 Hz, *H*-2), 4.37 (dd, 1H, J 0.5 Hz, 3.5 Hz, *H*-6a), 4..14 (dd, 1H, J 1.1 Hz, 2.5 Hz, *H*-6b), 4.21 (m, 1H, J 3.0 Hz, 3.5, 2.4 Hz, *H*-5), 4.03 (t, 2H, , J 7.4 Hz ,C*H₂*), 3.58 (t, 2H, , J7.4 Hz C*H₂*), 2.07,

2.06, 2.6 (s, 9H, 3 · COCH_3) 2.04 (s, 3H, NHCOCH_3).^{13}C NMR (CDCl$_3$, 101 MHz) δ: 172.3 (NHCOCH$_3$), 101.9 (C-1), 63.6 (CH$_2$), 62.6 (CH$_2$) 62.6 (C-6), 53.7 (C-2), 69.3 (C-4), 70.4 (C-3), 71.0(C-5), 21.8 (NHCOCH$_3$), 21.2, 21.3, 20.7 (3 XCOCH$_3$). Exact mass-Calcd for C$_{11}$H$_{17}$O$_6$N : 290.126; found m/z (M + H)-291.20.

Propargyl 2',3',4',6',2,4,6-Octa-*O*-acetyl-α-D-lactoside (7)
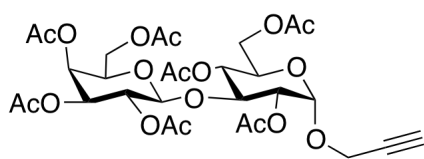
In a commercially available α-D-Lactose (342.3 mg, 1mmol) added azidoethanol (440 µl, 5 mmol) at rt and kept in ultrasonic for agitation for 5 min till all starting get dissolve then added a catalyst H$_2$SO$_4$-Silica (5mg). After 12 hrs TLC (MeOH: CH$_2$Cl$_2$, 2:5) shows a completion of reaction with higher running compound. The reaction is quenche with sodium bicarbonate (Na$_2$CO$_3$) and then was washed with diethyl ether (3 x 50 mL) to remove unreacted reagent. Propargyl-α-D-lactoside was isolated as pale yellow liquid (390mg, 98%). The product was dissolved in dry pyridine and Ac$_2$O (1.1 equiv/ OH) was added. After complete consumption of the starting material, the mixture was diluted with EtOAc, then extracted twice with 5% Acq. HCl. The organic layers were collected, dried over dry Na$_2$SO$_4$, filtered and concentrated to dryness. The residue was purified by flash chromatography using EP/EtOAc mixtures as eluent to obtained **7**.^{1}H NMR (CDCl$_3$, 400 MHz), δ (ppm): δ 6.28 (d, J = 3.5 Hz, 1H, H-1), 4.53 (d, J = 7.8Hz, 1H, H-1'), 5.43 (dd, J2, 3 = 9.7 Hz, J3, 4 = 9.7 Hz, 1H, H-3), 4.98 (dd, J$_{2-3}$ = 10.3 Hz, J$_{3-4}$ = 3.2 Hz, 1H, H-3'), 3.85 (dd, J$_{3-4}$ =9.73 Hz, J$_{4-5}$ = 9.64Hz, 1H, H-4), 5.34 (d, J = 3.1Hz, 1H, H-4'), 5.00 (dd, J$_{2-3}$ = 10.2 Hz,J$_{1-2}$ = 3.5 Hz, 1H, H-2), 5.11 (dd, J$_{2-3}$ = 10.1 Hz, J$_{1-2}$ = 8.0 Hz, 1H, H-2'), 4.44 (d, J = 11.6 Hz, 1H, H-6b), 4.09 –4.17 (m, 3H, H-6a, H-6'a,H-6'b) , 3.94 (dd, J$_{5-6}$ = 6.7 Hz, J$_{5-6a}$ = 6.6Hz, 1H, H-5'), 2.44(CH$_2$-C≡CH, 1H),

2.05, 2.04, 1.97, (7XCOCH$_3$). ^{13}C NMR (CDCl$_3$, 101 MHz) δ: 168.66, 168.87, 169.36, 169.65, 169.75, 169.87, 170.04 (2Ac), 100.81 (C-1'), 88.64 (C-1), 75.45 (C-4), 75.8 (CH$_2$-C≡CH),79.8 (CH$_2$-C≡CH),70.70 (C-3'), 70.41 (C-5', C-5), 69.32 (C-3), 69.14 (C-2), 68.88 (C-2'), 66.44 (C-4'), 61.27 (C-6), 60.63 (C-6'), 20.17 (3Ac), 20.32 (4Ac). Exact mass-Calcd for C$_{29}$H$_{38}$O$_{18}$: 674.60; found m/z (M + H) 675.71.

We had tried fisher type glycosylation on free sugars i.e monosaccharide and also disaccharide i.e lactose. We tried different acidic catalyst a) Dowex-50 resin at 80-90 ^{0}C , b) Sulfuric acid immobilized silica at 60-65 ^{0}C) Sulfuric acid immobilized silica with Ultrasonic at 35-40 ^{0}C. We showed that among all three method ultrasound assisted Fischer glycosylation catalysed by sulphuric acid immobilized on silica gel is an efficient method for the preparation of 2'azidoalkyl and propargyl glycosides, giving better yields and shorter reaction times then previously discuss and reported procedures, adding an improved tool for glycotechnology. The reported examples involve significant monosaccharides, usually engaged in relevant biological interactions.

Chapter-4

Synthetic approach towards monomer building blocks of HA

4.1: INTRODUCTION

Hyaluronic acid or hyaluronan (recent acronym HYA) is a ubiquitous glycosaminoglycan of high molecular weight acting as a structural component of extracellular matrices that mediates cell adhesions. The interest of the biomedical community into this biomacromolecule is constantly rising, as demonstrated by the high number of publications on this topic.

Most of the current applications of HYA in the biomedical field are based on its physical properties (hydration, viscosity, space filling), but it is nowadays clear that new and interesting opportunities araise from the exploitation of its specific and multifacet bilogical roles. This concept is excellently pointed out in a paper by Chen and co-workers[121], who state that "Currently HYA-based medical products are mostly classified as medical devices, utilising the physical attributes of HYA to achieve their intended functions. No doubt when the biology of HYA becomes better known, applications will also be developed to utilise its biological functions". Here I have given an overview of HYA biological roles, highlighting its fundamental interactions with proteins, and applications in medicinal chemistry. The use of HYA motifs or fragments of defined chemical structure and its mimetics will be described, covering the literature appeared since 2000. No mention will be made on applications of HYA based on its physical properties.

4.2: **Hyluronan: a simple picture**

Chemical Structure: Hyaluronan is a major carbohydrate component of the extracellular matrix and can be found in skin, joints, eyes and many other organs and tissues; it was originally discovered and biochemically purified from the vitreous

body of the eye in 1934[122], and its chemical structure solved in 1954[123]. Hyaluronic acid is a simple linear copolymer made of repeating units of glucuronic acid β(1-3) linked to *N*-acetyl glucosamine in turn β(1-4) linked to the subsequent unit, Fig. (**1**).
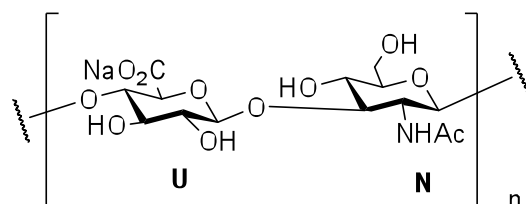
Fig-**1**: Disaccharide repeating unit of HYA.

This sequence is completely conserved throughout a large span of the evolutionary tree, indicating its fundamental biological importance. Hyaluronan is a member of the glycosaminoglycan (GAG) family[124], but it differs in many ways from other GAGs (Table 1).

Table 1. Different Classes of GAGs and Their Disaccharide Building Blocks.

Category	Disaccharide	U	N	Modification
Heparin / Heparan	$U_{2x\ (\alpha/\beta1,4)}N_{NY,3X,6X(\alpha1,4)}$	IdoA/GlcA	Glucosamine	X, sulfated; Y acetylated/ sulfated
Chondroitin / Dermatan	$U_{2X,\ 3X\ (\alpha/\beta1,3)}$ $N_{NAc,4X,6X(\alpha1,4)}$	IdoA/GlcA	Galactosamine	X, sulfated; 3-O, sulfated only for GlcA
Keratan	$U_{6X\ (\beta1,4)}, N_{NAc\ 6X(\beta1,3)}$	Gal	Glucosamine	X, sulfated
Hyaluronic Acid	$U_{(\beta1,3)}, N_{NAc\ 6X(\beta1,4)}$	GlcA	Glucosamine	None

D-Glucosamine
X= H or SO_2^-
Y= $COCH_3$ or SO_3^-

D-Galactosamine
N-acetylated
X= H or SO_3^-

L-Iduronic acid
X= H or SO_3^-

D-Glucuronic Acid
X= H or SO_3^-

D-Galactose
X= H or SO_3^-

IdoA = α-L-iduronic acid; GlcA or G = β-D-glucuronic acid, N = either α/β-D-glucosamine, or β-D-galactosamine depending on the GAG class; Gal = β-D-Galactose. Acetylation [$COCH_3$] is indicated using Ac and sulfation [SO_3^-] using S.
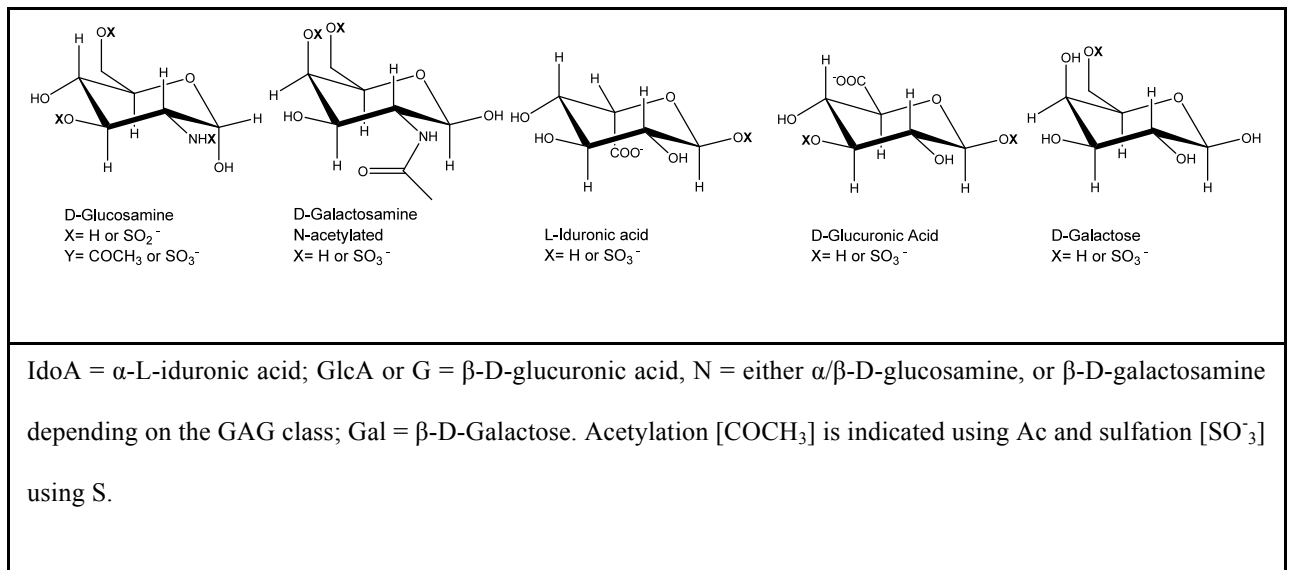
With respect to other GAG, HYA has the following peculiar features. First HYA is huge, usually with a molecular weight between 10^3 and 10^4 KDa and an extended length of 2–25 μm (the lenght of the unit is about 1 nm)[125]. Second, unlike other GAGs, HYA contains no sulfate groups or epimerized uronic acid residues. Third, the mechanism of synthesis of HYA is unique, being synthesized at the inner face of the plasma membrane as a free linear polymer, in contrast to the other glycosaminoglycans which are synthesized by resident Golgi enzymes and covalently attached to protein *cores*. Finally, HYA is most likely elongated at the reducing rather than at the non-reducing terminus.

Hyaluronan metabolism: It has been established that a single protein, hyaluronic acid synthases (HASs)[126-127] is responsible for both of the glycosyltransferase activities required for HYA synthesis. The synthesis of an average HYA chain, which contains ten thousand disaccharide-repeating units, represents considerable energy consumption for the cell. To form a single chain, around fifty thousand ATP equivalents, twenty thousand NAD cofactors, and ten thousand acetylCoA groups are

required, in addition to the monosaccharide components. Thus, it is not surprising that the synthesis of HYA is tightly regulated in the majority of cells. Hyaluronan is unique among matrix macromolecules since it is directly secreted into the extracellular space after it is being synthesised. Newly synthesized hyaluronan, protruding directly into the extracellular environment, provides a highly hydrated microenvironment at the sites of synthesis. This may represent a dynamic role by which hyaluronan synthesis may facilitate cell detachment during mitosis and migration. HASs, are integral plasma membrane glycosyltransferases that are proposed to coordinately polymerize and translocate HYA out of the cell into the extracellular matrix[128]. Three HASs, encoded by three separate but related genes, have been identified in vertebrates[129]. Any one of these synthases is capable of driving the *de novo* synthesis of HYA in transfected mammalian cells. Identification of the HYA synthases has provided an important jump-start to HYA biology and allows to directly manipulate a given cell's ability to synthesize HYA, either positively or negatively.

In *vivo*, catabolism of HYA is operated by the action of oxygen free radicals[130] and Hyaluronate Lyase enzymes (HYALs)[131]. Most HYA (80–90%) is cleared from the circulation by endocytosis in the lymph nodes and liver, *via* the HYA receptor for endocytosis, HARE[132]. Other HYA receptors including CD44, LYVE-1, RHAMM and layilin[133] have local, tissue specific roles in HYA endocytosis. This is particularly important in cartilage and bone where HYA is immobile and cannot reach the lymphatics. Once internalised, HYA is degraded in lysosomes by HYALs and exoglycosidases. Mammalian HYALs are endo-β-*N*-acetylhexosaminidases that catalyse the hydrolysis of HYA; some also degrade the related glycosaminoglycans,

chondroitin sulphate (CS) and dermatan sulphate. HYALs degrade hyaluronan, predominantly unsaturated disaccharide units, thereby destroying the normal connective tissue structure and exposing the tissue cells to various endo- and exogenous factors, including bacterial toxins[134].

Hyaluronan fragments: size-specific biological roles?

Despite their presumed importance for degrading HYA in development, morphogenesis, wound healing, inflammation and tumour metastasis, there are large gaps in what is known about HYALs. In addition, products of HYAL activity, that is HYA fragments, the existence of which in vivo is still debated, are the subjects of a vast literature describing their effects on numerous cellular events and disease processes, including those of the skeletal system[135]. In vivo HYA oligosaccharides of low relative molecular mass are inflammatory, angiogenic and immunomodulatory, in contrast to high molecular mass HYA fragments that are non-inflammatory, non-angiogenic and non-immunomodulatory[136]. Nevertheless, the sheer volume of data, coupled with the reproducible effects of specific fragments on critical biological processes such as angiogenesis, provide compelling reasons to believe that endogenous fragments do exist. HYA fragments may be short-lived and therefore difficult to detect, even if few studies have successfully identified HYAL-mediated HYA fragmentation *in vivo*[137]. For example, HYA synthesis and degradation are closely regulated in skeletal tissues and aberrant synthetic or degradative activity causes disease, hence HYA appears to regulate bone remodeling by controlling osteoclast, osteoblast and osteocyte behaviour. Bone remodelling involves resorption, activation, followed by new bone formation, which engages critical, local interactions between osteoblasts and osteoclasts. Non-contact co-cultures of osteoclasts with

osteoblasts, or with osteoblast-conditioned medium, showed that HYA facilitates interactions between osteoblasts and osteoclasts regulating osteoclast responses to parathyroid hormone (PTH). Exogenous HYA also promotes stromal cell proliferation and osteogenic gene expression, indicating a likely role in pre-osteoblast recruitment, proliferation and differentiation and osteoclast crosstalk. Toole and co-workers[138] showed that different developmental processes shared a common time sequence of HYA synthesis and subsequent removal by hyaluronidase, with a clear indication that accumulation of HYA coincided with periods of cellular migration in the tissue.

A dilemma for researchers at present is how to interpret increased HYAL expression. One interpretation is that bioactive HYA fragments (created by HYALs) have important physiological roles. Another interpretation is that removing HYA is important or necessary for the system. The latter interpretation is more compelling when increased HYAL activity is coordinated with decreased HAS activity, as in precartilage condensations of the skeletal elements[139]. These interpretations could be equally important and there is no reason why they should be mutually exclusive.

Hyaluronan conformations: structure-specific biological roles?

HYA physiological properties are controlled by molecular mass dependent transitions between tertiary structures (e.g., β sheets) and 2-fold helices, referred to as reversible "denaturation", which is central to HYA solution behavior. Aggregation of HYA oligosaccharides might be possible among oligomers of >20 disaccharides (MW ≈ 8000), while above 300 disaccharides (MW ≈ 120000) HYA chains are clearly aggregated. Hence, biological properties of HYA are controlled by its reversible tertiary structure[140]: bioactivity disappears whenever assembly in tertiary structure

69

masks direct communication between HYA 2-fold helices and the surrounding milieu and is made available whenever the tertiary structure denatures, releasing, in this way, HYA chains. In summary, HYA biological properties are controlled by molecular weight-dependent transitions between tertiary structures and 2-fold helices. Interestingly, Arrhenius plots show that HYA tertiary structures are on the edge of instability under physiological conditions, ready to switch from bioactivity to bioinertness as a response to external stimuli.
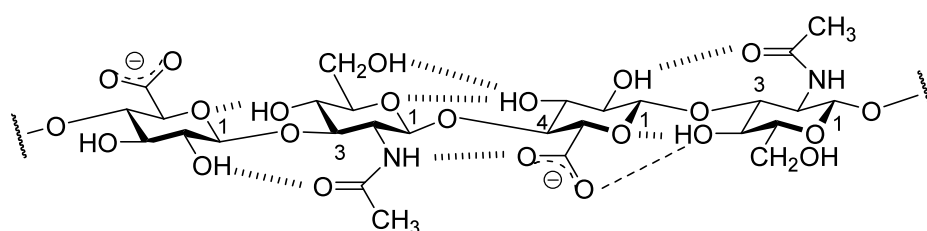
Fig-**2:** Extensive hydrogen bonding of a tetrasaccharide fragment of HYA comprising two repeating disaccharides, that help to maintain the 2-fold helix. The direct H bond between the acetamido NH and carboxylate seen in dimethyl sulfoxide solution is largely replaced in aqueous solution by a water bridge.

4.2.1: **Hyaluronan: Roles of a key extracellular molecule:**

From this concise picture, one can argue that the fascination, and opportunities of this macromolecule lie in the sharp contrast between the apparent simplicity of the primary molecular structure and the multiplicity of the roles HYA plays in cell and tissue biology. Learning how Nature can store so much information in such a simple structure can be a valuable tool in the design of bioactive molecules for applications in medicinal chemistry. Hyaluronan has multifaceted roles ranging from a purely structural function in the extracellular matrix to developmental regulation *via* control of the tissue macro- and microenvironments, and direct receptor mediated effects on gene expression.

The molecular functions of HYA fall into four partially overlapping categories[141].

i) First, HYA occupies an enormous hydrodynamic domain that greatly influences the hydration and physical properties of tissues.

ii) Second, it interacts with other ECM macromolecules, including the proteoglycans aggrecan and versican; these interactions are essential to the structure and assembly of several tissues.

iii) Third, HYA is an extracellular signalling molecule; interacting with cell surface receptors and thereby influencing cell behavior.

iv) Forth, HYA has also a significant presence and novel functions inside cell[142-143].

Short overview on physicochemical properties

The effects of HYA on cellular events were initially ascribed entirely to its physical interactions, and the evidence of extensive intramolecular hydrogen bonding[144], Fig. 2, were in agreement with a general view of HYA as an inert biomolecule[145]. This was considered an important property for the suggested role of HYA as a space-filling molecule. HYA is one of the most hygroscopic molecules in Nature. A detailed description of the physicochemical properties of hydrated, free colloidal hyaluronan are beyond the scope of the present review, and will be only summarised, while reviewed extensively elsewhere[146].

Hyaluronan's viscoelasticity is particularly relevant in its cushioning and lubricating effects as a component of the eye (aqueous humor) and synovial fluid. Because of its unique physicochemical properties, and, most importantly, nonimmunogenicity of the highly purified form, hyaluronan has already found medical applications for many

years, primarily in ocular and joint surgery[147-148]. More recently, the reported benefits of exogenously-applied hyaluronan in tissue repair have found application in hyaluronan-based biomaterials developed for tissue repair purposes[149].

Hyaluronan solutions are highly osmotic[150], a property further increased in many tissue fluids by the presence of serum albumin[151]. For example, in the skin, this property is likely to be relevant in controlling tissue hydration during periods of change, such as embryonic development, and during the inflammatory process (such as response to tissue injury) when hyaluronan levels are elevated. This is also of particular relevance for cell proliferation and migration, when hyaluronan synthesis contributes to local foci of tissue hydration. This results in weakening of cell anchorage to the extracellular matrix, allowing temporary detachment to facilitate cell migration and division[152]. The highly viscous nature of hyaluronan also contributes to retardation of viral and bacterial passage through the hyaluronan-rich pericellular zone[153]. Hyaluronan is fully ionized in physiological conditions. As a pericellular matrix, it may have effects on ion flux which are important in cellular signaling through membrane ion channels.

Since many HYA properties rely on its physicochemical properties, and due to the fact that native hyaluronic acid has limited use due to a short turnover rate and poor mechanical stability, chemically modified derivatives are therefore developed to obtain biomaterials with tailored properties. This is generally achieved by targeting the carboxylic acid on the glucuronic acid moiety or the hydroxyl groups found on both moieties of the disaccharide repeating unit. Prolonged *in vivo* residence time and improved mechanical properties can be obtained by cross-linking to form hydrogels

or by adding groups that lower the aqueous solubility. Several strategies to functionalize hyaluronic acid have been developed over the past decades[154-155].

4.2.2 : HYA-protein interactions: a relevant extracellular signalling molecule

According to the proposed structure, almost every polar group in HYA is involved in intramolecular interactions, Fig. 2, making potential interactions with other species less likely. This view came to an end by 1972, with the discovery of proteins that can specifically interact with HYA[156-157]. HYA was shown to aggregate cartilage proteoglycans[158-159] by specific binding to the *N*-terminal globular part of the proteoglycan, and a link protein[160]. The shift of the paradigm of HYA as an inert material to a biologically active molecule was then completed by the first demonstration that HYA activates signaling pathways[161]. Generally, HYA-mediated cell surface signaling events are correlated with either cell migration or cell proliferation responses.

It's now evident that the diverse biological roles of hyaluronan result, in part, from its solution properties, as described above, and also from the large number of hyaluronan-binding proteins[162] (hyaladherins/hyalectins) that might be able to capture and stabilise different conformers of the polysaccharide.

Interactions with ECM macromolecules

In the ECM, HYA is often bound by other matrix molecules such as the hyalectin class of proteoglycans. Small, globular Link proteins often stabilize HYA–hyalectin interactions. Actually, the majority of extracellular HYA-binding proteins belong to the Link protein superfamily. Members of this superfamily contain a conserved disulfide-linked domain of roughly 100 residues termed the Link module, which

73

resembles the sugar-binding domain of C-type lectins[163], from which it probably evolved[164].

The interaction between HYA and its intimately associated molecules is intertwined with their normal functions. Removing one part of the equation causes unraveling of tightly controlled biological systems, resulting in disaster. For instance, mice lacking cartilage Link protein, the protein that stabilizes the aggregate of aggrecan and HYA, died shortly after birth due to severe defects in cartilage development[165]. Localized synthesis of HYA may be critical for tissue volume changes and the creation of cell-free spaces. The stability of these cell-free spaces probably is dependent upon HYA–hyalectin interactions. HYA is able to stimulate cell migration indirectly by providing an extracellular or pericellular environment conductive to migration. This is partly dependent on its ability to bind to and complex with hyalectins, such as versican[166] and to modify the properties of other matrices, such as those composed of collagen and fibrin[167].

The picture emerging for hyalectins is that there is considerable diversity in the way that they bind hyaluronan[168]. A reasonable explanation for the diversity in hyaluronan–protein interactions is that hyalectins have evolved specific binding sites in order to capture different conformations of the glycosaminoglycan. For example, in TSG-6 (the secreted product of tumour necrosis factor stimulated gene-6), the link module alone supports the interaction with hyaluronan[169]. Aggrecan, an important component of cartilage extracellular matrix, uses an even larger domain that is composed of two contiguous link modules, both of which are necessary for high-affinity hyaluronan binding[170]; a similar domain is found in cartilage link protein and in the family of aggrecan-like proteoglycans[171].

74

Table 2. Some examples of hyaldherins and minimum sequence length of the HYA disaccharide repeating unit required for recognition[a]

Protein	N° of HYA disaccharides required	Features of the HYA binding domain
TSG-6	3	link module 90 amino acids
stabilin-1	3	link module 90 aminoacids
CAB61358	3	link module, 90 aminoacids
CD44	3	link module + extensions 160 aminoacids
Lyve-1	3-5	link module +extensions 160 aminoacids
Link protein	3-5	2 link modules 200 aminoacids
Aggrecan	5	2 link modules 200 aminoacids
Versican	5	2 link modules 200 aminoacid

Significantly, the size of the ligand-binding domain correlates broadly with the minimum length of hyaluronan recognised by the proteins of the link module superfamily[172], Table 2.

HYA repeating units involved range from three to five disaccharides, that is, the interaction involves continuous HYA segments of around 1200-2000 Da. It has been shown that the molecular basis of the link module-HYA interaction involves ionic interaction between HYA carboxylates and basic amino acids. In the case of CD44[172] and TSG-6[173-174], two arginines and two tyrosines play a critical role[175]. In general, specific interaction with HYA is driven and controlled by local ionic interaction between HYA carboxylate and cationic amino acids, even though both involved molecules can be depicted as highly negatively charged colloidal particles. Actually, an extensive network of interactions maintains the association of the receptors with HYA, and the overall energetics of the interactions is finely balanced, to the point that the loss of a single hydrogen bond or ionic interaction can be enough to abolish binding[176]. In addition, analysis of other link module sequences led to the prediction that, although the location of the hyaluronan-binding site might be conserved across the "link-module" superfamily, the residues that form the interaction surface might be distinct in each protein.

A significant finding arising since the first studies on hyalectins in general, and of CD44 in particular, is that the HYA receptor interaction is cooperative in nature. Already in the pioneering work by Underhill and Toole it was suggested that a single molecule of HYA could bind to multiple cell surface receptors, as pointed out by molecular weight-dependent binding inhibition studies[177-178].

4.3: HYA oligomers, mimetics and applications

Currently, hyaluronan-based products are designed to be used as medical devices because of their physicochemical properties; in addition, the two most important receptors of HYA, CD44 and RHAMM, are overexpressed by various tumors (i.e. epithelial, ovarian, colon, stomach, and acute leukemia). Consequently, these tumor cells show enhanced binding and internalization of HYA[179]. The high tumor specificity of the HYA–CD44 interactions and high biocompatibility of HYA prompted the design and synthesis of tumor-targeting bioconjugates bearing HYA and cytotoxic agents, that after internalisation into cancer cells through CD44 receptor-mediated endocytosis, release intracellularly the active drug [180].

As HYA biological role becomes better understood, simpler molecules or mimetics could be developed that support these processes as well. Blocking CD44, or regulation of other hyalderine function may have particular utility in the treatment of major inflammatory diseases, including chronic inflammation, and in the inhibition of tumor metastasis.

4.3.1: General method for HYA-synthesis

As described above, several studies have demonstrated that short oligosaccharides are the minimal feature necessary for recognition and binding by HYA proteins. The chemical synthesis of small HYA oligomers permits detailed studies of how structure influences function at a molecular level. In addition, the solution conformations of small, chemically synthesized HYA fragments are more easily characterized than that of the native polymeric form. Hence, in recent years there is growing interest in the synthesis of fragments and/or mimics of HYA as potential ligands that would bind to

and activate cell-surface HYA receptors. Such analogues could have important therapeutic uses in the treatment of cancer, wound healing, and arthritis, especially if such ligands are be designed to be resistant to degradation *in vivo*[181].
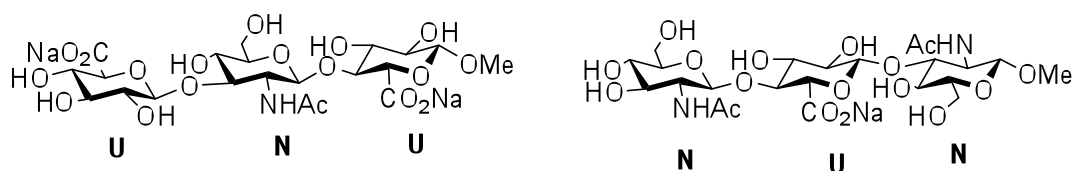
Fig-**3**: Structure of the two synthetic hyaluronan trisaccharides.

Several syntheses of HYA oligosaccharides have been reported to date[182]. Among these, Slaghek and Ogawa constructed a tetrasaccharide derivative with D-glucuronic acid at the reducing end[183] as well as a series of di-, tri-, and tetrasaccharides with *N*-acetyl-D-glucosamine at the reducing end[184-185]. These reported derivatives incorporated a *p*-methoxyphenyl ether moiety at C-1 of the reducing sugar that does not accurately mimic native HYA fragments. In this regard, *O*-methyl is a better structural mimic of native HYA because *O*-methyl is the smallest functional group available to minimize any potential secondary interactions and anomerization. Among the β-methyl HYA derivatives reported are the β(1,4) disaccharide[186], a series of tetra-, hexa-, and octasaccharides with D-glucuronic acid at the reducing end[187] and more recently, β-methyl HYA trisaccharides, UNU **1**, and NUN **2**, Fig. (**3**)[188], which represent the smallest fragments incorporating all of the structural features of polymeric hyaluronan.

Construction of the UNU trisaccharide utilized TMSOTf mediated glycosylation of trichloroacetimidate donor **4** with suitably protected β-(1,4) disaccharide **5**, obtained by glycosylation of donor **6** and methyl 2,3-di-*O*-benzyl-6-*O*-(4-methoxybenzyl)-*β*-

D-glucopyranoside **7** as acceptor (Scheme **1**). Partial deprotection of the trisaccharide, followed by the regioselective oxidation of the primary hydroxyls to the corresponding diacid by TEMPO, and finally last deprotections afforded the desired UNU trisaccharide.
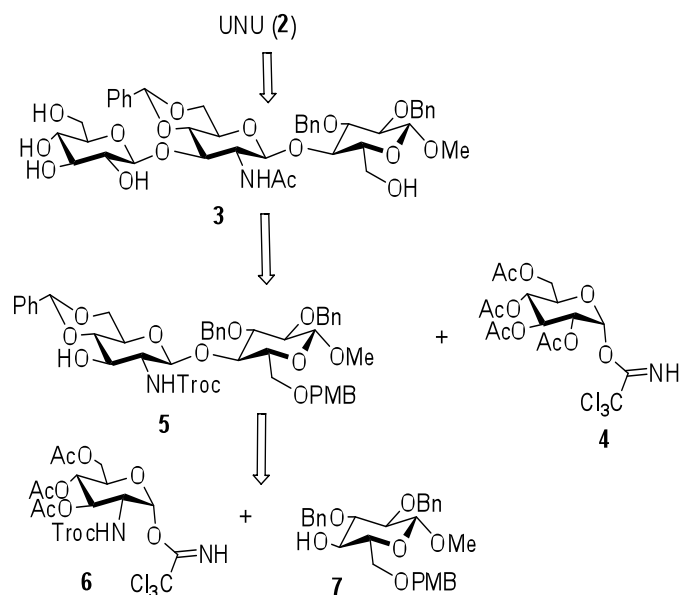
Scheme 1.:Retrosynthetic scheme towards UNU trisaccharide.
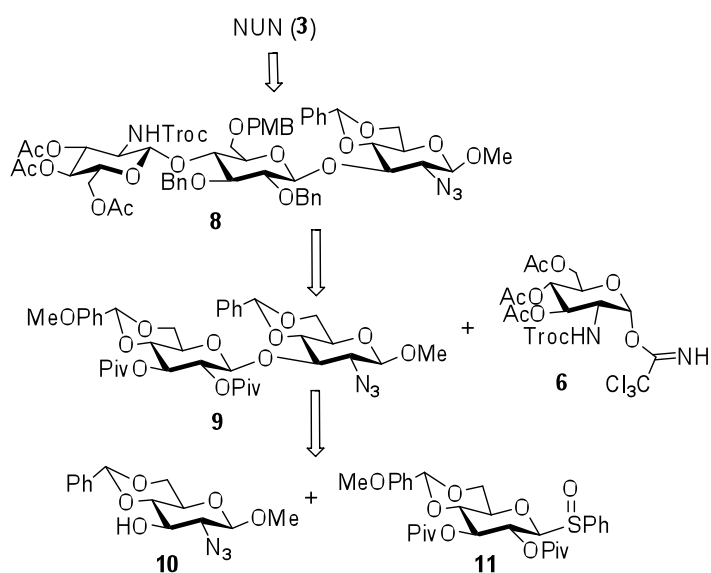
Scheme 2: Retrosynthetic scheme toward NUN trisaccharide.

The NUN trisaccharide contains the same monosaccharide units as the UNU trisaccharide, but alternate monomer precursor units are employed for the glycosylation steps, Scheme **2**.

The fully protected trisaccharide **8** was converted in the NUN trisaccharide by azide reduction, and acetylation, followed by several deprotection steps, and regioselective oxidation of the primary hydroxyl function of the central monosaccharide.

Another interesting report describes a linear strategy for the development of HYA-based oligomers consisting of [GlcAβ-(1→3)-GlcNAc]$_n$ separated by a flexible spacer, such as **12**, Scheme -**3**[189].
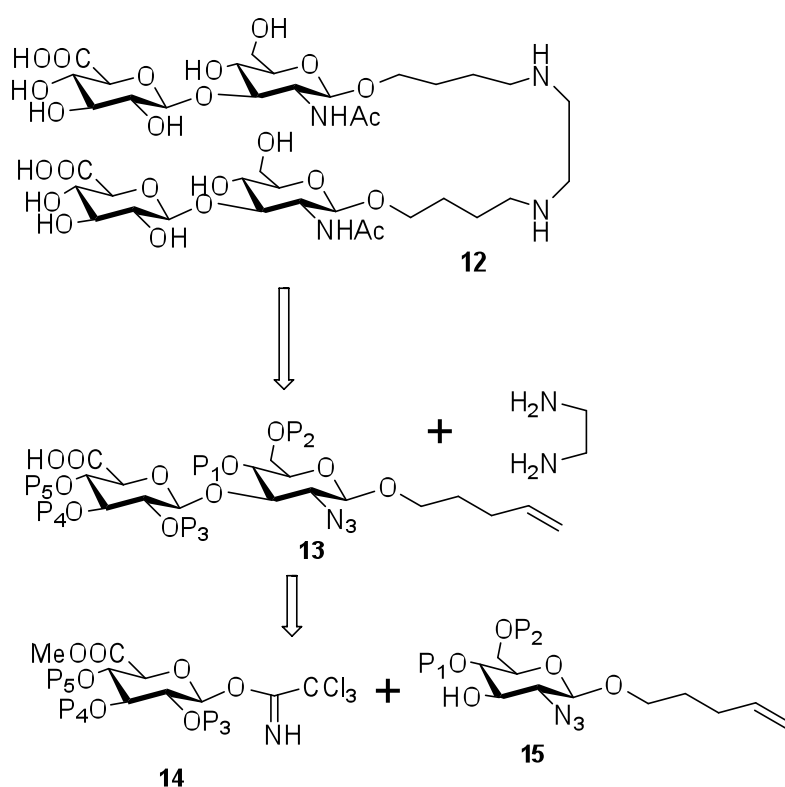
Scheme-**3**: Retrosynthetic strategy for the synthesis of dimers of β-(1→3) HYA disaccharides (P$_1$-P$_5$ = protecting groups).

While in previously reported syntheses the glucuronic acid residue is generated after

the construction of the oligosaccharide backbone by selective oxidation of the primary position of a D-glucose residue, in this work acetobromo D -glucuronic acid methyl ester was used as a precursor for the synthesis of the trichloroacetimidate glycosyl donor. Significantly, a *n*-pentenyl glycoside was designed as the acceptor. The pentenyl moiety was chosen since carbon-carbon double bound could be readily attached to spacers, carrier proteins or polymer backbone providing direct access to glyco-dendrimers and/or glycopolymers.

By this approach, Gemini disaccharides were produced via reductive amination with ethylenediamine, after conversion of the terminal olefin to an aldehyde. The selection of the ethylenediamine linker in the glycomimetic design was based on the consideration that it provides a sufficiently flexible chain possessing head-to-head HYA-based disaccharides. Since the ligand affinity and specificity is often dependent upon the proper spacing and orientation of the carbohydrate residues, such compounds would then be able to pre-organize and fold into a conformation suitable for fitting and complexing with the specific receptor binding site, a fundamental requirement for bioactivity. It's a matter of fact that the intrinsic binding affinity of oligosaccharide mimetics to target proteins depends upon the distance and appropriate orientation of the sugar epitopes, as well as the carbohydrate conformational flexibility. Moreover, small and subtle differences in configuration, conformation and functionality can have a profound influence on the biological activity of glycoconjugates. To this end, while the β-linked neoglycoconjugate **12** resembles the native β-(1→3) linked HYA structure, compounds based on β-linked disaccharides were also synthesised, since may exhibit different receptor binding affinities.

The same synthetic strategy was applied to the synthesis of β-(1,3)-GlcA-GlcNAc dimeric and tetrameric glycoclusters through the conjugation of disaccharide groups onto a diaminodiamide aromatic scaffold (**17**) by reductive amination, Scheme (**4**) [190].
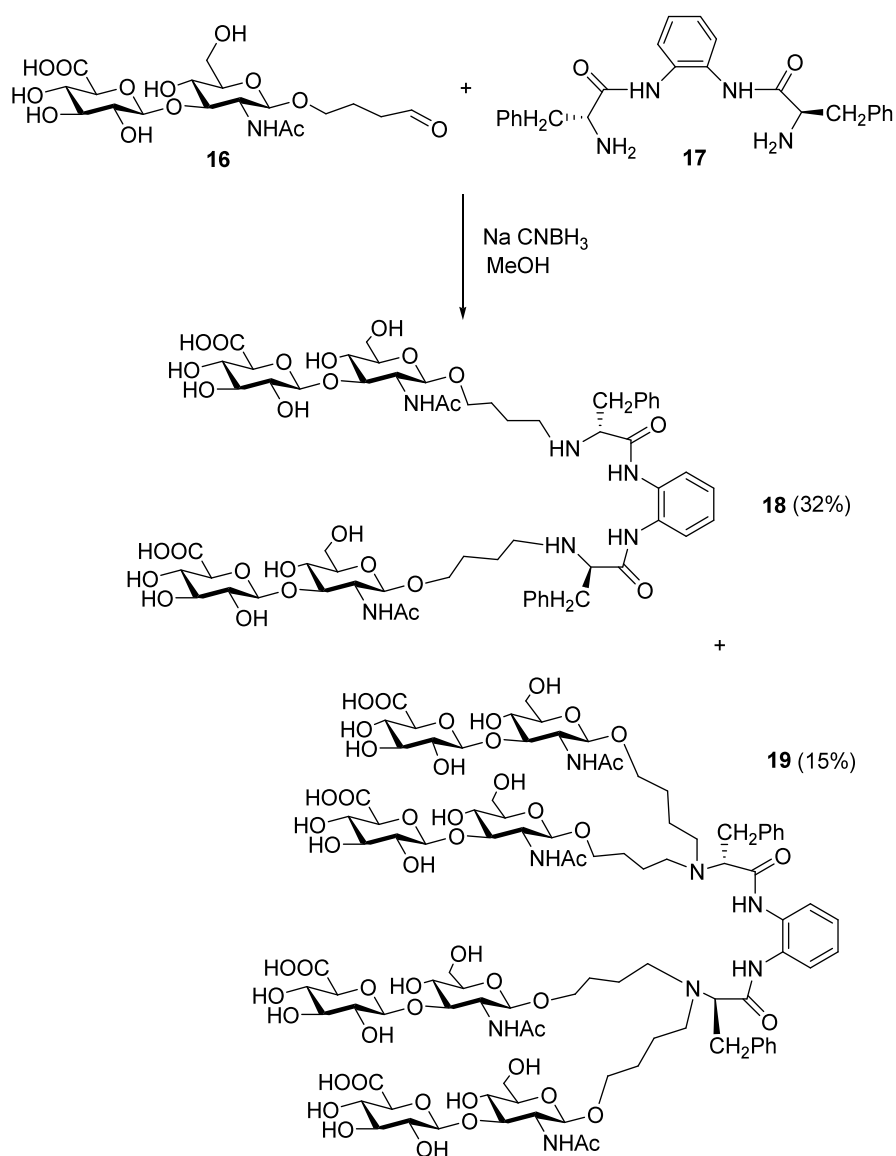
Scheme -**4**: HYA multidentate glycoclusters.

The synthetic approach involves the synthesis of an HYA-like β-(1,3)-linked disaccharide with a pentenyl spacer arm, the generation of conformationally rigid

aromatic diamidodiamine scaffold; and the chemical conjugation of the disaccharide to the diamine template via reductive amination.

The aromatic diamide scaffold for the assembly of head-to-head HYA oligomers comes from the postulation by the authors that glycoligand–protein binding affinity would be further augmented by the potential for secondary hydrophobic and hydrogen-bonding interactions provided, respectively, by the aromatic and amide/amine groups in the short peptide skeleton. In addition, by incorporating different substituents in the scaffold backbone, the spatial presentation and conformational mobility of the pendant saccharides could be altered as additional structural variables for optimized binding. Furthermore the incorporation of HYA disaccharide epitopes onto a restricted scaffold via a flexible aliphatic linker would minimize direct steric interactions between carbohydrate residues and the diamide scaffold.

A *C*-disaccharide **20** mimetic of the repeating unit of HYA has been proposed, Scheme (**5**)[191]. This mimic is resistant to enzymatic degradation.
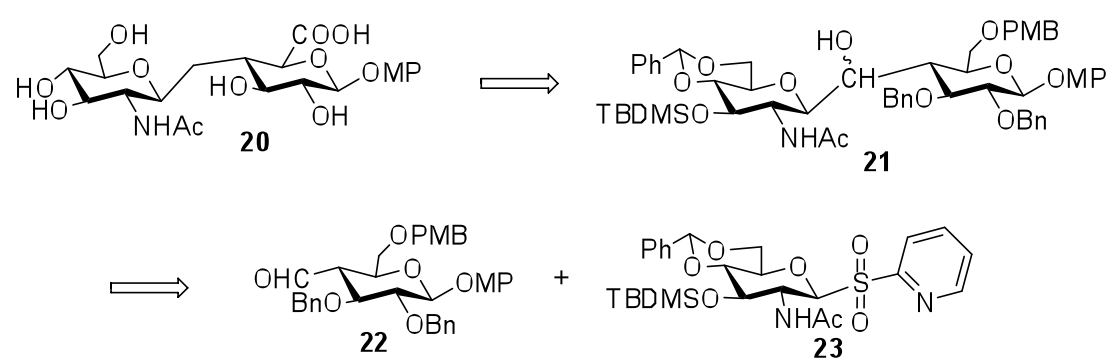
Scheme-**5:** Retrosynthetic scheme towards C-glycosidic analogues of HYA repeating unit

The target compound was obtained via the SmI$_2$-promoted coupling reaction of the sulfone, 2-acetamido-4,6-O-benzylidene-3-O-tert-butyldimethylsilyl-1,2-dideoxy-1-pyridinylsulfonyl-b-D-glucopyranose (**23**), and the aldehyde, p-methoxyphenyl 2,3-di-O-benzyl-4-deoxy-4-C-formyl-6-O-p-methoxybenzyl-b-D-glucopyranoside (**22**). Biological studies of this synthetic HYA mimetic are not yet available.

Several syntheses of HA oligosaccharides have been previously reported[192]. Among these, Slaghek and Ogawa constructed a tetrasaccharide derivative with D-glucuronic acid at the reducing end[193] as well as a series of di-, tri-, and tetrasaccharides with *N*-acetyl-D-glucosamine at the reducing end[194]. However, all of the derivatives reported incorporated a *p*-methoxyphenyl ether moiety at C-1 of the reducing sugar that facilitates chain elongation but does not accurately mimic native HA fragments. In this regard, *O*-methyl is a better structural mimic of native HA because (1) *O*-methyl is the smallest functional group available to minimize any potential secondary interactions and (2) anomerization, which significantly complicates any NMR solution study, can be eliminated by capping C-1 of the reducing end sugar. Among the *α*-methyl HA derivatives previously reported are the *β* (1,4) disaccharide[195] and a series of tetra-, hexa-, and octasaccharides with D-glucuronic acid at the reducing end[196].

There are three central considerations in the synthesis of glycosaminoglycans:

(1) The mode of glycosylation, or formation of the glycosidic linkages;

(2) The installation of the acetamido group; and

(3) The oxidation of C-6 on the glucuronic acid .

Another part of synthesis is cyclitols. Cyclitols are cycloalkanes containing one hydroxyl group on three or more ring atoms.

4.4: Aim of work:-

With the aim to prepare the monomer building blocks for HA oligomers that can be functionalized and used for biomaterial functionalisation studies, we set out to develop a general synthesis protocol. Here i have shown monomer building block synthesis that will be useful for the synthesis of HA polymers and HA mimic shown below. Each with a glucuronic acid moiety as the reducing end sugar.
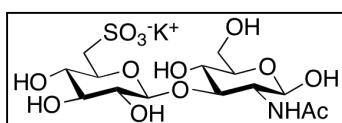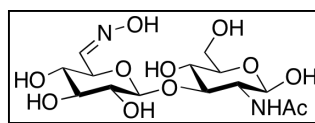
HA-1   HA-2
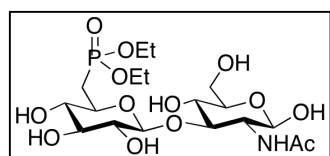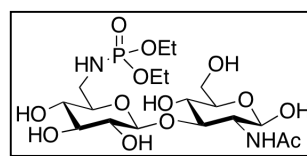
HA-3   HA-4
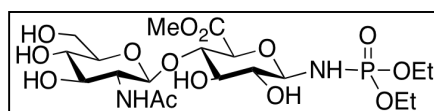
HA-5

Our main goal within this research topic was to synthesize different kind of acceptor and donor moiety of sugar. I have successfully synthesized monomer building blocks i.e. **27, 34, 37, 43, 49, 52, 54** and **57**. For synthesizing the HA mimic i.e cyclitol the monomer **63** is also synthesized. ***These all monomer are useful tool for synthesizing the mimic of HA described above.Which could consider as future prospectus for further synthetic studies.***

I have demonstrated that HA oligomers that are suitably functionalized for future biological studies can be conveniently prepared by making use of thioglycosides and

1-hydroxyglycosides, and the combination of the presence of acid-labile benzylidene protective groups and the propensity of orthoester formation requires that the glycosylations be monitored with care.

However, I believe our general strategy to be convenient, in that useful quantities can be prepared from synthesized monomer building blocks. Therefore confident that our strategy will be of use for the large-scale synthesis of HA oligomers, including compounds with a glucosamine residue at the reducing end and oligomers assembled from more than five monosaccharide residues. These compounds in turn will prove to be useful in the assessment of the biological properties of HA oligomers.

4.4.1: **Results and discussion:-**

Scheme-1:
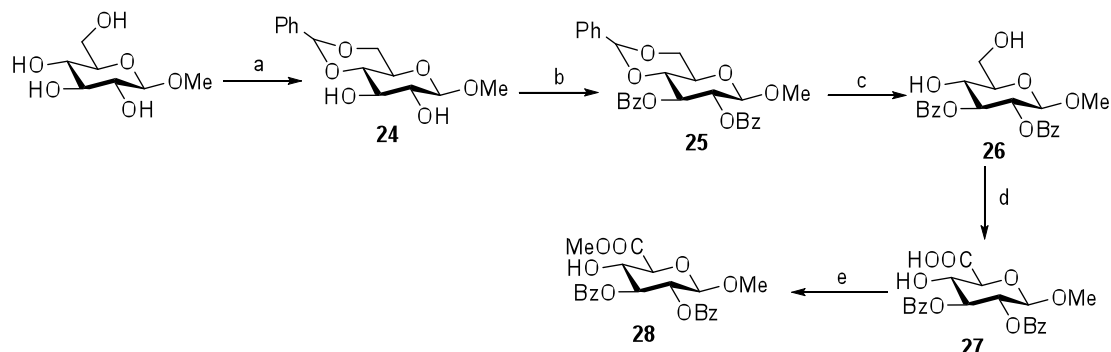
a) PhCH(OMe)$_2$, CSA (cat.), DMF at 60^{0}C b) Bz-Cl, Py, DMF C) TFA 95%, DCM, d) Tempo, BIAB, DCM-H$_2$O e) MeI, K$_2$CO$_3$, DMF

In a first phase the synthesis of the protected 2,3-benzoyl-1-O-methoxy glucuronate was carried on, using a highly selective and great yielding procedure. Treatment of methyl-D-glucopyranoside with benzaldehyde dimethyl acetal and *p*-toluenesulfonic acid afforded the corresponding benzylidene derivatives **24**. Benzoylation of at 2-OH & 3-OH has been achieved by treatment with benzoyl chloride and pyridine to afford **25** subsequently deprotection of benzylidene with 95% TFA gives **26** without affecting the benzoyl group**.** The oxidation at 6-OH wih tempo & BIAB afford **23** and esterification of **27** with methyl iodide and potassium carbonate in DMF which leads to deprotection of benzoyl groups also due to basic condition.

Scheme-2:
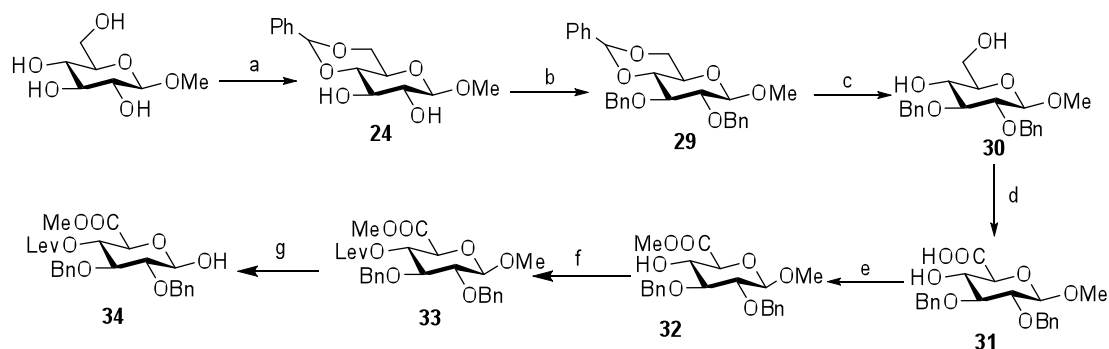
Reagent and condition: a) PhCH(OMe)$_2$, CSA (cat), DMF at 60^{0}C, b) BnBr, NaH, DMF, c)TFA 95%, DCM, d) Tempo, BIAB, DCM-H$_2$O, e) MeI, K$_2$CO$_3$, DMF, f)Lev-acid, DCC, DMAP, DCM, g) H$_2$SO$_4$-H$_2$O, reflux

The commercially available methyl-D-glucopyranoside with benzaldehyde dimethyl acetal and *p*-toluenesulfonic acid afforded the corresponding benzylidene derivatives **20**. Benzylation of at 2-OH & 3-OH has been achieved by treatment with benzyl bromide and sodium hydride in DMF to afford **29** subsequently deprotection of benzylidene with 95% TFA gives **30** without affecting the benzyl group**.** The oxidation at 6-OH wih tempo & BIAB afford **31** and esterification of **31** with methyl iodide and potassium carbonate in DMF gives **32** in a quantitative yield. The protection of 4-OH with levlinic group by using levlinic acid, dimethyl aminopyridine, DCC afford **33** the subsequently hydrolysis of **33** in sulphuric acid and water in refluxing condition afford **34**.

Scheme-3:
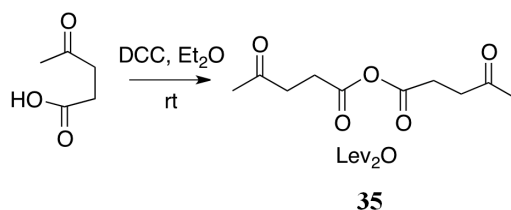
The commercially available levulinic acid is treated with DCC in diethyl ether at room temperature to afford a levulinic anhydride **35**.
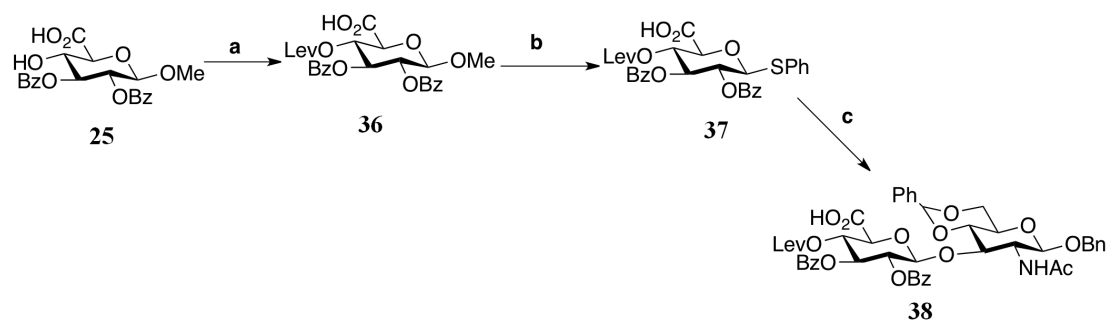
Reagent and condition: a) Lev$_2$O, DMAP, DCC,DCM, b)Thiophenol, BF$_3$:Et$_2$O, DCM, c) Tf$_2$O, DPS, DCM at -78^{0}C

The levelinic derivative **36** was prepared from **25** which then thioglycosylated by using BF$_3$:Et$_2$O ,thiophenol in dichloromethane to give thio donor **37** which is then coupled with acceptor **43** in the presence of diphenly sulphoxide, triflic anhydride at -78^{0}C in dichloromethane to afford dissachride **38**.

Scheme-4:
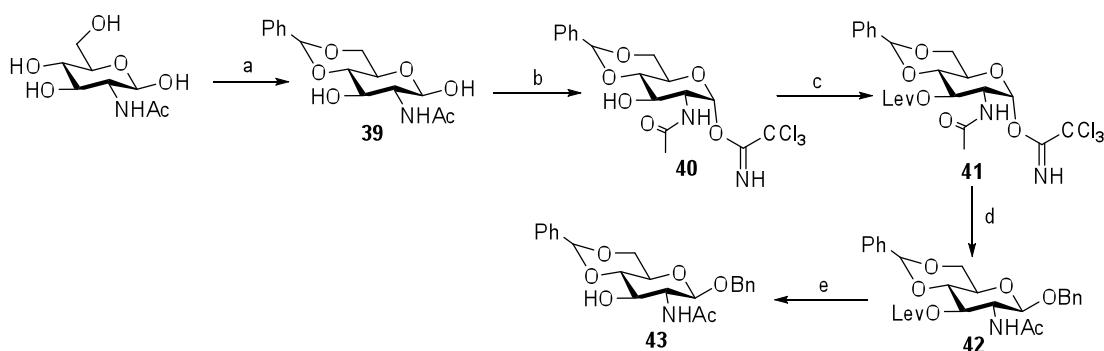
Reagent and condition: a) PhCH(OMe)$_2$, CSA (cat.), DMF at 60^{0}C b) CCl$_3$CN, DCC, DBU, DCM C) Lev$_2$O, DCC, DMAP, DCM d) Bn--Br, NaH, DMF e) Pyridine, AcOH, NH$_2$NH$_2$

The commercially available N-Acetyl glucosamine with benzaldehyde dimethyl acetal and camphorsulfonic acid afforded the corresponding benzylidene derivatives **39**. The benzylidene derivative **39** then treated with trichloroacetonitrile, DCC, DBU in dichloromethane to afford selective formation trichloroacetamide at anomeric

position,the **40** is then subsequently protected at 4-OH with levelinic group by using levulinic anhydride , DCC, dimethyl aminopyridine in dichloromethane gives **41.** The bezylation of **41** at anomeric position by replacing trichloroacetamide group in presence of benzyl bromide, sodium hydride in DMF afford **42.** Deprotection levulinic group of **42** **w**ith acetic acid, hydrazine in pyridine afford a donor **43** in a good yield.

Scheme-5: A)
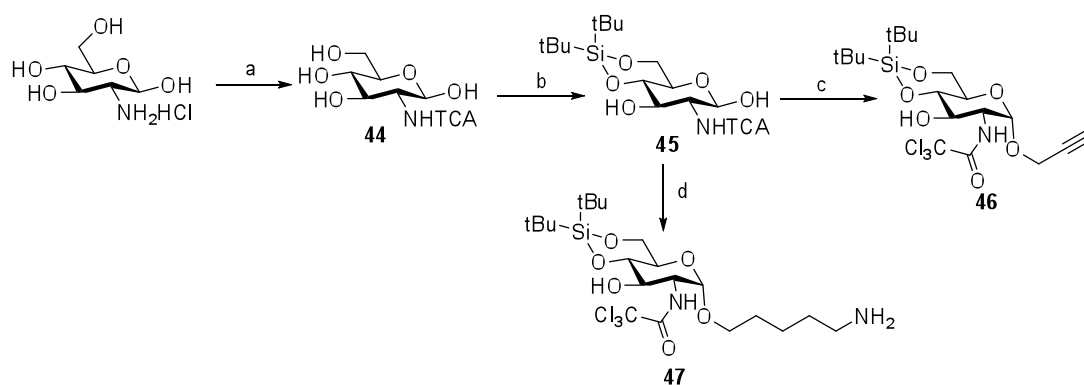
Reagent and condition: a)Cl_3CCOCl, MeOH, Et_3N, 5days b) tBuSi OTf_2 , DMF, -30^0C C) Silica-H_2SO_4, Propargyl alcohol d) Silica-H_2SO_4, Pentane-1-ol-amine

The synthesis of the glucosamine building blocks started with the introduction of the trichloroacetyl group on the amino function of glucosamine, using trichloroacetylchloride and triethylamine in methanol (Scheme 5 A) result *N*-TCA glucosamine **44.** Thus, regioselective silylation of the C6-OH and C4-OH in **44** using di-*tert*-butylsilyl bistriflate in DMF at -30^0C quantitatively yielded 4,6-*O*-di-*tert*-butylsilylidene glucosamine. The **45** was then tried transformed by introducing propargyl **46** and amino **47** functionality at anomeric position by glycosylation.

B)
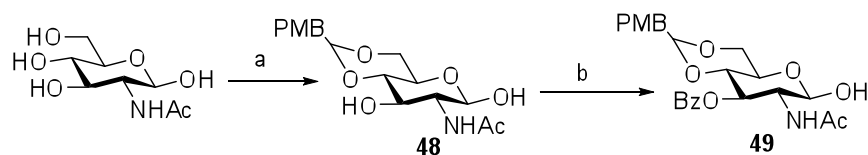
Reagent and condition: a)PMB, CH$_3$CN, CSA b) Bz-Cl, Pyridine

N-acetyl glucosamine is treated with p-methoxy-benzaldehyde dimethyl in presence of camphor sulphonic acid in acetonitrile in refluxing condition afford **48** in 2hrs. The selective protection of 3-OH with benzoyl group with benzoyl chloride in pyridine afford **49** in good yield.

Scheme-6:- (A)
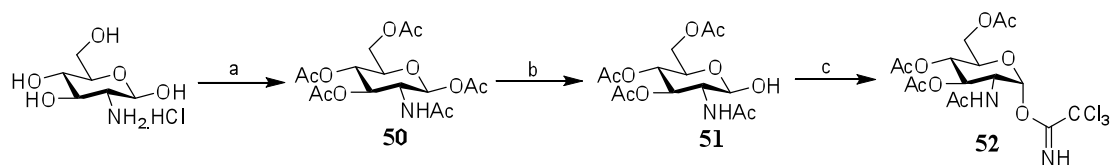
Reagent and condition: a)Ac$_2$O, Py at rt, b) MeNH$_2$, MeOH-THF at rt, c) Cl$_3$CCN,DBU, DCM.

The commercially available D-glucosamine hydrochloride is treated with acetic anhydride in pyridine at room temperature afford **50** in a quantitative yield. Selective deprotection of anomeric hyd roxyl group by methylamine in MeOH & THF at room temperature afford **51** which subsequently treated with trichloroacetonitrile, DBU in dichloromethane at room temperature to afford **52.**

B)
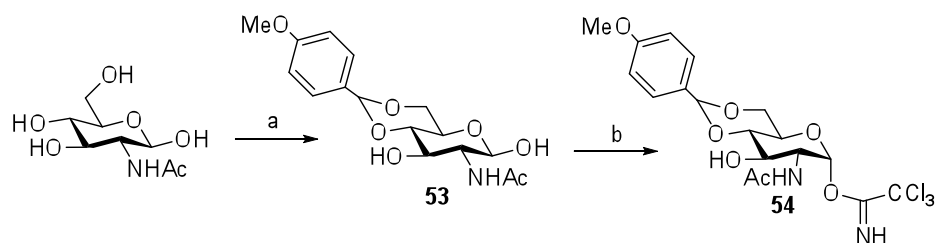
Reagent and condition: PMB, CSA, CH$_3$CN, B) Cl$_3$CCN, DBU, DCM.

N-acetyl glucosamine is treated with p-methoxy-benzaldehyde dimethyl in presence of camphor sulphonic acid in acetonitrile in refluxing condition afford **53** which is the treated with trichloroacetonitrile, DBU in dichloromethane at room temperature to afford **54** (scheme 6B).

Scheme-7:-
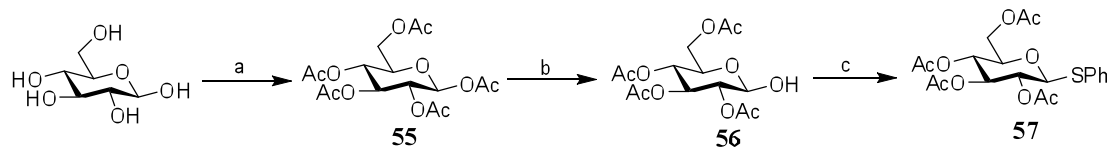
Reagent and condition: a)Ac$_2$O, Py, DCM b) MeNH$_2$, MeOH-THF at rt, c) Thiophenol, BF$_3$:Et$_2$O, DCM,

The commercially available D-glucose is treated with acetic anhydride in pyridine with quantitative yield, Selective deprotection of anomeric hydroxyl group by methylamine in MeOH & THF at room temperature afford **56.** Which is then converted to its thioglycoside by treating with BF$_3$:Et$_2$O and thiophenol in dichloromethane to afford **57.**

Scheme-8:-
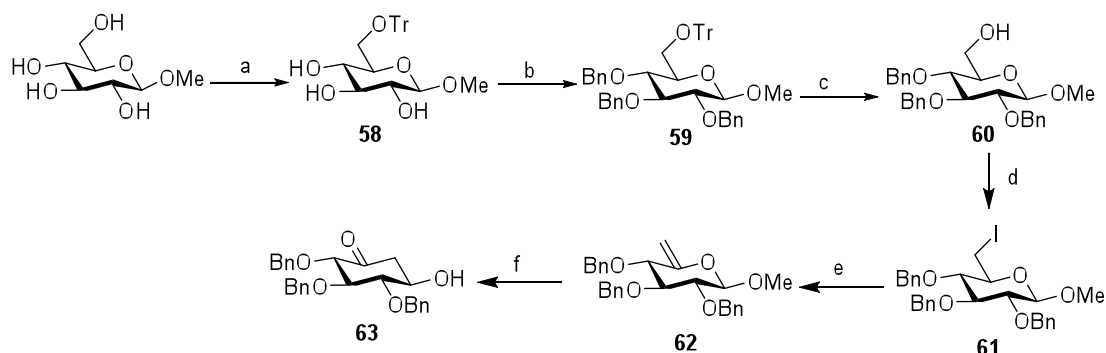
Reagent and condition: a) trityl chloride, DMAP, pyridine, 30 h; b) BnBr, NaH, DMF, 16 h, 0 °C → RT, 61% over two steps; c) P-TSA 26 h, 80 °C, 92%; d) Iodine, Ph$_3$P, DEAD,Et$_2$O e) DBU, Toulene f) HgCl$_2$, Acetone-Water, 3hrs

The commercially available1-methyl-glucopyranose is treated with trityl chloride to selective protect 6-OH to afford **58**, which is then benzylated with benzyl bromide, sodium hydride in DMF to afford **59** in a quantitative yield. The selective deprotection of 6-OTr with *p*-toulenesulphonic acid at 80^{0}C to give 6-OH **60** whose primary hydroxyl group was selectively replaced by iodide with a Mitsunobu reaction to give **58** in 74% yield. Dehydroiodination of **61** was accomplished by treatment with l,8-diazabicyclo[5.4.0]undec-7- ene (DBU) to afford 5-enopyranoside **62**.
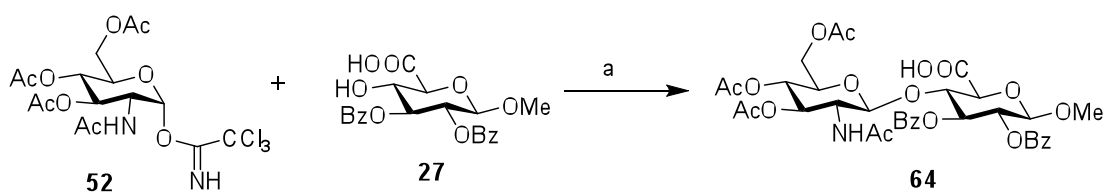
Construction of **64** utilized TMSOTf mediated glycosylation of methyl 2,3-di-*O*-benzoyl-glucouronic acid as a acceptor (**27**) with the trichloroacetimidate donor **52** to afford the corresponding (1,4) disaccharide, **64** in 87% yield

94

Scheme-9:-
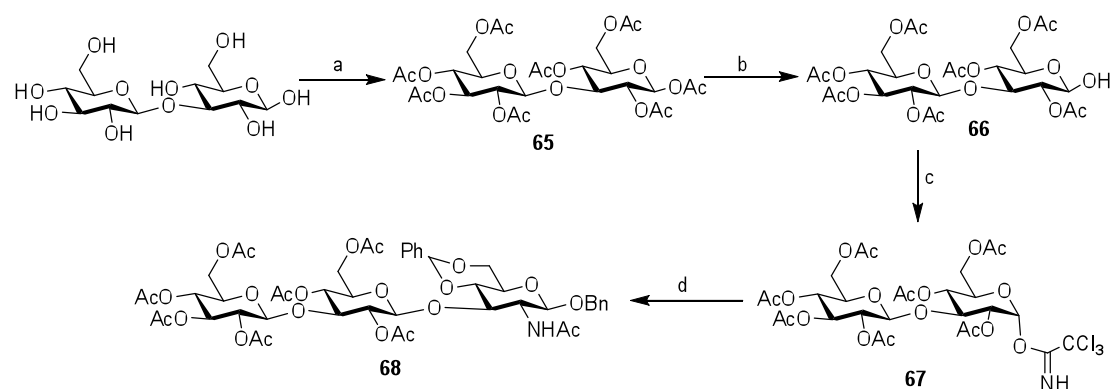
Reagent and condition: a) Ac$_2$O, Py, DCM, b) MeNH$_2$, MeOH-THF at rt, c) Cl$_3$CCN, DBU, DCM, d) TfOH, 3A^0 MS at 0^{0}C

The commercially available D-lactose is treated with acetic anhydride in pyridine with quantitative yield afford **65**, Selective deprotection of anomeric hydroxyl group by methylamine in MeOH & THF at room temperature afford **66**. which is the treated with trichloroacetonitrile, DBU in dichloromethane at room temperature to afford acceptor **67**.The donor **67** is coupled with acceptor **43** in the presence of 3 A^0 Moleculer sieve and TfOH at 0^{0}C to afford trisaccharide **68**.

4.4.2: Experimental Part:-

General Method for benzylidene protection (24, 39)

for e.g α-Methyl 4,6-*O*-benzylidene-D-glucopyranoside(24).
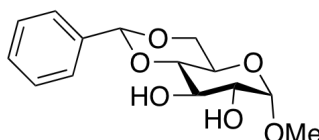
α-Methyl glucopyranoside (21.5 g, 111 mmol) and benzaldehyde diethyl acetal (27.9 g, 155 mmol) were added to CHCl₃ (350 mL) in a distillation flask, followed by camphorsulfonic acid (65 mg). The resultant suspension was placed in a preheated oil bath (bath temp. 90 °C), and the distillate was collected. After approximately 75 mL was collected, the same volume of CHCl₃ was added. This process was repeated. Then, a final 100 mL of distillate was collected, and the reaction mixture was filtered while hot. The remaining volatile material was removed on a rotary evaporator to give a white solid, which was triturated twice with petroleum ether and filtered to give α-methyl 4,6-*O*-benzylidene- D-glucopyranoside (28.5 g, 92%) as a white solid.

^{1}H NMR (400 MHz, CDCl₃) δ 7.49 (m, 2H), 7.36 (m, 3H), 5.54 (s, 1H), 4.92 (d, J = 3.1 Hz, 1H), 4.27 (m, 2H), 4.07 (dd, J = 12.4, 1.6 Hz, 1H), 3.90 (m, 2H), 3.69 (s, 1H), 3.44 (s, 3H), 2.41 (br s, 2H).

α-Methyl 2-*O*-benzoyl-4,6-*O*-benzylidene-D-glucopyranoside (25).
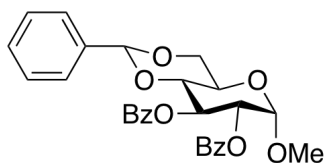
Pyridine (2.0 g, 2 mmol) were added to a solution of α-methyl 4,6-*O*-benzylidene-D-glucopyranoside (3.6 g, 1 mmol) in THF (20 mL). The solution was stirred briefly, and benzoyl chloride (2.3 mL, 2.7 g, 1.5 mmol) was added drop-wise. The resultant solution was stirred at rt for 30 min. The THF is evaporated on rote and then diluted

with CH_2Cl_2 (150 mL), and washed with H_2O (100 mL), 1N HCl (100 mL), and brine (100 mL). The organic layer was then dried ($MgSO_4$) and concentrated. The residue was purified by chromatography on silica gel (toluene/Et2O 3:2) to give **21** (0.63 g, 23%) as a white solid:

^{1}H NMR (400 MHz, $CDCl_3$) δ 8.10 (d, J = 7.4 Hz, 2H), 7.54 (m, 3H), 7.42 (m, 5H), 5.60 (s, 1H), 5.37 (dd, J = 9.9, 3.6 Hz, 1H), 5.12 (d, J = 3.5 Hz, 1H), 4.32 (m, 3H), 4.12 (d, J = 12.3 Hz, 1H), 3.79 (s, 1H), 3.43 (s, 3H),; ^{13}C NMR (100 MHz, CDCl3) δ 194.6, 165.8, 153.2, 137.5, 133.5, 130.0, 129.5, 129.5, 128.6, 128.3, 126.7, 126.3, 121.7, 100.8, 98.1, 80.0, 73.4, 69.3, 69.1, 62.3, 55.9.

General method for deprotection of benzylidene group (26, 30):

To a solution of **21** (1 g, 7.49 mmol) in DCM (75 mL) was added a solution of 95%TFA in H_2O dropwise at 0°C. After 5 h the mixture was neutralized with Na_2CO_3. The organic layer was dried over $MgSO_4$ and concentrated *in Vacuo*. Yielded **22** as a colorless oil (90%).

General Method for the Oxidation of Saccharides (27, 31):

In a typical experiment a solution of a saccharide (800 mmol), TEMPO (7.5 mg, 48 *i*mol), KBr (179 mg, 2.4 mmol), and deionized water (15 mL) was cooled to 0 °C, and NaOCl (5% aqueous solution, 0.72 mL, 10.6 mmol) was slowly added. After TLC showed disappearance of starting material and intermediate products (1-2 h), MeOH (3 mL) was added to quench the reaction. The mixture was concentrated, the solid residue was extracted with MeOH, and the extract was evaporated to dryness. The title compounds were obtained after purification by column chromatography (CH_2Cl_2-MeOH-AcOH, 25:25:1).

General procedure for esterification (28, 32):

Methyl (phenyl 2,3-di-*O*-benzyl-1-thio-α-D-glucopyranoside) uronate:
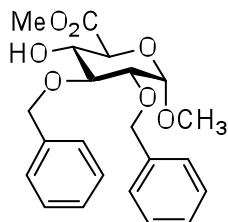
To a stirred solution of 965 mg compound **27** (2.1 mmol) in 10 mL DMF was added 0.3 mL MeI (5 mmol, 2.5 equiv.) and 200 mg K2CO3. The solution was stirred overnight and quenched by the addition of 2 mL MeOH. The reaction mixture was taken up in EtOAc and washed with H2O. The water layer was extracted with EtOAc. The collected organic layers were dried (MgSO4), filtered and concentrated under reduced pressure. Flash column chromatography (EtOAc/PE) afforded 0.96 g of the title compound **28** (1.9 mmol, 95%) as a colorless oil. TLC: 35% EtOAc/PE;

^{1}H NMR (400 MHz, CDCl$_3$) δ = 2.98 (s, 1H, OH-4), 3.71 (dd, H-3), 3.78 (s, 3H, CH3 COOMe), 4.95 (dd, H-2), 4.38 (t, 1H, $J4,3$ = 7.2 Hz, H-4), 4.57 (d, 1H, J = 9.6 Hz, CH*H*Ph), 4.60 (d, 1H, J = 9.6 Hz, CH*H*Ph), 4.61 (s, 1H, H-5), 4.66 (d, 1H, J = 9.6 Hz, C*H*HPh), 4.69 (d, 1H, J = 9.6 Hz, C*H*HPh), 5.61 (d, 1H, $J1,2$ = 1.6 Hz, H-1), 7.24 – 7.45 (m, 10H, H Arom); ^{13}C NMR (100 MHz, CDCl3) δ = 52.6 (CH3 COOMe), 68.5 (C-4), 72.3 (CH2 Bn), 72.5 (CH2 Bn), 72.6 (C-5), 75.7 (C-2), 78.1 (C-3), 86.2 (C-1), 127.6 – 131.5 (CH Arom), 137.6 (Cq Bn), 137.9 (Cq Bn), 170.3 (C=O COOMe);

General method for the benzylation (29, 42):-

2,3-di-*O*-benzyl-4,6-*O*-benzylidene-β-D-glucopyranoside.
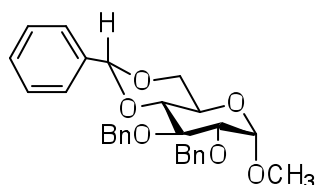
NaH (60% in mineral oil, 1.4 g, 35 mmol) was added to DMF (35 mL), and a mixture of benzyl bromide (4.0 g, 23 mmol) and 4,6-*O*-benzylidene-β-D-glucopyranoside (2.1

g, 5.8 mmol) was added dropwise at 0 °C under N$_2$. The reaction mixture was stirred overnight at rt. MeOH was used to quench the excess NaH. The reaction mixture was then poured over ice water. The mixture was extracted with Et$_2$O (3 x 50 mL), and the combined organic extracts were dried (MgSO$_4$) and concentrated. Purification by flash chromatography on silica gel (petroleum ether/EtOAc 95:5) afforded 2,3-di-*O*-benzyl-4,6-*O*-benzylidene-β-D-glucopyranoside (2.1 g, 67%) as a pale yellow oil.

^{1}H NMR (400 MHz, CDCl$_3$) δ 7.56–7.50 (m, 4H), 7.41–7.30 (m, 11H), 5.61 (s, 1H), 4.96 (d, *J* = 11.0 Hz, 1H), 4.89–4.77 (m, 4H), 4.13 (dd, *J* = 10.5, 5.0 Hz, 1H), 3.88–3.80 (m, 2H), 3.73 (t, *J* = 9.0 Hz, 1H), 3.56–3.47 (m, 2H); ^{13}C NMR (100 MHz, CDCl3) δ 138.5, 138.2, 137.4, 132.6, 129.2, 129.2, 128.6, 128.5, 128.4, 128.3, 128.1, 128.0, 126.2, 101.3, 88.5, 83.2, 81.7, 80.6, 76.1, 75.5, 70.4, 68.9.

General method for Lev$_2$O protection (33, 41, 36)

To a solution of **32** (3.81 g, 7.49 mmol) in pyridine (75 mL) was added a solution of Lev$_2$O in dioxane (0.5 M, 37.5 mL, 18.7 mmol). After 18 h the mixture was diluted with EtOAc (200 mL) and washed with 1 M HCl (aq), NaHCO$_3$ (aq), and brine. The organic layer was dried over MgSO$_4$ and concentrated *in Vacuo*. Purification by column chromatography yielded **33** as a colorless oil (3.91 g, 86%).

General method for synthesis of thioglycoside (37, 57):-

e.g Phenyl 2,3,4,6-tetra-*O*-acetyl-1-thio-β-D-glucopyrvanoside.
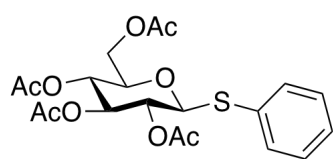
Penta-*O*-acetyl-D-glucose (10.0 g, 25.6 mmol) was dissolved in CH$_2$Cl$_2$ (250 mL), and the solution was cooled to 0 °C under N$_2$. Then, thiophenol (5.10 g, 46.0

mmol) was added. After 30 min BF$_3$.Et$_2$O (11.1 mL, 89.0 mmol) was slowly added, and the reaction mixture was stirred overnight at rt. The reaction mixture was washed with saturated aqueous NaHCO$_3$ (100 mL) and brine (100 mL), dried (MgSO$_4$) and concentrated. Purification by flash chromatography on silica gel (petroleum ether/EtOAc 60:40) afforded phenyl 2,3,4,6-tetra-O-acetyl-1-thio-β-D-glucopyranoside as a white solid (5.3 g, 46%)

^{1}H NMR (400 MHz, CDCl$_3$) δ 7.50–7.46 (m, 2H), 7.32–7.25 (m, 3H), 5.20 (dd, $J =$ 9.3, 9.3 Hz, 1H), 5.02 (dd, $J =$ 9.8, 9.8 Hz, 1H), 4.95 (dd, $J =$ 9.6, 9.6 Hz, 1H), 4.68 (d, $J =$ 10.1 Hz, 1H), 4.19 (m, 2H), 3.71 (m, 1H), 2.07 (s, 3H), 2.06 (s, 3H), 2.00 (s, 3 H), 1.97 (s, 3H); ^{13}C NMR (100 MHz, CDCl$_3$) δ 170.8, 170.4, 169.6, 169.5, 133.3, 131.9, 131.6, 129.1, 128.8, 85.9, 75.9, 74.1, 70.1, 68.4, 62.3, 20.9, 20.8.

Synthesis of Levulinic anhydride (35):-

A reaction of levulinic acid (20 mmol) with dicyclohexylcarbodide (10 mmol) in 65 ml of ether for *5* hr followed by filtration and evaporation of the solvent.

General method for synthesis of trichloroacetimidate (40, 52, 54, 67)

To a stirred solution of **48** (0.63 g, 1.8 mmol) in dry dichloromethane (10 mL) were added trichloroacetonitrile (7.2 mL, 7.2 mmol) and DBU (0.054 mL, 0.36 mmol). The reaction mixture was stirred for 3 hr at RT. The crude product was then concentrated and purified by flash column chromatography on silica gel (EtOAc/hexane = 1:3) to give imidate **49** as a white solid (0.64 g, 73%).

2-Acetoamido-1-O-Benzyl-4,6 benzylidene-β-D-glucopyranose (43):-

The crude concentrate 39 was then dissolved in a mixture of pyridine (16 mL) and

AcOH (4 mL), after which hydrazine monohydrate (0.48 mL, 10 mmol) was added. The mixture was stirred for 15 min, diluted with EtOAc (50 mL), and washed with 1 M HCl (aq), NaHCO$_3$ (aq), and brine. The organic layer was dried over MgSO$_4$ and concentrated *in Vacuo*. Purification by column chromatography yielded **40** as a colorless oil.

2-Deoxy-2-trichloroacetamido-D-glucopyranose (44).
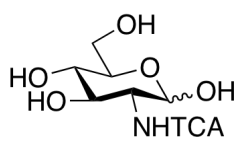
To a mixture of D-glucosamine-HCl (53.9 g, 250 mmol) in MeOH (625 mL) and Et$_3$N (70 mL, 500 mmol) trichloroacetyl chloride (TCACl) (28 mL, 250 mmol) was added dropwise at 0 ¢XC. After 5 days, the mixture was filtered and concentrated *in Vacuo*. Purification by column chromatography (EtOAc, MeOH) yielded **41** as an off-white solid (37.8 g, 46%). Analytical data were identical to those described in literature previously.

4,6-*O*-di-*tert*-butylsilylidene-2-deoxy-2-trichloroacetamido-D-glucopyranose (45).
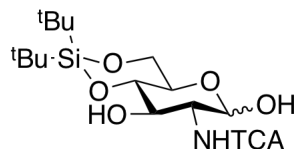
To a solution of **41** (13.9 g, 43.0 mmol) in DMF (215 mL) at -30^{0}C was added di-*tert*-butylsilylidene bistriflate (13.6 mL, 42.0 mmol). The reaction was warmed to -10^{0}C in 1 h after which pyridine (10.9 mL, 129 mmol) was added and subsequently the reaction was diluted with Et$_2$O and washed with H$_2$O. The organic layer was dried over MgSO$_4$ and concentrated *in Vacuo* to afford **42** as white amorphous solid (18.5 g, 95%).

^{1}H NMR (400 MHz, CDCl3): δ) 0.99, (s, 9H, *t*Bu), 1.06 (s, 9H, *t*Bu), 3.30 (bs, 1H, OH), 3.74-3.82 (m, 1H), 3.87-3.94 (m, 2H), 3.96-4.13 (m, 3H, H-2, H-6), 5.34 (d, 1H, *J*) 3.2 Hz, H-1), 6.98 (d, 1H, *J*) 8.4 Hz, NH);^{13}C NMR (100 MHz): δ) 19.7 (Cq *t*Bu), 22.7 (Cq *t*Bu), 26.9 (CH3 *t*Bu), 27.4 (CH3 *t*Bu), 54.4 (C-2), 66.3 (C-6), 66.4 (C-5),

71.9 (C-3), 77.7 (C-4), 91.7 (C-1), 162.3 (CdO TCA). HRMS: $C_{16}H_{28}Cl_3NO_6Si + H^+$ requires 464.0824, found 464.0823.

General procedure for glycosylation of (46,47):-

In compound **42** (308.4 mg, 1 mmol) added propargyl alcohol (290µl, 5 mmol) at rt and kept in ultrasonic for agitation for 5 min till all starting get dissolve then added a catalyst H_2SO_4-Silica (5mg). after 2 days The reaction is quenche with sodium bicarbonate (Na_2CO_3) and then was washed with diethyl ether (3 x 50 mL) to remove unreacted reagent. No reaction occur starting material is recovered.

2-Acetamido-4,6-*O*-*p*-methoxybenzylidene-β-D-glucopyranoside (48, 52).
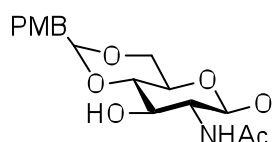
The procedure for the preparation of **45** was adapted from Ye *et. al.*1 2-acetoamido-β-D-glucopyranoside (36.7 g, 128 mmol) was dissolved in DMF (30.0 mL) and CH3CN (300 mL). *p*-Anisaldehyde dimethyl acetal (44.0 mL, 256 mmol) and camphorsulfonic acid (6.00 g, 25.6 mmol) were added. The reaction was stirred at rt for 12 h. The reaction was quenched with TEA and concentrated to afford an orange syrup. The product was purified by flash chromatography (50% → 70% EtOAc:hexanes) to afford **45** (36.3 g, 70%) as a white crystalline solid. Rf- 0.26 (50% EtOAc:hexanes).

^{1}H NMR (400 MHz, CDCl$_3$): δ = 7.39 (d, *J* = 9.0 Hz, 2H, C$_6$*H*$_4$OMe), 7.15 (d, *J* = 7.5 Hz, 2H, SC$_6$*H*$_4$Me), 6.88 (d, *J* = 9.0 Hz, 2H, C$_6$*H*$_4$OMe), 5.48 (s, 1H, MeOPhC*H*), 4.56 (d, *J* = 9.9 Hz, 1H, H-1), 4.35 (dd, *J* = 3.9, 10.5 Hz, 1H), 3.85 − 3.72 (m, 5H), 3.50 − 3.39 (m, 3H), 2.80 (br s, 1H, O*H*), 2.67 (br s, 1H, O*H*),; ^{13}C NMR (75 MHz, CDCl3): δ = 138.8, 138.2, 133.6, 132.1, 129.9, 129.4, 127.7, 113.7, 101.8, 88.7, 80.2, 74.5, 72.5, 70.5, 68.6, 55.3, 21.2.

3-O-Benzoyl-2-deoxy-4,6-O-p-methoxybenzylidene glucosepyranosyl (49):-
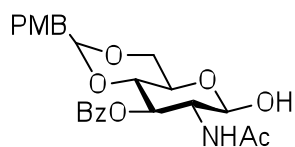
This glucosamine derivative (100mg, 0.29mmol) was dissolved in dry pyridine (2ml) and cooled to 0^0C.Benzoyl chloride (0.04ml, 0.32 mmol) was added and the reaction is stirred for 2 hrs.The reaction mixture was diluted with CH_2Cl_2, washed with $NaHCO_3$, brine and dried with Na_2SO_4.The concentrated material was chromatographed (toulene-acetone 2:1to 3:2) to give compound **46** (73mg, 57%).

^{1}H NMR (400 MHz, CDCl$_3$): 8.05 (2H, d, BzO), 7.56 (1H, t, BzO), 7.40-7.48 (4H, m, BzO, C$_6$H$_4$), 6.88 (2H, d,C$_6$H$_4$), 6.22 (1H, d, NH), 5.45 (1H, s,C$_6$H$_4$CH), 5.41 (1H, H-3), 5.39 (1H, H-1), 4.85 (1H, ddd, H-2), 4.23-4.29 (2H, m, H-4, H-6a), 3.99 (1H, d, H-6b), 3.94(1H,s, H-5), 3.75 (3H, s, OCH$_3$), 1.89 (3H, s, OCOCH$_3$); ^{13}C NMR (100 MHz, CDCl$_3$) ∂ 171.49, 167.25, ,160.37, 133.78, 130.59, 130.49, 130.39, 129.95, 128.94, 128.80, 127.92, 113.92, 100.83, 92.79, 74.28, 70.30, 69.85, 62.64, 55.65, 48.50, 23.67.

2-Acetamido-1,3,4,6-tetra-O-acetyl-2-deoxy-α-D-glucopyranose (50)
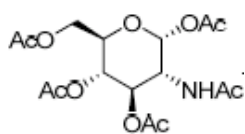
A solution of D-glucosamine hydrochloride (2.0 g, 9.3 mmol) in a mixture of 15 mL of anhydrous pyridine and 10 mL of acetic anhydride was stirred overnight at RT. The mixture was diluted with 60 mL of chloroform and washed successively with 50 mL of cold water, 50 mL of saturated sodium bicarbonate solution and then with portions of a 10% solution of cupric sulfate until disappearance of the deep blue pyridine-copper complex, and finally with water. After drying over Na_2SO_4, the chloroform was removed *in vacuo* and the crude product **47** was used directly to the next step without purification (75%).

^{1}H NMR (400 MHz, CDCl$_3$) δ: 1.92 (s, 3H), 2.03 (s, 3H), 2.04 (s, 3H), 2.07 (s, 3H), 2.18 (s, 3H), 3.97-4.00 (m, 1H), 4.05 (dd, J = 2.3, 12.5 Hz, 1H), 4.23 (dd, J = 4.1, 12.5 Hz, 1H), 4.47 (ddd, J = 3.6, 9.1, 10.4 Hz, 1H), 5.17-5.25 (m, 2H), 5.64 (d, J = 9.1 Hz, 1H), 6.15 (d, J = 3.6 Hz, 1H) ppm; ^{13}C NMR (100 MHz, CDCl$_3$) δ: 20.5, 20.6, 20.7, 20.9, 23.0, 51.0, 61.5, 67.4, 69.7, 70.6, 90.6, 168.6, 169.1, 169.9, 170.7, 171.7 ppm.

2-Acetamido-3,4,6-tri-O-acetyl-2-deoxy-α-D-glucopyranose (51)
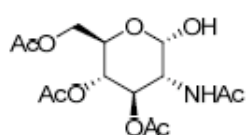
 A solution of methylamine in methanol (2 M, 4 mL) was added to a solution of **47** (1.64 g, 4.2 mmol) in THF (20 mL) at RT and the mixture was stirred for 2 hr. The mixture was concentrated *in vacuo* and the residue was purified by flash column chromatography on silica gel (EtOAc/CH$_2$Cl$_2$ = 1:1 to 3:1) to give compound **48** as a colorless oil (1.02 g, 70%).

^{1}H NMR (400 MHz, CDCl$_3$) δ: 1.94 (s, 3H), 1.99 (s, 3H), 2.00 (s, 3H), 2.01 (s, 3H), 4.06-4.11 (m, 1H), 4.17-4.27 (m, 3H), 5.07-5.12 (m, 2H), 5.21 (t, J = 3.7 Hz, 1H), 5.27 (t, J = 10.1 Hz, 1H), 6.10 (d, J = 9.4 Hz, 1H) ppm; ^{13}C NMR (100 MHz, CDCl$_3$) δ: 20.6, 20.7 (2C), 23.0, 52.3, 62.1, 67.3, 68.3, 71.0, 91.4, 169.5, 170.6, 171.0, 171.4 ppm.

General method for acetylation of sugar(55, 65):
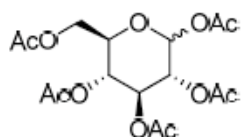
 Acetic anhydride (7.9 mL, 84 mmol) was added dropwise to a stirred solution of D-glucose(2.0 g, 11 mmol) in anhydrous pyridine (10 mL) at 0 °C, and the stirring continued at the same temperature for 17 hr [S3]. After addition of ice into the reaction mixture a powdery white solid precipitated. The precipitate was washed by water, NaHCO$_3$ solution, 2 N HCl

solution and water successively. After drying *in vacuo*, **52** (α and β mixture) was obtained as a white solid (3.96 g, 90%).

¹H NMR (400 MHz, CDCl3) δ: 2.00 (s, 6H), 2.01 (s, 12H), 2.02 (s, 3H),2.07 (s, 3H) 2.10 (s, 3H), 2.16 (s, 3H), 3.83 (dt, *J* = 2.0, 10.0 Hz, 1H), 4.06-4.11 (m, 3H), 4.27 (dd, *J* = 4.0, 8.4 Hz, 2H), 5.06-5.15 (m, 4H), 5.24 (t, *J* = 9.4 Hz, 1H), 5.45 (t, *J* = 9.8 Hz, 1H), 5.70 (d, *J* = 8.0 Hz, 1H), 6.31 (d, *J* = 3.6 Hz, 1H) ppm; ¹³C NMR (100 MHz, CDCl3) δ: 20.4, 20.5, 20.6 (2C), 20.8 (2C), 61.4, 67.7, 67.8, 69.1, 69.8, 70.2, 72.7 (2C), 89.0, 91.6, 168.7, 168.9 169.2, 169.3, 169.6, 170.0, 170.2, 170.5, 170.6 ppm.

2,3,4,6-Tetra-O-acetyl-α-D-glucopyranose (56, 66)
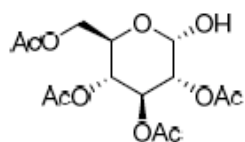
A solution of methylamine in methanol (2 M, 2.7 mL) was added to a solution of **52** (1.05 g, 2.7 mmol) in THF (10 mL) at RT and the mixture was stirred for 2 hr. The mixture was concentrated in vacuo and the residue was purified by flash column chromatography on silica gel (EtOAc/Hexane = 1:3 to 1:1) to give compound **53** as a colorless oil (0.64 g, 68%).

¹H NMR (400 MHz, CDCl₃) δ: 2.01 (s, 3H), 2.03 (s, 3H), 2.08 (s, 3H), 2.09 (s, 3H), 3.44 (br s, 1H), 4.11-4.14 (m, 1H), 4.21-4.28 (m, 2H), 4.89 (dd, *J* = 3.6, 9.9 Hz, 1H),

5.08 (t, *J* = 9.9 Hz, 1 H), 5.45-5.46 (m, 1H), 5.53 (t, *J* = 9.9, Hz, 1H) ppm. ¹³C NMR (100 MHz, CDCl₃) δ: 20.6, 20.7 (3C), 61.9, 67.2, 68.5, 69.8, 71.0, 90.1, 169.6, 170.1, 170.2, 170.8 ppm.

6-*O*-trityl-1-methoxy-D-glucopyranoside (58).
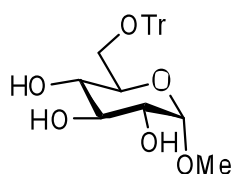
1-methoxy-α-D-glucopyranoside (Tetrol) (12.3 g, 0.04 mol) and trityl chloride (13.2 g, 0.05 mol) were dissolved in pyridine (100

ml) and stirred under argon. After 24 h dimethylaminopyridine (500 mg, 4.67 mmol) and trityl chloride (10 g, 0.04 mol) were added and the mixture stirred for a further 5 h, at which point t.l.c. (ethyl acetate) indicated the formation of a major product (*R*f 0.5) and the absence of starting material (*R*f 0.1). The reaction mixture was concentrated *in vacuo* and the residue taken up in dichloromethane (200 ml), washed with ammonium chloride (2 × 200 ml of a saturated aqueous solution), sodium hydrogen carbonate (2 × 200 ml of a saturated aqueous solution) and brine (200 ml). The organic layer was then dried (MgSO$_4$) and concentrated *in vacuo* to afford the crude triol.

2,3,4-tri-*O*-benzyl-6-*O*-trityl-1-methoxy-D-glucopyranoside (59).
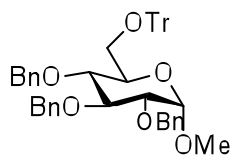
The crude residue of 55 was dissolved in dimethylformamide (100 ml) and benzyl bromide (27 ml, 0.23 mol) was added. The solution was cooled to 0 °C and sodium hydride (11 g of a 60% dispersion in mineral oil, 0.28 mol) was added portion wise to the stirred solution over 15 min. The reaction mixture was allowed to warm to room temperature overnight. After 16 h, t.l.c. (ethyl acetate : petrol, 1 : 3) indicated the formation of a major product (*R*f 0.5) and the absence of starting material (*R*f 0.1). Methanol (100 ml) was added and the solution stirred for 30 min, the reaction mixture was then concentrated *in vacuo* (co-evaporation with toluene, 3 × 100 ml) and the residue taken up in dichloromethane (200 ml). The resulting solution was washed with water (200 ml) and brine (3 × 100 ml), dried (MgSO$_4$) and concentrated *in vacuo*. The residue was purified by flash column chromatography (ethyl acetate : petrol, 1 : 4) to afford fully protected glycoside **56** (21 g, 61%) as a white crystalline solid.

^{1}HNMR (400 MHz, CDCl$_3$) 3.45 (3H, s, OC*H*3), 3.32 (1H, dd, *J*5,6 4.1 Hz, *J*6,6′ 10.1

Hz, H-6), 3.37–3.50 (1H, m, H-5), 3.62 (1H, at, J 9.1 Hz, H-2), 3.67 (1H, dd, J5,6′ 1.4 Hz, H-6′), 3.70 (1H, at J 9.0 Hz, H-3), 3.82 (1H, at, J 9.4 Hz, H-4), 4.37, 4.71 (2H, ABq, JAB 10.4 Hz, PhCH2), 4.70 (1H, d, J1,2 9.6 Hz, H-1), 4.81, 4.97 (2H, ABq, JAB 10.2 Hz, PhCH2), 4.86, 4.91 (2H, ABq, JAB 10.8 Hz, PhCH2); ^{13}C (100.6 MHz, CDCl$_3$) 62.4 (t, C-6), 75.0, 75.4, 76.0 (3 × t, 3 × PhCH2), 77.2, 86.5, 137.7, 138.2, 138.3, 143.9 (6 × s, ArC), 77.8 (d, C-4), 78.8 (d, C-5), 80.7 (d, C-2), 86.8 (C-3), 87.7 (d, C-1), 127.0, 127.7, 127.8, 127.9, 128.0, 128.1, 128.2, 128.5, 128.8, 129.7, 129.8, 132.8 (12 × d, ArCH);

6-hydroxyl-2,3,4-tri-*O*-benzyl-1-methoxy-α-D-glucopyranoside (60).
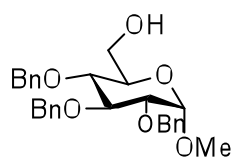
Fully protected glycoside **56** (2.0 g, 2.51 mmol) was suspended in a p-Toulensulphonic acid and refluxed at 80 °C for 26 h at which point t.l.c. (ethyl acetate : petrol, 1 : 4) indicated the formation of a major product (*R*f 0.3) and almost complete consumption of starting material (*R*f 0.6). The reaction mixture was concentrated *in vacuo* (co-evaporation with toluene) and the residue taken up in dichloromethane (200 ml), washed with sodium hydrogen carbonate (200 ml of a saturated aqueous solution), brine (200 ml), dried (MgSO$_4$) and concentrated *in vacuo* to afford alcohol **57** (1.26 g, 92%) as a white crystalline solid,

^{1}H (400 MHz, CDCl$_3$) 1.98 (1H, at, J 6.6 Hz, OH), 3.39 (1H, ddd, J4,5 9.8 Hz, J5,6 5.0 Hz, J6,6′ 10.1 Hz, H-6), 3.37–3.50 (1H, m, H-5), 3.62 (1H, at, J 9.1 Hz, H-2), 3.67 (1H, dd, J5,6′ 2.7 Hz, H-5), 3.48 (1H, dd, J1,2 8.8 Hz, J2,3 9.5 Hz, H-2), 3.56 (1H, at, J 9.4 Hz, H-4), 3.61–3.74 (1H, m, H-6), 3.74 (1H, at, J 9.1 Hz, H-3), 3.90 (1H, ddd, J5,6′ 2.3 Hz, J6,6′ 11.8 Hz, J6′,OH 5.4 Hz, H-6′), 4.67 (1H, d, H-1), 4.67, 4.88 (2H, d ABq, JAB 11.1 Hz, PhCH2), 4.79, 4.95 (2H, ABq, JAB 10.3 Hz, PhCH2), 4.89, 4.94 (2H, ABq, JAB 10.8 Hz, PhCH2), 7.13–7.46 (19H, m, ArH).

^{13}C (100.6 MHz, CDCl$_3$) 62.1 (t, C-6), 75.1, 75.5, 75.8 (3 × t, 3 × PhCH2), 77.6 (d, C-4), 79.2 (d, C-5), 81.1 (d, C-2), 86.6 (C-3), 87.8 (d, C-1), 127.8, 127.9, 128.0, 128.2, 128.5, 129.8, 132.7 (7 × d, 19 × ArCH).

2,3,4-Tri-O-benzyl-6-iodo-1-methoxy-α-D-glucopyranoside (61):-

To a stirred solution of 57 (4.39 g, 11.7 mmol) and Ph$_3$P (3:69 **g,** 14.1 mmol) in THF (25 mL) at 0^{0}C under N$_2$ was added diethyl azodicarboxylate (2.22 mL, 14.1 mmol). After the solution was stirred at 0^{0}C for 5 min, iodine (1g) was added, and the resulting mixture was stirred at room temperature for 19 h. The mixture was diluted with EtOAc and washed with saturated aqueous NaHCO$_3$, solution and brine and dried. Evaporation of the solvent left a syrup, which was purified on a column of silica gel (150 g) with EtOAc-toluene (1:20) to afford **58** (4.19 g, 74%) **as** a colorless syrup:

^{1}H NMR (400 MHz CDCl$_3$) 3.39 (1H, ddd, J4,5 9.8 Hz, J5,6 5.0 Hz, J6,6′ 10.1 Hz, H-6), 3.37–3.50 (1H, m, H-5), 3.62 (1H, at, J 9.1 Hz, H-2), 3.67 (1H, dd, J5,6′ 2.7 Hz, H-5), 3.48 (1H, dd, J1,2 8.8 Hz, J2,3 9.5 Hz, H-2), 3.56 (1H, at, J 9.4 Hz, H-4), 3.61–3.74 (1H, m, H-6), 3.74 (1H, at, J 9.1 Hz, H-3), 3.90 (1H, ddd, J5,6′ 2.3 Hz, J6,6′ 11.8 Hz, J6′,OH 5.4 Hz, H-6′), 4.67 (1H, d, H-1), 4.67, 4.88 (2H, d ABq, JAB 11.1 Hz, PhCH2), 4.79, 4.95 (2H, ABq, JAB 10.3 Hz, PhCH2), 4.89, 4.94 (2H, ABq, JAB 10.8 Hz, PhCH2), 7.13–7.46 (19H, m, ArH);

^{13}C (100.6 MHz, CDCl3) 62.1 (t, C-6), 75.1, 75.5, 75.8 (3 × t, 3 × PhCH2), 77.6 (d, C-4), 79.2 (d, C-5), 81.1 (d, C-2), 86.6 (C-3), 87.8 (d, C-1), 127.8, 127.9, 128.0, 128.2, 128.5, 129.8, 132.7 (7 × d, 19 × ArCH).

2, 3, 4-tri O-benzyl-6-deoxy-β-L-arabino-hex-5-enopyranoside (62):-
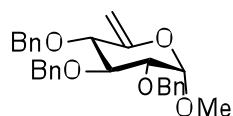
A mixture of 58 (31mg) and DBU (0.035 ml) in Toulene (3ml) was heated at 80^0C for 2 days. The mixture was dilutes with ethyl acetate and washed successively with diluted Hydrochloric acid solution, saturated aq.sodium hydrogenchloric acid solution and brine,and dried. Evaporation of solvent left a residue, which was purified on a column of silica gel with acetone –hexane (1:6) to give 25mg (95%) of compound 59 as a colourless syrup.

^{1}HNMR (400 MHz, CDCl₃): 3.60 (3H, s, OMe), 3.64 (1H dd, H-3), 3.78 (1H, dd, H-2), 4.45 (1H, d, H-1), 4.58 (1H, d, benzyl), 4.67 (1H, bs, H-6), 4.70 (1H, d, benzyl), 4.73 (1H, d, benzyl), 4.80 (1H, bs, H-6'), 4082 (1H, d, benzyl), 5.73 (1H, d, H-4), and 7.26-7.36 (15H, m, Phenyl).

2, 3, 4,-di-O-benzyl-2, 3, 4, 5-tetrahydroxycyclohexanone (63):-
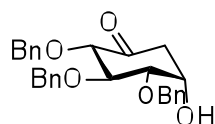
Treatment of compound 58 (398mg) with mercury (II) Chloride (43 mg) in acetone-water stirred at rt for 3 hrs. The mixture was partially evaporated to remove acetone and extracted with ethyl-acetate. The solvent is removed on rota to gave 303 mg (80%) of a 59 as a colourless syrup.

General method for synthesis of disaccharide and trisaccharide (61, 63, 67):A mixture of 1-hydroxy donor (0.514 g, 1.00 mmol), Ph₂SO (0.485 g, 2.40 mmol), and TTBP (0.248 g, 1.00 mmol) was coevaporated with toluene two times to remove traces of water, dissolved in DCM (20 mL), and further dried by stirring over molecular sieves for 15 min. At -60 °C Tf₂ O (0.177 mL, 1.05 mmol) was added and the temperature was raised to -40 °C. After 1 h. a solution of acceptor **5** (0.505 g, 1.00 mmol) in DCM (20 mL) was slowly added, and the reaction mixture was allowed to

warm to 0 °C. Dry Et$_3$N (1.35 mL, 10 mmol) was added, the reaction was washed with NaHCO3 (aq), and the organic layer was dried over MgSO$_4$ and concentrated *in Vacuo*. Purification by column chromatography yield a white solid.

Chapter-5

Natriuretic Peptides

5.1: Natriuretic Peptide

Natriuresis is the process of excretion of abnormally large amounts of salt in the urine. The word comes from the Latin term *natrium*, which means "sodium" and the Greek term *ouresis*, which means, "making water." Natriuresis is similar to diuresis, the excretion of an unusually large quantity of urine, except that in natriuresis the urine is exceptionally salty[197]. Natriuretic peptides are endogenous hormones that are released by the heart in response to myocardial stretch and overload[198]. Three mammalian NPs have been identified and characterized, including atrial natriuretic peptide (ANP or atrial natriuretic factor), B-type natriuretic peptide (BNP), and C-type natriuretic peptide (CNP)[199-200]. Moreover, Dendroaspis natriuretic peptide (DNP) was isolated from the venom of Dendroaspis angusticeps (the green mamba snake) [201] and DNP-like immunoreactivity has also been detected in the human plasma and myocardium[202]. However, the gene for DNP has yet to be identified in the human genome[203], whereas ANP, BNP, and CNP are known to be genetically distinct[199-200]. In addition, urodilatin (URO) is an NP that has been isolated in human urine. Urodilatin originates from the same common precursor as ANP, but is differentially processed[204]. All five NPs share structural similarities in a 17-amino acid core ring and a cysteine bridge (Fig. 1)[199,201].

Both ANP and BNP are produced by myocardial cells[205]. They bind to natriuretic peptide receptor A (NPR-A)[206], which is widely distributed in the human myocardium[207]. Both NPs are released in response to myocardial wall stretch[205] which is exaggerated in heart failure (HF) where cardiac filling pressures are elevated[208-209]. Activation of NPR-A results in an increase in cyclic guanosine monophosphate (cGMP), which mediates natriuresis, inhibition of renin and aldosterone, as well as

vasorelaxant, anti-fibrotic, anti-hypertrophic, lusitropic and other effects (Fig. 2)[200,205].

C-type natriuretic peptide was first identified in porcine brain[210]. It is of endothelial and renal cell origin with a wide distribution in the vasculature, brain, bone, epithelium, and other tissues[200,211–213]. It is thought to act via a paracrine mechanism[214]. CNP preferentially binds to the natriuretic peptide receptor-B (NPR-B) [206, 215], which is in abundance in veins as compared with arteries[216]. Activation of NPR-B by CNP increases cGMP in vascular smooth muscle cells and mediates vasorelaxation[217]. Additional actions of CNP include reduction in cardiac preload in vivo[218]; regulation of vascular tone[217] inhibition of vascular smooth muscle cell proliferation, hypertrophy of cardiac myocytes and growth of fibroblasts [217, 219–221]; suppression of aldosterone release[222-223]; attenuation of myocardial ischemia-reperfusion injury (IRI) [224-225]; and prevention of remodeling following myocardial infarction[226]. CNP might also contribute to the anti-mitogenic and vasodilatory effects of ANP and BNP, as CNP secretion can be stimulated by ANP and BNP [227]. However, it lacks significant natriuretic or diuretic effects [218, 223].

The natriuretic family

Four peptides related to each other through biochemistry and physiological function:
- Atrial natriuretic peptide (ANP)
- Brain (or B-type) natriuretic peptide (BNP)
- C-type natriuretic peptide (CNP)
- Urodilatin, a slightly extended form of ANP
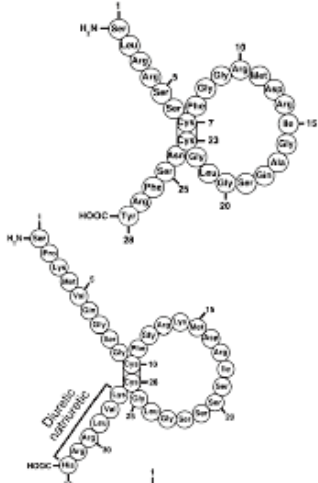
Biochemistry
- Common 17-amino-acid ring structure
- Ring structure highly conserved
- 11/17 Amino acids are homologous
- Ring structure essential for physiologic activity

Physiologic function
- Diverse effects on tissues involved in sodium regulation and blood pressure homeostasis

ANP
- Diuretic
- Natriuretic
- Vascular relaxation
- Inhibition of RAAS, SNS
- In atria

CNP
- No natriuresis or diuresis
- Potent vasodilator

URODILATIN

113

Fig-1: Structures of natriuretic peptides and multiple sequence alignment of NPs.
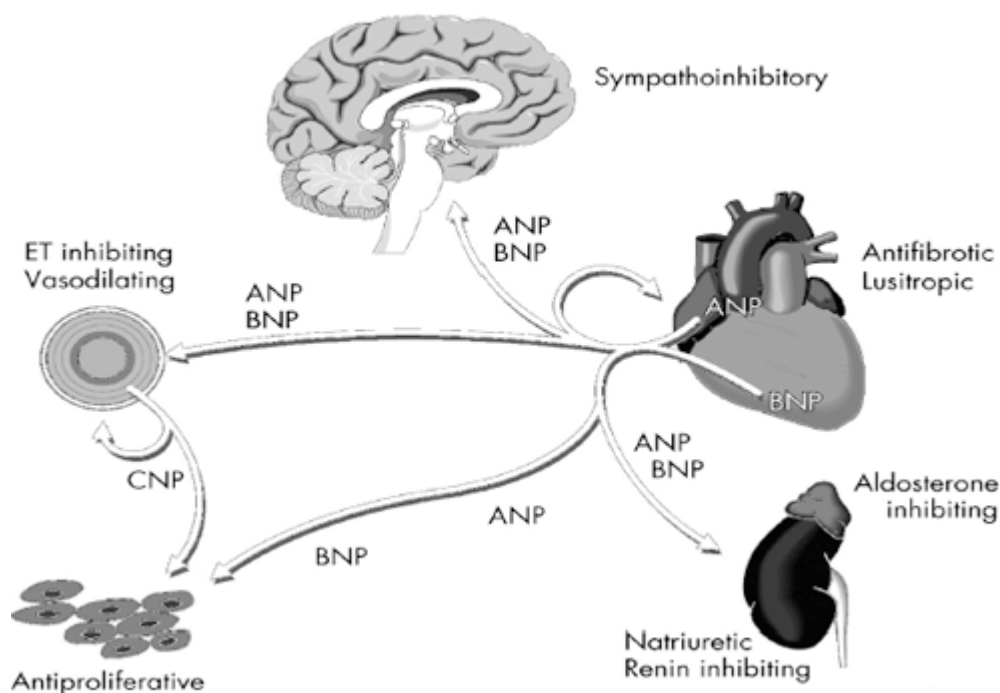
The above diagram shows interaction of heart, kidney, vasculature, brain, and renin angiotensin-aldosterone system with natriuretic peptide system. ET=endothelin; ANP=A-type natriuretic peptide; BNP=B-type natriuretic peptide; CNP=C-type natriuretic peptide. Reprinted with permission from Congest Heart Fail. 2004;10(5 suppl 3):1–30.

Atrial natriuretic peptide

Atrial natriuretic peptide (ANP), is a powerful vasodilator, and a protein (polypeptide) hormone secreted by heart muscle cells[228-229]. It is involved in the homeostatic control of body water, sodium, potassium and fat (adipose tissue). It is released by muscle cells in the upper chambers of the heart (atrial myocytes), in response to high blood pressure. ANP acts to reduce the water, sodium and adipose loads on the circulatory system, thereby reducing blood pressure[228].

Physiological endocrine and cardiac actions of atrial natriuretic peptide (ANP).
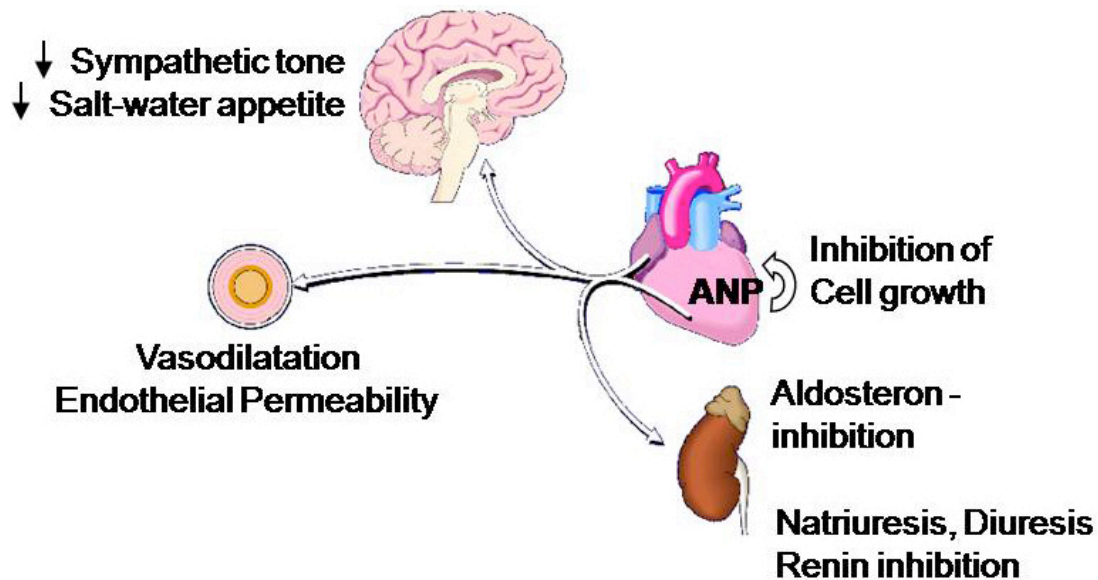
Fig-2: Physiological endocrine and cardiac actions of atrial natriuretic peptide (ANP).

Structure of ANP:-

ANP is a 28-amino acid peptide with a 17-amino acid ring in the middle of the molecule. The ring is formed by a disulfide bond between two cysteine residues at positions 7 and 23. ANP is closely related to BNP (brain natriuretic peptide) and CNP (C-type natriuretic peptide), which all shares the same amino acid ring.

The circulating (biological active) form of human ANP, as shown in the figure, comprises a 28 amino acid peptide with a 17 amino acid ring closed by a disulfide bond between two cysteine residues. Its amino acid sequence is highly conserved across species.
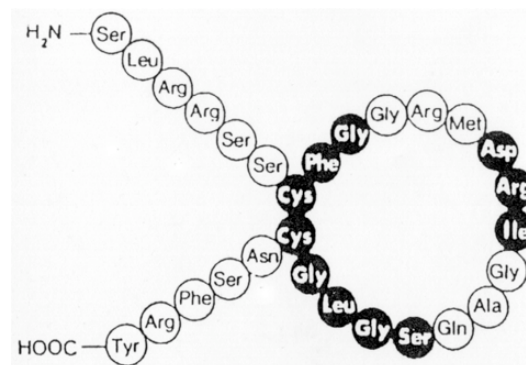
Fig-3: ANP (1-28) - the biologically active hormon

Function of Natriuretic Peptides

The natriuretic peptides can affect systemic blood pressure by several mechanisms, including modification of renal function and vascular tone, counteracting of the renin-angiotensin aldosterone system and action on brain regulatory sites. These systems maintain a balance which ensures relative constancy of body electrolyte and water content and circulatory homeostasis.

Main biologic actions of natriuretic peptides

•cause of natriuresis and diuresis

•cause of vasodilatation

•suppression of renin action

•suppression of aldosterone action

•suppression of sympathetic activity

•suppression of antidiuretic hormone (ADH)

•inhibition of growth of vascular smooth muscle

Brain-type natriuretic peptide

A second natriuretic peptide (brain-type natriuretic peptide; BNP) is a 32-amino acid peptide that is synthesized within the ventricles (as well as in the brain where it was first identified). BNP is first synthesized as prepro-BNP, which is then cleaved to pro-BNP and finally to BNP. Like ANP, BNP is released by the same mechanisms that release ANP, and it has similar physiological actions. Proteolysis of pro-BNP (108 amino acids) results in BNP (32 amino acids) and the N-terminal piece of pro-BNP (NT-pro-BNP; 76 amino acids). Both BNP and NT-pro-BNP are sensitive, diagnostic markers for heart failure in patients. It's produced in response to stretching of the ventricles due to the increased blood volume and higher levels of extracellular fluid (fluid overload) that accompany congestive heart failure. It acts as a natural diuretic,

116

eliminating fluid, relaxing blood vessels and funneling sodium into the urine.

When your heart is damaged, your body secretes very high levels of B-type natriuretic peptide into your bloodstream in an effort to ease the strain on your heart. The levels may also rise if you have new or increasing chest pain or after a heart attack. BNP is co-secreted along with a 76 amino acid N-terminal fragment (NT-proBNP) that is biologically inactive. BNP binds to and activates the atrial natriuretic factor receptors NPRA, and to a lesser extent NPRB, in a fashion similar to atrial natriuretic peptide (ANP) but with 10-fold lower affinity. The biological half-life of BNP, however, is twice as long as that of ANP, and that of NT-pro BNP is even longer, making these peptides better targets than ANP for diagnostic blood testing[230].
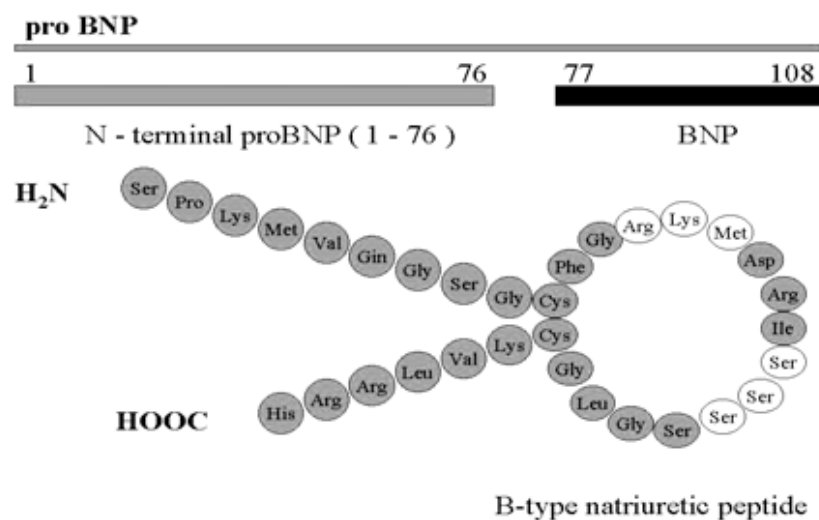
Fig-4: B-type natriuretic peptide

Brain natriuretic peptide (BNP) is synthesized as a high molecular weight precursor; Biologicaly active form BNP has amino acid sequence 77-108 and the N-terminal proBNP the sequence 1-76. Lower diagram gives the amino acid sequence and 17 amino acid ring structure that is common to all natriuretic peptides.

C-type natriuretic peptide

CNP was originally isolated as a 22-amino-acid peptide from the porcine brain[231]. C-type natriuretic peptides are produced by cells that line the blood vessels. They cause relaxation of blood vessels, helping to lower blood pressure. Unlike A-type and B-type natriuretic peptides, they don't have direct natriuretic activity.

The biological effects of CNP show important differences from those of ANP and BNP.C-type natriuretic peptide (CNP) has recently been identified as an important anabolic regulator of endochondral bone growth, but the molecular mechanisms mediating its effects are not completely understood[232].

Bone formation occurs through the related, but distinct processes of intramembranous and endochondral ossification[233-234]. While the former is responsible for the formation of bones directly from precursor cells, such as the majority of the skull, the latter is responsible for the development of long bones, ribs, and vertebrae through a cartilage intermediate. In endochondral ossification, mesenchymal cells condense and begin to differentiate into chondrocytes, some of which later form the growth plate that controls longitudinal growth of endochondral bones[235]. The growth plate zones consists of resting, proliferating, and terminally differentiated hypertrophic chondrocytes, each of which are characterized by the expression of specific markers[236-237]. This organization of the growth plate and the coordinated proliferation and hypertrophy of chondrocytes are responsible for elongation of bones and eventually determine final bone length. Hypertrophic chondrocytes are thought to undergo apoptosis, and simultaneously their surrounding cartilaginous matrix is degraded and replaced by bony tissue, produced by cells entering through vascularization of hypertrophic cartilage. The intricate control mechanisms regulating the proliferation, differentiation and apoptosis of chondrocytes as well as the

118

subsequent vascular invasion are not completely understood. However, disturbances of these processes can result in numerous diseases such as chondrodysplasias and other growth disorders, demonstrating the need for a better understanding of the pathways involved[236-238, 241].

C-type natriuretic peptide (CNP) has recently been shown to be an important regulator of endochondral ossification. Earlier studies have demonstrated that CNP stimulates bone growth through enhanced proliferation, mineralization and extracellular matrix synthesis[242,244-245]. Recently a patent appeared on its application in the treatment of skeletal dysplasia[246].

Structure

C-type natriuretic peptide is structurally related to atrial natriuretic peptide (ANP) and brain natriuretic peptide (BNP).
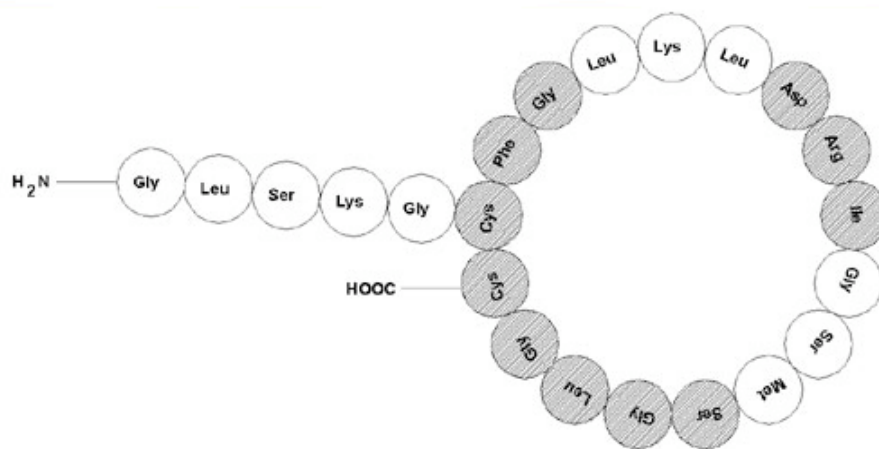
Fig-5: C-type natriuretic peptide

Natriuretic peptides (NPs) are a family of structurally related hormone/paracrine factors. NPs mediate a diverse array of physiological effects ranging from blood pressure control to endochondral ossification[247-248]. This broad array of responses is achieved from the distinct actions of individual natriuretic peptides interacting with specific guanylyl cyclase receptors. Atrial natriuretic (ANP) and B-type natriuretic

119

(BNP) peptides are secreted prevalently from the cardiac atria and ventricles, respectively. C-type natriuretic peptide (CNP) primarily stimulates long bone growth and its function is still not well understood. Moreover, a fourth class of NPs, the Dendoraspis natriuretic peptide (DNP), was isolated from the venom of *Dendroaspis angusticeps*[249-250].

The action of NPs is mediated through their cell-surface receptors, NPRs, which are a family of homologous single-transmembrane gylcosylated receptors (NPR-A, NPR-B, NPR-C). NPR-A and B transduce the NP signal through a large cytoplasmic domain with guanylyl cyclase activity[251-252]. ANP and BNP activate the transmembrane guanylyl cyclase NPR-A, whereas CNP activates the related cyclase NPR-B. A third natriuretic peptide receptor, natriuretic peptide receptor-C (NPR-C), clears natriuretic peptides from the circulation through receptor-mediated internalization and degradation. However, a signaling function for the receptor has been suggested as well[253-255]. Intriguingly, the C-terminal fragments generated by proteolysis of osteocrin (Ostn) are homologous to the NPs, specifically in the region matching the ring structure of the NPs, where the residues demonstrated to be essential for binding of NPs to their receptors are highly conserved. Proteolytic Ostn fragments have been shown to selectively bind the NPR-C receptor, but not the guanylate cyclase receptors NPR-A and B[256-257].

Natriuretic peptides are also relevant for their potential therapeutic and clinical applications[248,258-259]. In fact, measurement of serum BNP levels is used as a diagnostic indicator for heart failure, and synthetic analogues of ANP and BNP have been approved for heart failure treatment[260-261].

Bifunctional chimeric natriuretic peptides have also been proposed as therapeutics[262-263]. From an evolutionary perspective, previous studies indicated that

ANP and BNP evolved from CNP gene duplication events, suggesting that CNP is the most ancient family member[264]. From a structural perspective, NPs share a common ring structure of 17 amino acids, in which a disulfide bond between two conserved cysteine residues is formed. The common ring is generally accompanied by short head and tail segments, i.e., extensions from the amino acid carboxyl termini of the ring (Fig. 1A). Notably, extensive structure-activity studies of NPs have converged on the idea that the residues within the cyclic loop are largely responsible for receptor selectivity, whereas the flanking residues outside the ring can modulate affinity [265-266].

Natriuretic peptides have therapeutic potential[267] and have already found application into the clinics, especially ANP and BNP. Measurement of serum BNP levels is used in the clinic as a diagnostic indicator for heart failure, and synthetic analogues of both of these peptides have been approved in some countries for the treatment of heart failure [268]; trials are underway to determine the most effective use of these peptides.

Table 1. Genetically engineered mice with alterations in the natriuretic peptide system

Genetic alteration	Cardiovascular phenotype	References
ANP knockout	Salt sensitive hypertension	John *et al.* 1995
ANP overexpression	Hypotension	Steinhelper *et al.* 1990
BNP knockout	Normal blood pressure, cardiac fibrosis, no LVH	Tamura *et al.* 2000
BNP overexpression	Hypotension	Ogawa *et al.* 1994
NPR_A knockout	Hypertension, LVH with cardiac fibrosis, sudden death	Lopez *et al.* 1995, Oliver *et al.* 1997
NPR_A overexpression (cardiomyocytes)	Normal blood pressure, decreased LV weight	Kishimoto *et al.* 2001
NPR_A overexpression (non tissue specific)	Hypotension, protection from high dietary salt	Oliver *et al.* 1998
NPR_C knockout	Hypotension	Matsukawa *et al.* 1999
ANP, atrial natriuretic peptide; BNP, B-type natriuretic peptide; LVH, left ventricular hypertrophy; NPR_X, natriuretic peptide receptor subtype.		

5.2: Aim of work:

Concerning CNP, recently a patent appeared on its application in the treatment of skeletal dysplasia[269]. The significance of the CNP/GC-B/NPR-C axis in longitudinal bone growth is now widely recognized[270-272] while the functional consequences of the CNP/GC-B/NPR-C axis on osteoblasts are still unknown.

We present here computational structural analysis of the three human NP in solution, the synthesis and preliminary biological assays of a short fragment of CNP, $I^{14}GSM^{17}$, together with one small mimetic, GGSM. To date, only few full-length mutants of CNP have been prepared[273] but no data are available on biological activity for short peptide sequences derived thereof.

In our studies, we have also present some preliminary results regarding an ongoing research project focused on the study of the effect of different fragments of CNP on osteogenesis and chondrogenesis compared to the full-length peptide. At first, sequence similarity among the NPs class and a conformational investigation by molecular dynamics simulations of CNP in comparison to ANP and BNP were carried out. The primary sequence of CNP was aligned to the other NPs known sequences and to the C-terminal fragment of the osteocrin peptide, which has been recently shown to present homology to NPs and to interact with the NPR-C receptor (see Figure 1)[276]. Extensive structure-activity studies of NPs have converged on the idea that the residues within the cyclized loop are largely responsible for receptor selectivity[274].

5.2.1: Studies on NP's

Therefore we focused on the analysis of the cyclic portion of the peptides. From the sequence alignment of NPs, it turns out that ANP and BNP present higher similarity when compared to CNP (see Figure 1). In particular, differences between CNP and ANP/BNP are located mainly in two regions of the cyclized loop (4–6 and 10–12). The action of the three main members of the NP family (ANP, BNP, and CNP) is mediated through their cell-surface receptors, NPRs.[1] In particular, NPR-A and NPR-B transduce the NPs signal through a large cytoplasmic domain and they are specific for ANP/BNP and CNP, respectively. The differences in the cycle primary sequences between ANP/BNP and CNP can reflect differences in the activity and specificity for different NPRs.
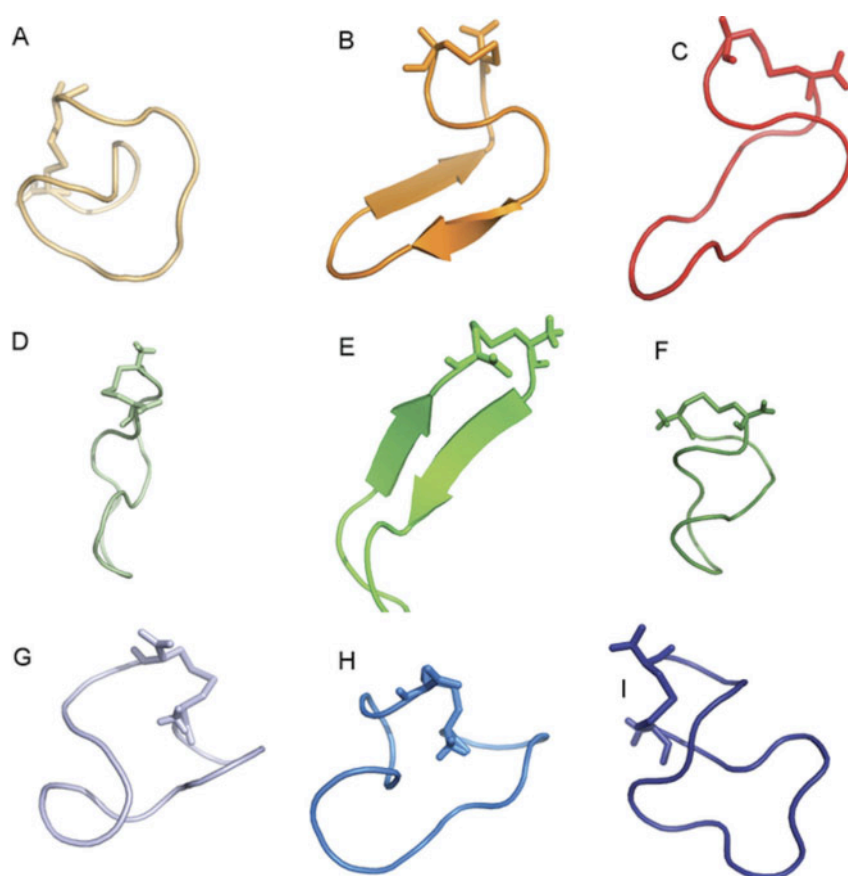
Fig-6: Average structures from cluster analysis of peptide simulations. The average

structures from the three-main populated clusters of ANP (A–C), BNP (D–F) and, CNP (G–I) simulations are shown.

5.2.2: Study of NPs in Solution

The X-ray structure of NPs used as initial structure for MD simulations are derived by the complexes between the receptor NPR-C and the peptides. No intramolecular stabilization of the peptides were observed in these complexes, suggesting that they are not stable solution structures. In fact, the structure of the free peptides rapidly diverged during MD simulations from the bound-conformations (see Figure 2). Therefore, to better characterize the conformations assumed from the peptides in solutions, cluster analysis of main chain rmsd matrices were carried out and the average structures from the main populated clusters were reported in Figure 2. Several conformations are explored during the simulations indicating a high flexibility of the peptides.

Moreover it turns out that transient formation of b-strand structures are observed only in ANP (Figure 2B) and BNP (Figure 2E) simulations. They involve some of the ANP and BNP typical residues, such as the polar ones at position 17, replaced by methionine in CNP (see Figure 1).

The high conformational variability of the peptides is also confirmed by analysis of rmsf as flexibility index. The Ca rmsf per residue indicates the intensity of fluctuation of each residue with respect to the average structure. Coherently with the high conformational variability of the peptides, the rmsf profiles for each residue are characterized by significantly high values, indicating the absence of stable secondary structure elements. Moreover, the rmsf profiles of ANP and BNP present a higher similarity than rmsf profiles of CNP, suggesting that the dynamics of peptides with different specificity for NP receptors are strictly different.

In summary, none NP structure corresponding to the bound conformation to the NPRs can be isolated during the simulations in agreement with the hypothesis that NP bound conformations are not stable in solution and that induced-fit mechanisms are involved in the formation of NP-NPR complexes. The differences in activity and NPR specificity of CNP and ANP/BNP seems to be correlated to different amino acid composition of the cyclized loop, different flexibility patterns (see Figure 7) and free conformations (see Figure 6) explored during the simulations. These observations prompted the study of the biological activity of significant fragments of CNP, with particular regard to the 14–17 region of the peptide, in which differences in the amino acid composition seem to be strongly correlated with conformational properties, activity, and specificity of the three NPs (op. seems to be determinant for different conformational properties, activity and specificity of the three NPs).
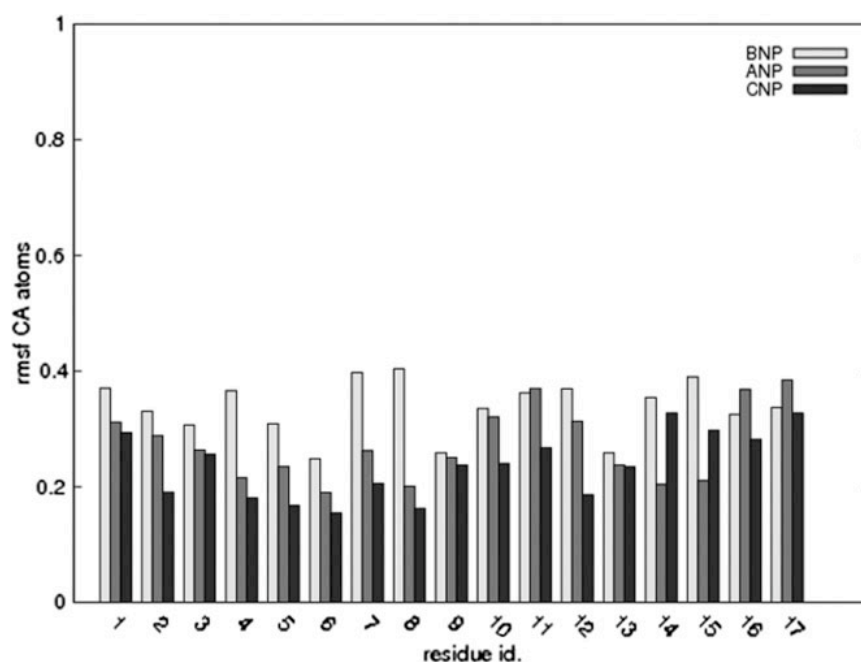
FIGURE-7: Rmsf as a flexibility index. Ca rmsf per residue calculated on peptide simulations discarding the first 3 ns of each simulation.
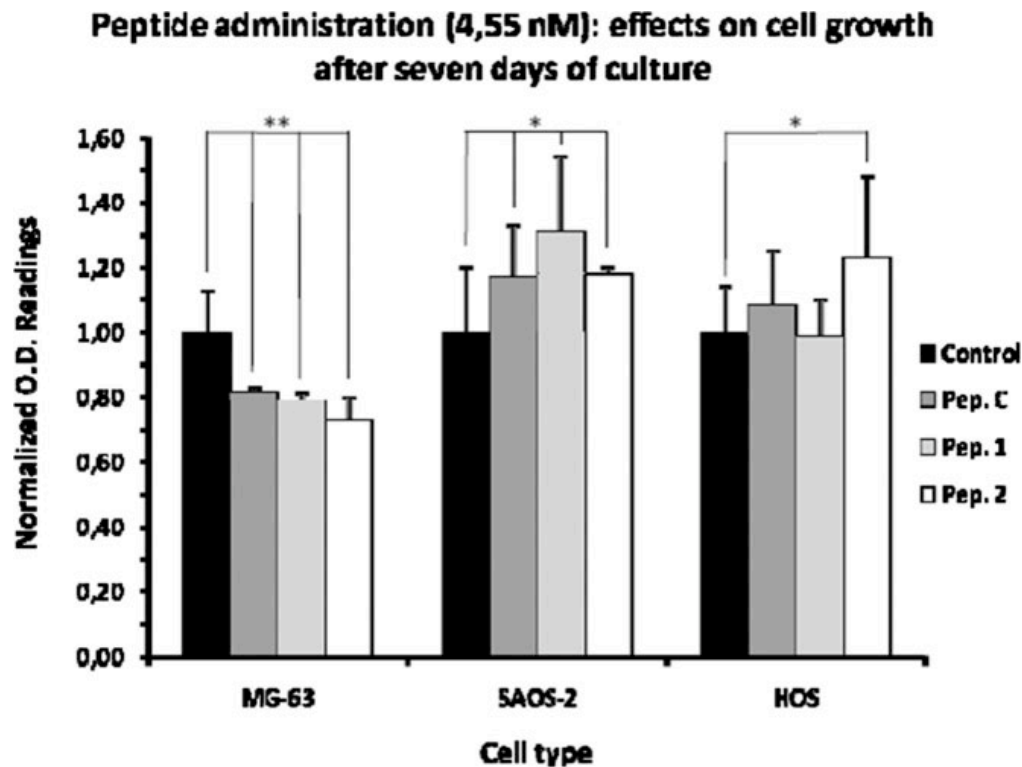
FIGURE 8 Effects of the administration of the peptides under testing on the growth kinetics of MG-63, SAOS-2, and HOS cells; depicted results refer to data obtained exposing cells to peptides at the concentration of 4.55 nM for 7 days. Results are normalized to control values for each cell type used. Each data point represents the average of six determinations performed in two different experiments. Error bars depict standard deviation values (n 1/4 6); *: $P < 0.05$; **: $P < 0.001$ (P values refer to control vs. treated cells).

5.2.3: **Synthesis and Biological assay:-**

Since it's not clear whether the full-length form of CNP is the only active molecule or if short fragments can exert biological effects, we started our study with the synthesis of a very short sequence, $I^{14}GSM^{17}$ (Peptide 1), containing one of the two putative sequences responsible for the biological activity, which are not conserved in the natriuretic peptide family. In addition, we also prepared a mimetic where the fully conserved isoleucine is changed into glycine, that is, $G^{14}GSM^{17}$ (Peptide 2). The peptides were synthesized manually using standard Fmoc chemistry protocols. The two fragments were then evaluated in three different osteosarcoma cell lines, using

126

the full length CNP peptide (CAS number 127869-51-6, Calbiochem USA) as control.

 Peptides were preliminary tested for their ability to influence cell growth of human osteosarcoma cell lines, since the CNP peptide was previously shown to be involved in endochondral ossification and bone formation. Growth kinetics were assessed at three different peptide concentrations (455, 45.5, or 4.55 nM) for peptide 1, peptide 2, and CNP on three human osteosarcoma cell lines, MG-63,[277] Saos-2,[278] and HOS[279]. Control cells, cultured in the absence of peptide, were assessed in parallel. Results are shown in Figure 4, for the minimum concentration tested. Peptides displayed different effects upon the cell type used. All peptides slightly reduced proliferation of MG-63 cells already after 5 days of culture (data not shown), peptide 2 being the most active after 7 days (-27% with respect to controls). By converse, in SAOS-2 cells, proliferation was increased, although to a relative extent, with peptide 1 inducing the maximal effect (+31%). A similar induction was obtained in HOS cells, but only when peptide 2 was added to the growth medium (see Figure 4). Cell cycle arrest and activation of bone matrix proteins transcription are sequential events that lead to osteoblast differentiation[280]. Any variation of the cell proliferation rates, then—although limited—may be of interest, particularly considering that those are human osteoblast-like tumor cell lines, with relative high growth rates. In addition, osteogenesis is associated with reduction of the proliferative bursts and cell differentiation: the former may depend upon the availability of a properly assembled hyaluronan-rich matrix,[281] while the latter coincides with increased alkaline phosphatase activity,[282] osteocalcin biosynthesis, and matrix component deposition.[281,283] However the proliferative and differentiative potentials of bone precursors change during osteogenesis. In living bone, in fact, osteocytes derive from pre-osteoblasts and osteoblasts after polarization,[284] a process that allows bone growth

127

through a concerted control of proliferation (needed to generate new cells) and differentiation (needed to induce the cells to produce matrix and become resident in it). Pre-osteoblasts are normally proliferating cells and typically express osteogenic transcription factors, later downregulated in the osteoblast/osteocyte stages. Collagen I/III, osteopontin and osteonectin, fibronectin, tenascin C, and thrombospondins are also expressed. However, from the stage of osteoblast, osteocalcin, and bone sialoprotein become expressed, while type III collagen is downregulated.

In this light, then, a reduced proliferation of MG-63 cells upon CNP treatment is in accordance with the proposed role for the peptide in the osteogenic differentiation of cartilage and bone precursors.[285-286] On the contrary, in SAOS-2, proliferative events and matrix deposition are contemporary and possibly controlled through cell morphology and tensegrity by molecular components of the matrix itself[287]; this event may partially explain the results obtained exposing SAOS-2 or HOS cells to the tested peptides, where cell proliferation was slightly increased. The used cell lines, in fact,— although not derived from the same tumor source— could be related to slight ''different stages'' of the osteoblastic differentiation, being SAOS-2 and HOS cells in a more immature one, possibly displaying a lesser dependency upon matrix production and a higher proliferative potential. Moreover, it should be remembered that other studies, have tributed opposite effect to the administration of the same molecule to different osteoblast-like cells: it was reported that anti-tenascin antibodies reduced alkaline phosphatase activity and type I collagen production in UMR-106, ROS- 17/2.8, and SAO-2 cells lines. However proliferation was slightly increased only in SAOS-2 cells, while it was inhibited in the other two[286] indicating that more than one single stimuli was probably needed to overcome the proliferative potential of SAOS-2. The relevance of the cell ''responsiveness,'' when in different stages is also

evidenced by the CNP administration to an osteogenic cell line (ROB-C26) that maintains potentials for differentiating into myoblasts, osteoblasts, and adipocytes. The effects of the peptide were clearly different when the same cells were primed toward the separate lineages[287]. In our settings, however, the effects of the peptides could be minimized by the cells used, already addressed toward an osteoblast-like phenotype. The peptides osteogenic potential could be fully exploited using human skeletal progenitor cells, such as bone marrow stromal cells, particularly considering that the receptors for the natriuretic peptides have already been detected in the chicken, mouse, and rat cell counterparts [287-289]. As a whole, the proliferation results, although limited, are in accordance with previous work, reflect the cells' osteogenic potential and indicate that full length CNP can be successfully substituted by biologically effective synthetic peptides. Indeed the molecular mechanisms underlying their action are yet to be disclosed.

5.3: EXPERIMENTAL PROCEDURE

Peptide synthesis ad its biological assay

Purification of peptides was performed by preparative reversed phase HPLC on a Jasco HPLC system, model PU-2080 PLUS (Intelligent isocratic HPLC, High pressure binary gradient Pump) equipped with a Merck LiChrosper 100 RP18 column (250 310 mm2; 10 lm), and eluting with a flow rate of 5 mL/min with eluent A (0.1% TFA in water) and eluent B (0.1% TFA in 90% aq acetonitrile). Analytical HPLC purity checks were performed using a Merck LiChrosper 100 RP18 column (250 3 4 mm 2 ; 5 lm), eluting at a flow rate of 1 mL/min and with the same eluent system. Detection was at 280 nm. The purified peptides were characterized by RP-HPLC, LC/MS/MS system Q-TRAP AB Applied Biosystem. Purification of the crude peptides was performed by preparative scale HPLC (eluent: linear gradient 0–30% eluent B in eluent A over 30 min afforded 13 mg of peptide 1 (60% yield) and 14 mg of peptide 2 (65% yield). The purity of both peptides was checked by analytical

HPLC (eluent: linear gradient 0–30% eluent B in eluent A; analysis time 30 min, tR 1/4 9.58 min for peptide 1, and tR 1/4 9.9 min, for peptide 2, respectively). Peptide 1: Exact mass: calcd 406.50, found m/z (M + H) 407.50. Peptide 2: Exact mass: calcd 350.39, found m/z (M + H) 351.39.

References

1. Vacanti, J.P.; Langer R. Tissue engineering: the design and fabrication of living replacement devices for surgical reconstruction and transplantation. *Lancet* 1999, 354 (suppl I):32–4.

2. Lee, K.Y.; Mooney, D.J. Hydrogels for tissue engineering. *Chem. Rev.* 2001, 101:1869–79

3. Sakiyama-Elbert, S.E.; Hubbell, J.A. Functional biomaterials: design of novel biomaterials. *Annu. Rev. Mater. Res.* 2001, 31:183–201.

4. Shin, H.; Jo, S.; Mikos, A.G. Biomimetic materials for tissue engineering *Biomaterials* 2003*,* 24:4353–64.

5. Lutolf, M.P.; Hubbell, J.A. Synthetic biomaterials as instructive extracellular microenvironments for morphogenesis in tissue engineering. *Nature Biotechnol.* 2005, 23:47–55.

6. Peppas, N.A.; Langer, R. New challenges in biomaterials. *Science* 2004, 263:1715–20.

7. Hubbell, J.A. Biomaterials in tissue engineering. *Bio/Technology* 1995, 13:565–76.

8. Langer, R. Tirrell, D.A. Designing materials for biology and medicine. *Nature* 2004, 428, 487–492.

9. Putnam, A.J.; Mooney, D.J. Tissue engineering using synthetic extracellular matrices. *Nature Med.* 1996, 2:824–6.

10. Heath, C.A. Cells for tissue engineering. *TIBTECH* 2000, 18:17–9.

11. Griffith, L.G. Naughton, G. Tissue engineering–current challenges and expanding opportunities. *Science* 2002, 295:1009–14.

12. Chaikof, E.L. Biomaterials and scaffolds in reparative medicine. *Ann. N. Y. Acad. Sci.* 2002, 961:96–105.

13. Drury and Mooney, Hydrogels for tissue engineering: scaffold design variables and applications. Biomaterials. 2003, 24:4337-4351.

14. Roew, Raymond, "Adipic Acid", *Handbook of Pharmaceutical Excipients*, 2009, pp. 11–12

15. Puleo, D.A.; Kissling, R.A.; Sheu, M.-S. A technique to immobilize bioactive proteins, including bone morphogenetic protein-4 (BMP-4), on titanium alloy. *Biomaterials* 2002, 23:2079–87.

16. Goddarda, J.M. Polymer surface modification for the attachment of bioactive compounds J.M. Goddard̲a and J.H. Hotchkiss *Progress in Polymer Science* 2007, 32:698-725.

17. Whittlesey, K. J.; Shea, L. D. Delivery systems for small molecule drugs, proteins, and DNA: the neuroscience/biomaterial interface. *Exp. Neurol*. 2004, 190:1–16.

18. Simmons, C. A.; Alsberg, E.; Hsiong, S.; Kim, W. J.; Mooney, D. J. Dual growth factor delivery and controlled scaffold degradation enhance in vivo bone formation by transplanted bone marrow stromal cells. *Bone* 2004, 35,562-9.

19. Kroese-Deutman, H. C.; Ruhe, P. Q.; Spauwen, P. H.; Jansen, J. A. Bone inductive properties of rhBMP-2 loaded porous calcium phosphate cement implants inserted at an ectopic site in rabbits. *Biomaterials* 2005, 26:1131–8.

20. Zisch, A. H.; Lutolf, M.; Ehrbar, P. M. et al. *et al*. Cell-demanded release of VEGF from synthetic, biointeractive cell ingrowth matrices for vascularized tissue growth. *FASEB J.* 2003, 17:2260–2.

21. Lutolf, M.P.; Raeber, G.P.; Zisch, A.H.; Tirelli, N.; Hubbel, J.A. Cell responsive synthetic hydrogels. *Adv. Mater.* 2003, 15, 888-892.

22. Haugh, J. M.; Schooler, K.; Wells, A.; Wiley, H. S.; Lauffenburger, D. A. Effect of epidermal growth factor receptor internalization on regulation of the phospholipase C-gamma1 signaling pathway. *J. Biol. Chem.* 1999, 274: 8958-65.

23. Wiedlocha, A.; Sorensen, V. Signaling, internalization, and intracellular activity of fibroblast growth factor. *Curr. Top. Microbiol. Immunol.* 2004, 286: 45–79.

24. Zhang, Y.; Moheban, D. B.; Conway, B. R.; Bhattacharyya, A.; Segal, R. A. Cell surface Trk receptors mediate NGF-induced survival while internalized receptors regulate NGF-induced differentiation. *J. Neurosci.* 2000, 20:5671–78.

25. Ye, H.; Kuruvilla, R.; Zweifel, L. S.; Ginty, D. D. Evidence in support of signaling endosome-based retrograde survival of sympathetic neurons. *Neuron* 2003, 39:57–68.

26. Bronfman, F. C.; Tcherpakov, M.; Jovin, T. M.; Fainzilber, M. Ligand-induced internalization of the p75 neurotrophin receptor: a slow route to the signaling endosome. *J. Neurosci.* 2003, 23:3209–20.

27. Kuhl, P. R.; Griffith-Cima, L. G. Tethered epidermal growth factor as a paradigm for growth factor-induced stimulation from the solid phase. *Nat. Med*. 1996, 2:1022–7.

28. Kirkwood, K.; Rheude, B.; Kim, Y. J.; White, K.; Dee, K. K. C. In vitro mineralization studies with substrate-immobilized bone morphogenetic protein peptides. *J. Oral Implantol*. 2003, 29:57–65.

29. Karageorgiou, V.; Meinel, L.; Hofmann, S.; Malhotra, A.; Volloch, V.; Kaplan, D. Bone morphogenetic protein-2 decorated silk fibroin films induce osteogenic differentiation of human bone marrow stromal cells. *J. Biomed. Mater. Res. A* 2004, 71:528–37.

30. Sakiyama-Elbert, S. E.; Hubbell, J. A. Controlled release of nerve growth factor from a heparin-containing fibrin-based cell ingrowth matrix. *J. Control. Release* 2000, 69:149–58.

31. Sakiyama-Elbert, S. E.; Hubbell, J. A. Development of fibrin derivatives for controlled release of heparin-binding growth factors. *J. Control. Release* 2000, 65:389–402.

32. Lee, A. C.; Yu, V. M.; Lowe, J. B. Controlled release of nerve growth factor enhances sciatic nerve regeneration. *Exp. Neurol*. 2003, 184:295–300.

33. Taylor, S. J.; McDonald, J. W. Controlled release of neurotrophin-3 from fibrin gels for spinal cord injury. *J. Control. Release* 2004, 98:281–94.

34. Seliktar, D.; Zisch, A. H.; Lutolf, M. P.; Wrana, J. L.; Hubbell, J. A. MMP-2 sensitive, VEGF-bearing bioactive hydrogels for promotion of vascular healing. *J. Biomed. Mater. Res. A* 2004, 68:704–16.

35. Dinbergs, I. D.; Brown, L.; Edelman, E. R. Cellular response to transforming growth factor-beta1 and basic fibroblast growth factor depends on release

kinetics and extracellular matrix interactions. *J. Biol. Chem*. 1996, 271:29822–29.

36. Hersel, U.; Dahmen, C.; Kessler, H. RGD modified polymers: biomaterials for stimulated cell adhesion and beyond. *Biomaterials* 2003, 24:4385-415.

37. a) Hersel, U.; Dahmen, C.; Kessler, H. RGD modified polymers: biomaterials for stimulated cell adhesion and beyond. *Biomaterials 2003,* 24:4385-415. b) Hern, D.L., Hubbell, J.A. Incorporation of adhesion peptides into nonadhesive hydrogels useful for tissue resurfacing. *J. Biomed. Mater. Res*. 1998, 39:266–76.

38. Kam, L.; Shain, W.; Turner, J. N.; Bizios, R. Selective adhesion of astrocytes to surfaces modified with immobilized peptides. *Biomaterials* 2002*,* 23:511–5.

39. Rezania, A.; Healy, K.E. Biomimetic peptide surfaces that regulate adhesion, spreading, cytoskeletal organization, and mineralization of the matrix deposited by osteoblast-like cells. *Biotechnol Prog*.1999, 15:19–32.

40. Schuler, M. Hamilton, D.W.; Kunzler, T.P. et al. Comparison of the response of cultured osteoblasts and osteoblasts outgrown from rat calvarial bone chips to nonfouling KRSR and FHRRIKA-peptide modified rough titanium surfaces. *J. Biomed. Mater. Res*.2009*, B.* 91B: 517−27.

41. La Ferla, B.; Zona, C.; Nicotra, F. Easy silica gel supported desymmetrization of PEG. *Synlett*, 2009, 14:2325−7.

42. Weetall, H.H. Preparation of immobilized proteins covalently coupled through silane coupling agents to inorganic. *Supports Appl. Biochem. Biotechnol*. 1993, 41:157−88.

43. Dubruel, P.; Vanderleyden, E.; Bergadà, M. Et al. Comparative study of silanisation reactions for the biofunctionalisation of Ti-surfaces. Surface Science 2006, 600:2562–71.

44. The Organic Chemistry of Sugars, Edited by Daniel E. Levy Péter Fügedi, Published in 2006 by CRC Press, Taylor & Francis Group 6000 Broken Sound Parkway NW, Suite 300 Boca Raton.

45. Nicolaou, K. C.; Mitchell, H. J. Angew. Chem. Int. Ed. 2001, 40, 1576-1624.

46. Linhardt, R. J.; Toida, T. Carbohydrates in Drug Design; Witczak, Z. J., Nieforth, K. A., Eds.; Marcel Dekker: New York 1997.

47. Balazs, E.A, Laurent, T.C. In *The Chemistry, Biology and Medical applications of hyaluronan and its derivatives*. Laurent, T.C., Ed. London, Portland Press, 1998, 325–36.

48. Wang, Q., Dordick J. S. Synthesis and application of carbohydrate containing polymers. *Chem. Mater*. 2002, 14:3232-44.

49. Varki, A. Biological roles of oligosaccharides: all of the theories are correct. *Glycobiology*. 1993, 3:97–130.

50. Ashwell, G.,. Harford J. Carbohydrate-specific receptors of the liver. *Ann Rev Biochem*.1982, 51:531–54.

51. Weigel, P.H., Schnaar, R.L., Kuhlenschmidt, M.S., et al. Adhesion of hepatocytes to immobilized sugars. *J. Biol. Chem*. 1979, 254:10830–8.

52. Oka, J.A., Weigel, P.H. Binding and spreading of hepatocytes on synthetic galactose culture surfaces occur as distinct and separable threshold responses. *J. Cell Biol*. 1986, 103:1055–60.

53. Kobayashi, A., Akaike, T., Kobayashi, K., Sumitomo, H. Enhanced adhesion and survival efficiency of liver cells in culture dished coated with a lactose-

carrying styrene homopolymer. *Makromol. Chem. Rapid Commun.* 1986, 7:645–50.

54. Kobayashi, A., Goto, M., Kobayashi, K., Akaike. T. Receptor- mediated regulation of differentiation and proliferation of hepatocytes by synthetic polymer model of a sialoglycoprotein. *J. Biomater. Sci. Polym. Edn. 1994,* 6:325–42.

55. Yang, J., Goto, M., Ise, H., Cho, C.-S., Akaike, T. Galactosylated alginate as a scaffold for hepatocytes entrapment. *Biomaterials, 2002,* 23:471–9.

56. Yoon, J.J., Nam, Y.S., Kim, J.H, Park, T.G. Surface immobilization of galactose onto aliphatic biodegradable polymers for hepatocyte culture. *Biotechnol. Bioeng.* 2002, 78:1–10.

57. Gotoh, Y., Tsukada, M., Aiba, S-I, Minoura, N. Chemical modification of silk fibroin with N-acetyl-chito-oligosaccharides. *Int. J. Biol. Macromol.* 1996, 18:19–26.

58. Gotoh, Y.; Minoura, N.; Miyashita, T. Preparation and characterization of conjugates of silk fibroin and chitooligosaccharides. *Colloid Polym. Sci.* 2002, 280:562–8.

59. Miura, Y.; Sato, H.; Ikeda, T.; Sugimura, H.; Takai, O.; Kobayashi. K. Micropatterned carbohydrate displays by self-assembly of glycocojugate polymers on hydrophobic templated on silicon. *Biomacromolecules* 2004, 5:1708-13.

60. Love, C.; Ronan, J.L.; Grotenbreg, G.M.; van der Veen, A.G.; Ploegh. H.L. A microengraving method for rapid selection of single cells producing antigen-specific antibodies. *Nat. Biotechnol.* 2006, 24:703-707.

61. Umezewa, Y. Aoki, H. Ion Channel Sensors Based on Artificial Receptors. *Anal. Chem*.2004, 76:320-326.

62. Lindahl, U; Lidholt, K; Spillmann, D; Kjellén, L. More to "heparin" than anticoagulation. *Thrombosis Res.1994,* 75:1-32.

63. Sato, H.; Miura, Y.; Saito, N.; Kobayashi, K.; Takai, O. A micropatterned carbohydrate display for tissue engineering by self-assembly of heparin , Surface Science 2007, 601:3871–3875.

64. Foster, A.B. Chemistry of Carbohydrate. *Ann. Rev. Biochem*. 1961, 30: 45-70.

65. Verli, H.; Guimaraes, J.A. Molecular dynamics simulation of a decasaccharide fragment of heparin in aqueous solution. *Carbohydr. Res*. 2004, 339:281-90.

66. Varki A. Biological roles of oligosaccharides: all of the theories are correct. *Glycobiology* 1993, 3, 97–130.

67. Helenius A, Aebi M. Intracellular functions of *N*-linked glycans. *Science* 2001, 291, 2364–2369.

68. Bertozzi CR, Kiessling LL. Chemical glycobiology. *Science* 2001,291, 2357–2364.

69. Rudd PM, Elliott T, Cresswell P, Wilson IA, Dwek RA. Glycosylation and the immuno system. *Science* 2001, 291, 2370–2376.

70. Gabius H-J (2009) The sugar code: fundamentals of glycoscience. Wiley-Blackwell.

71. Ritchie GE, Moffatt, Sim BE, Morgan BP, Dwek RA, Rudd PM. Glycosylation and the complement system. *Chem. Rev*. 2002, 102, 305–319.

72. Dove A. The bittersweet promise of glycobiology. *Nat. Biotechnol.* 2001*, 19,* 913–917.

73. Ohtsubo K, Marth JD. Glycosylation in cellular mechanisms of health and disease. *Cell* 2006, 126, 855–867.

74. Hakomori S, Zhang Y. Glycosphingolipid antigens and cancer therapy. *Chem. Biol.* 1997*,* 4, 97–104.

75. Nangia-Makker P, Conklin J, Hogan V, Raz A. Carbohydrate-binding proteins in cancer, and their ligands as therapeutic agents. *Trends Mol. Med.* 2002, 8, 187–192.

76. van Kooyk Y, Rabinovich GA. Protein–glycan interactions in the control of innate and adaptive immune responses. *Nat. Immunol.* 2008, 9, 593-601.

77. Marth JD, Grewal PK. Mammalian glycosylation in immunity. *Nat. Rev. Immunol.* 2008, 8, 874–887.

78. Dwek RA, Butters TD, Platt FM, Zitzmann N. Targeting glycosylation as a therapeutic approach. *Nat. Rev. Drug Discov.* 2002, 1, 65–75.

79. Koeller KM, Wong C-H. Emerging themes in medicinal glycoscience. *Nat. Biotech.* 2000, 18, 835–841.

80. von Itzstein M, Wu WY, Kok GB *et al.* Rational design of potent sialidase-based inhibitors of influenza virus replication. *Nature* 1993, 363 (6428), 418–423.

81. Lew W, Chen X, Kim CU. Discovery and development of GS 4104 (oseltamivir): an orally active influenza neuraminidase inhibitor. *Curr. Med. Chem.*2000, 7, 663–672.

82. Weinreb NJ, Barranger JA, Charrow J, Grabowski GA, Mankin HJ, Mistry P. Guidance on the use of Miglustat for treating patients with type 1 Gaucher disease. *Am. J. Hematol.* 2005, 80, 223–229.

83. *Carbohydrate-Based Drug Discovery Volumes 1 & 2.* Wong C-H (Ed.). Wiley-VCH, Wheineim, Germany (2003).

84. Rosner H: US 6683098 (2004).

85. V. V. Rostovtsev, L. G. Green, V. V. Fokin and K. B. Sharpless, Angew. Chem., Int. Ed., 2002, 41, 2596–2599.

86. C.W. Torn.e, C. Christensen and M. Meldal, J. Org. Chem., 2002,67, 3057–3064.

87. For a recent review see: C. W. Torn.e and M. Meldal, Chem. Rev., 2008, 108, 2952–3015.

88. E. M. Sletten and C. R. Bertozzi, Angew. Chem., Int. Ed., 2009, 48, 6974–6998

89. L. M. Gaetke and C. K. Chow, Toxicology, 2003, 189, 147–163.

90. J. A. Prescher, D. H. Dube and C. R. Bertozzi, Nature, 2004, 430, 873–877.

91. A. Padwa, 1,3-Dipolar Cycloaddition Chemistry, Wiley-Interscience Publication, New York, 1984, vol. 1.

92. R. Huisgen, Angew. Chem., Int. Ed. Engl., 1963, 2, 565–598.

93. N. J. Agard, J. A. Prescher and C. R. Bertozzi, J. Am. Chem. Soc., 2004, 126, 15046–15047.

94. R. D. Chambers, Fluorine in Organic Chemistry, Blackwell, Oxford, 2004, pp.14–15, 224–225.

95. N. J. Agard, J. M. Baskin, J. A. Prescher, A. Lo and C. R. Bertozzi, ACS Chem. Biol., 2006, 1, 644–648.

96. J. M. Baskin, J. A. Prescher, S. T. Laughlin, N. J. Agard, P. V. Chang, I. A. Miller, A. Lo, J. A. Codelli and C. R. Bertozzi, Proc. Natl. Acad. Sci. U. S. A., 2007, 104, 16793–16797.

97. S. S. van Berkel, A. J. Dirks, M. F. Debets, F. L. van Delft, J. J. L. M. Cornelissen, R. J. M. Nolte and F. P. J. T. Rutjes, ChemBioChem, 2007, 8, 1504–1508.

98. M. L. Blackman, M. Royzen and J. M. Fox, J. Am. Chem. Soc., 2008, 130, 13518–13519.

99. N. K. Devaraj, R. Weissleder and S. A. Hilderbrand, Bioconjugate Chem., 2008, 19, 2297–2299.

100. R. Pipkorn, W. Waldeck, B. Didinger, M. Koch, G. Mueller, M. Wiessler and K. Braun, J. Pept. Sci., 2009, 15, 235–241.

101. R. Huisgen, Angew. Chem., Int. Ed. Engl., 1968, 7, 321–328.

102. W. Song, Y. Yang, J. Qu, M. M. Madden and Q. Lin, Angew. Chem., Int.Ed., 2008, 47, 2832–2835.

103. W. Song, Y. Wang, J. Qu and Q. Lin, J. Am. Chem. Soc., 2008, 130, 9654–9655.

104. For another fluorogenic system see: M. J. Hangauer and C. R. Bertozzi, Angew. Chem., Int. Ed., 2008, 47, 2394–2397; and references therein.

105. K. Gutsmiedl, C. T. Wirges, V. Ehmke and T. Carell, Org. Lett., 2009, 11, 2405–2408.

106. Huisgen, M. Seidel, G. Wallbillich and H. Knupfer, Tetrahedron, 1962, 17, 3-29.

107. Feizi T, Fazio F, ChaiW, Wong C-W (2003) Carbohydrate microarrays-a new set of technologies at the frontiers of glycomics. Curr Opin Struct Biol 13: 637–645.

108. (a) Kappe, C. O. Angew. Chem., Int. Ed. 2004, 43, 6250–6284; (b) Heard, D. D.; Barker, R. J. Org. Chem. 1968, 33,740–746; (c) Ferrier, R. J.; Hatton, L. R. Carbohydr. Res.1968, 6, 75–86; (d) Freudenberg, K. Adv. Carbohydr.Chem. 1966, 21, 2–38.

109. For the use of H_2SO_4–silica in carbohydrate synthesis see: (a) Mukhopadhyay, B. Tetrahedron Lett. 2006, 47, 4337–4341; (b) Rajput, V. K.; Mukhopadhyay, B. Tetrahedron Lett. 2006, 47, 5939–5941; (c) Rajput, V. K.; Roy, B.;Mukhopadhyay, B. Tetrahedron Lett. 2006, 47, 6987–6991; (d) Dasgupta, S.; Roy, B.; Mukhopadhyay, B.Carbohydr. Res. 2006, 341, 2708–2713; For the use of H2SO4–silica in organic synthesis see: (e) Zolfigol, M. A.;Bamoniri, A. Synlett 2002, 1621–1623; (f) Zolfigol, M. A.Tetrahedron 2001, 57, 9509–9511; (g) Zolfigol, M. A.;Shirini, F.; Ghorbani Choghamarani, A.; Mohammadpoor-Baltork, I. Green Chem. 2002, 4, 562–564; (h) Shirini,F.; Zolfigol, M. A.; Mohammadi, K. Bull. Korean Chem.Soc. 2004, 25, 325–327.

110. Hölemann A, Seeberger PH Carbohydrate diversity: synthesis of glycoconjugates and complex carbohydrates. Curr Opin Biotechnol 2004,15:615–622.

111. Bornaghi LF, Poulsen S-A Microwave-accelerated Fischer glycosylation. Tetrahedron Lett 2005, 46:3485–3488.

112. Kappe CO. Controlled microwave heating in modern organic synthesis. AngewChem Int Ed Engl 2004, 43:6250–6284.

113. Heard DD, Barker R. Investigation of the role of dimethyl acetals in the formation of methyl glycosides. J Org Chem 1968, 33: 740–746.

114. Ferrier RJ, Hatton LR. Studies with radioactive sugars: Part I. Aspects of the alcoholysis of -xylose and -glucose; the role of the acyclic acetals. Carbohydr Res 1968, 6:75–86.

115. Freudenberg K. Emil Fischer and his contribution to carbohydrate chemistry. Adv Carbohydr Chem. 1966, 21:2–38.

116. Ferrières V, Bertho J-N, Plusquellec D. A new synthesis of O-glycosides from totally O-unprotected glycosyl donors. Tetrahedron Lett 1995, 36:2749–2752.

117. Sanki AK, Mahal L. A one-step synthesis of azide-tagged carbohydrates: versatile intermediates for glycotechnology. Synlett 2006, 455–459.

118. Roy B, Mukhopadhyay B. Sulfuric acid immobilized on silica: an excellent catalyst for Fischer type glycosylation. Tetrahedron Lett 2007, 48:3783–3787.

119. Yeoh KK, Butters TD, Wilkinson BL, Fairbanks AJ. Probing replacement of pyrophosphate via click chemistry; synthesis of UDP-sugar analogues as potential glycosyl transferase inhibitors. Carbohydr Res 2009, 344:586–591.

120. Brochette-Lemoine S, Trombotto S, Joannard D, Descotes G, Bouchu A, Queneau Y. Ultrasound in carbohydrate chemistry: sonophysical glucose oligomerisation and sonocatalysed sucrose oxidation. Ultrason Sonochem 2000, 7:157–161.

121. Chen, J. W. J., Abatangelo, G. Functions of hyaluronan in wound repair. *Wound Rep. Reg.*, 1999, *7*, 79-89.

122. Meyer, K.; Palmer, J.W. J. The polysaccharide of the vitreous humor. *Biol. Chem.*, 1934, *107*, 629-634.

123. Weissmann, B., Meyer, K. The structure of hyalubiuronic acid and hyaluronic acid from umbilical cord. *J. Am. Chem. Soc.*, 1954, *76* (7), 1753–1757

124. Raman, R., Sasisekharan, V., Sasisekharan, R.. Structural insights into biological roles of protein-glycosaminoglycan Interactions. *Chemistry & Biology*, 2005, 12, 267–277.

125. Evered, D., Whelan, J., *The Biology of Hyaluronan*, Wiley: Chichester, U.K., 1989.

126. Weigel, P.H., Hascall, V.C., Tammi, M. Hyaluronan synthases. *J. Biol. Chem.*, 1997, 272, 13997-14000.

127. Toole, B.P. Hyaluronan in morphogenesis and tissue remodeling. 1998. Glycoforum: science of hyaluronan today. http://www.glycoforum.gr.jp/science/hyaluronan/HA08/HA08E.html.

128. DeAngelis, P. L. Hyaluronan synthases: fascinating glycosyltransferases from vertebrates, bacterial pathogens, and algal viruses. *Cell Mol Life Sci.,* 1999, 56, 670-682.

129.   Tien, J. Y., Spicer, A. P. Three vertebrate hyaluronan synthases are expressed during mouse development in distinct spatial and temporal patterns. *Dev. Dyn.*, 2005, 233, 130–141.

130.   Schiller, J., Fuchs, B., Arnhold, J. and Arnold, K. Contribution of reactive oxygen species to cartilage degradation in rheumatic diseases: molecular pathways, diagnosis and potential therapeutic strategies. *Curr. Med. Chem.*, 2003, 10, 2123–2145.

131.   Stern, R. Devising a pathway for hyaluronan catabolism: Are we there yet? *Glycobiology,* 2003, 13, 105R-115R.

132.   Weigel, J., Weigel, P. H. Characterization of the recombinant rat 175-kDa hyaluronan receptor for endocytosis (HARE). *J. Biol. Chem.*, 2003, 278, 42802–42811.

133.   Lesley, J., Hyman, R., Kincade, P.W. CD44 and its interaction with extracellularmatrix. *Adv. Immunol*, 1993, 54, 271–335.

134.   Jedrzejas, M. J, Mello, L. V., de Groot, B.L., Li, S. Mechanism of Hyaluronan Degradation by Streptococcus pneumoniae Hyaluronate Lyase. *J. Biol. Chem.*, 2002, 277, 28287-28297.

135.   Bastow, E. R. Byers, S., Golub, S. B., Clarkin, C. E., Pitsillides, A. A., Fosang, A. J. Hyaluronan synthesis and degradation in cartilage and bone. *Cell. Mol. Life Sci.*, 2008, 65, 395 – 413

136.   Sterna, R., Akira, A. A., Kazuki, N. Sugaharac Hyaluronan fragments: An information-rich system. *Eur. J.Cell Bio*. 2006, 85, 699–715.

137.   Teder, P., Vandivier, R.W., Jiang, D., Liang, J., Cohn, L., Pure, E., Henson, P. M., Noble, P. W. Resolution of lung inflammation by CD44. *Science* 2002, 296, 155–158.

138.   Toole, B. P.; Gross, J. The extracellular matrix of the regenerating newt limb: synthesis and removal of hyaluronate prior to differentiation. *Dev. Biol.* 1971, 25, 57-77.

139.   Li, Y., Toole, B. P., Dealy, C. N. and Kosher, R. A. Hyaluronan in limb morphogenesis. *Dev. Biol*. 2007, 305, 411–420.

140.   a) Scott, J. E.; Heatley, F. Biological properties of hyaluronan in aqueous solution are controlled and sequestered by reversible tertiary structures, defined by NMR spectroscopy. *Biomacromolecules,* 2002, 3, 547-553; b) Scott, J. Secondary and tertiary structures of hyaluronan in aqueous solution. Some Biological consequences. http://www.glycoforum.gr.jp/science/hyaluronan/HA02/ HA02.pdf, Mar 1998.

141.   Toole, B.P. Hyaluronan in morphogenesis and tissue remodeling. Glycoforum: science of hyaluronan today. 1998. http://www.glycoforum.gr.jp/science/hyaluronan/HA08/HA08E.html.

142.   Hascall, V. C., Majors, A. K., De La Motte, C. A., Evanko, S. P., Wang, A., Drazba, J. A., Strong, S. A. and Wight, T. N. Intracellular hyaluronan: A new frontier for inflammation? *Biochim. Biophys*. Acta, 2004, 1673, 3–12.

143.   Schulz, T., Schumacher, U. and Prehm, P. Hyaluronan export by the A. B.C transporter M. R.P5 and its modulation by intracellular cGMP. *J. Biol. Chem*., 2007 282, 20999–21004.

144. Day, A. J., Sheehan, J., K. Hyaluronan: polysaccharide chaos to protein organisation. *Curr. Opin. Struct. Biol.* 2001, 11:617–622 and references cited therein.

145. Scott, J. E. In *The Chemistry, Biology and Medical Applications of Hyaluronan and its Derivatives*; Laurent, T. C., Ed.; Portland Press Ltd.: London, 1998; pp 7-15.

146. a) Fraser JRE, Laurent TC. Hyaluronan. In: *Extracellular matrix*. Comper WD Ed. The Netherlands: Harwood Academic Publishers, 1996, vol. II, 141–99; b) Hascall, V. C. Hyaluronan: Structure and Physical properties.

   http://www.glycoforum.gr.jp/science/hyaluronan/HA01/HA01.pdf;

   c) Almond, A., Hardingham, T. E., Hyaluronan: Current macromolecular and micromolecular views,

   http://www.glycoforum.gr.jp/science/hyaluronan/HA31/HA31E.html

147. Balasz, E. A., Denlinger, J. L. Clinical uses of hyaluronan. In *The biology of hyaluronan*. Evered, D., Whelan, J., Ed. Chichester, J. Wiley & Sons, 1989, 265–80.

148. Balazs, E.A, Laurent, T.C. In *The Chemistry, Biology and Medical applications of hyaluronan and its derivatives*. Laurent, T.C., Ed. London, Portland Press, 1998, 325–36.

149. a) Kogan, G., Ladislav, S., Stern, R., Gemeiner, P. Hyaluronic acid: a natural biopolymer with a broad range of biomedical and industrial applications, *Biotechnol. Lett.,* 2007, 29, 17–25; b) Price, R. D., Berry, M. G., Navsaria, H. A. Hyaluronic acid: the scientific and clinical evidence, *J. Plast., Recons. & Aesth.*

Surg. 2007, 60, 1110-1119; c) Prestwich, G. D.,Vercruysse, K. P., Therapeutic applications of hyaluronic acid and hyaluronan derivatives, *PSTT*, Vol. 1, 1998, 42-43. d) Morra, M. Engineering of Biomaterials Surfaces by Hyaluronan, *Biomacromolecules*, 2005, 6, 1205-1223

150. Tammi, M., Day, A. J., Turely, E. A. Hyaluronan and homeostasis: a balancing act. *J. Biol. Chem.* 2002, 277, 4581-4584.

151. Laurent, T. C., Ogston, A. G. The interactions between polysaccharides and other macromolecules. 4. The osmotic pressure of mixtures of serum albumin and hyaluronic acid. *Biochem. J.* 1963;89: 249–53.

152. Culp, L. A., Murray, B. A., Rollins, B. J. Fibronectin and proteoglycan as determinants of cell- substratum adhesion. *J. Supramol. Struct.*1979, 11, 401–27.

153. Clarris, B. J., Fraser, J. R. E. On the pericellular zone of some mammalian cells in vitro. *Exp. Cell. Res.* 1968, 49, 181–93.

154. a) Della Valle, F., Romeo, A. *U.S. Pat.* 4,851,521, 1989.; b) Pouyani, T., Prestwich, G. D. Functionalized derivatives of hyaluronic acid oligosaccharides: drug carriers and novel biomaterials. *Bioconjugate Chem.* 1994, 5, 339-347.

155. Wang, W. A novel hydrogel crosslinked hyaluronan with glycol chitosan. *J Mater Sci Mater Med.* 2006, 12, 1259-65.

156. Toole, B. P. Hyaluronan is not just a go! *J. Clin. InVest.*, 2000, 106, 335-336.

157. A) Day, A. J, Prestwich, G. D: Hyaluronan-binding proteins: tying up the giant. *J. Biol. Chem.,* 2002, 277: 4585-4588. b) Tammi, M., Day, A. J., Turely, E. A. Hyaluronan and homeostasis: a balancing act. 2002, *J. Biol. Chem.* 277, 4581-4584.

158. Hardingham, T. E.; Muir, H. The specific interaction of hyaluronic acid with cartilage proteoglycans. *Biochim. Biophys. Acta,* 1972, *279*, 401-405.

159. Hardingham, T. E.; Muir, H. Binding of oligosaccharides of hyaluronic acid to proteoglycans. *Biochem. J.* 1973, *135*, 905-908.

160. Hascall, V. C.; Heinegard, D. Aggregation of cartilage proteoglycans. The role of hyaluronic acid. *J. Biol. Chem.* 1974, 249, 4232-4241.

161. Turley, E. A. Hyaluronic acid stimulates protein kinase activity in intact cells and in an isolated protein complex. *J. Biol. Chem.* 1989, 264, 8951-8955.

162. Day, A. J. Understanding hyaluronan-protein interaction. http://www.glycoforum.gr.jp/science/hyaluronan/HA16/HA16E.html.

163. Kohda, D., Morton, C. J., Parkar, A. A., Hatanaka, H., Inagaki, F. M., Campbell, I. D., Day A. J: Solution structure of the link module: a hyaluronan-binding domain involved in extracellular matrix stability and cell migration. *Cell,* 1996, 86, 767-775.

164. Bono, P, Rubin, K, Higgins, J. M., Hynes, R. O. Layilin, a novel integral membrane protein, is a hyaluronan receptor. *Mol. Biol. Cell.* 2001, 12, 891-900.

165. Watanabe, H., Yamada, Y. Mice lacking link protein develop dwarfism and craniofacial abnormalities. *Na.t Genet.* 1999, 21, 225-229.

166. Evanko, S. P., Angello, J. C., Wight, T. N. Formation of hyaluronan- and versican-rich pericellular matrix is required for proliferation and migration of vascular smooth muscle cells. *Arterioscler. Thromb. Vasc. Biol.* 1999, 19, 1004-1013.

167. Hayen, W., Goebeler, M., Kumar, S., Rieben, R., Nehls, V. Hyaluronan stimulates tumor cell migration by modulating the fibrin fiber architecture. *J. Cell. Sci.* 1999, 112, 2241-2251.

168. Day, A. J., Sheehan, J. K. Hyaluronan: polysaccharide chaos to protein organisation. *Curr. Opinion Struct. Biol.* 2001, 11, 617–622.

169. Kahmann, J. D., O'Brien, R, Werner, J. M., Heinegård, D., Ladbury, J. E., Campbell, I. D., Day, A. J. Localization and characterization of the hyaluronan-binding site on the link module from human TSG-6. *Structure* 2000, 8:763-774.

170. Watanabe, H, Cheung, S. C., Itano. N., Kimata, K., Yamada, Y. Identification of hyaluronan-binding domains of aggrecan. *J. Biol. Chem.* 1997, 272, 28057-28065.

171. Hardingham, T. E. Aggrecan-link protein-Hyaluronan aggregates. http://www.glycoforum.gr.jp/science/hyaluronan/HA05/HA05E.html

172. Bajorath, J., Greenfield, B., Munro, S. B., Day, A. J., Aruffo, A. Identification of CD44 residues important for hyaluronan binding and delineation of the binding site. *J. Biol. Chem.* 1998, 273, 338-343.

173. Mahoney, D. J., Blundell, C. D., Day, A. J. Mapping the hyaluronan-binding site on the link module from human TSG-6 by site-directed mutagenesis. *J. Biol. Chem.* 2001, 276, 22764-22771.

174. Kohda, D., Morton, C. J., Parkar, A. A., Hatanaka, H., Inagaki, F. M., Campbell, D, Day, A. J. Solution Structure of the Link Module: A Hyaluronan-Binding Domain Involved in Extracellular Matrix Stability and Cell Migration. *Cell*, 1996, 86, 767–775.

175. Peach, R. J.; Hollenbaugh, D.; Stamenkovic, I.; Aruffo, A. Identification of hyaluronic acid binding sites in the extracellular domain of CD44. *J. Cell Biol.* 1993, *122*, 257-264.

176. Day, A. J. The structure and regulation of hyaluronan-binding proteins. *Biochem. Soc. Trans.* 1999, *27*, 115-121.

177. Underhill, C. B.; Toole, B. P. Binding of hyaluronate to the surface of cultured cells. *J. Cell Biol.* 1979, 82, 475-484.

178. Underhill, C. B.; Toole, B. P. Physical characteristics of hyaluronate binding to the surface of simian virus 40-transformed 3T3 cells. *Biol. Chem.* 1980, 255, 4544-4549.

179. Hua, Q., Knudson, C. B., Knudson, W. Internalization of hyaluronan by chondrocytes occurs via receptor-mediated endocytosis, J. *Cell Sci.* 1993, 106, 365–375.

180. a) Luo, Y.; Prestwich, G. D. Synthesis and Selective Cytotoxicity of a Hyaluronic Acid-Antitumor Bioconjugate., *Bioconjugate Chem.* 1999, 10(5), 755–763; b) Luo, Y., Ziebell, M. R.; Prestwich, G. D. A hyaluronic acid-taxol antitumor bioconjugate targeted to cancer cells. *Biomacromolecules* **2000**, 1, 208–218.

181. Dinkelaar, J., Gold, H.; Overkleeft, H. S, Codée, J. D. C; Van der Marel, G. A. Synthesis of hyaluronic acid oligomers using chemoselective and one-pot strategies. *JOC* 2009; 74, (11), 4208-16.

182. a) Takanashi, S., Hirasaka, Y., Kawada, M. *J. Am. Chem. Soc.* 1962, 84, 3029. (b) Jeanloz, R. W., Flowers, H. M. *J. Am. Chem. Soc.* 1962, 84, 3030. (c)

Flowers, H. M., Jeanloz, R. W. *Biochemistry* 1964, 3, 123. (d) Walker-Nasir, E., Jeanloz, R. W. *Carbohydr. Res.* 1979, 68, 343. (e) Klaffke, W., Warren, C. D., Jeanloz, R. W. *Carbohydr. Res.* 1993, 244, 171.

183. Slaghek, T. M., Hypponen, T. K., Ogawa, T., Kamerling, J. P., Vliegenthart, J. F. G. *Tetrahedron Lett.* 1993, 34, 7939.

184. Slaghek,T., Nakahara,Y., Ogawa, T. Stereocontrolled synthesis of hyaluronan tetrasaccharide. *Tetrahedron Lett.* 1992, 33, 4971.

185. Slaghek, T. M.; Nakahara, Y.; Ogawa, T.; Kamerling, J. P.; Vliegenthart, J. F. G. Synthesis of hyaluronic acid-related di-, tri-, and tetra-saccharides having an N-acetylglucosamine residue at the reducing end. *Carbohydr. Res.* 1994, 255, 61.

186. Carter, M. B.; Petillo, P. A.; Anderson, L.; Lerner, L. E. The 1,4-linked disaccharide of hyaluronan: synthesis of methyl 2-acetamido-2-deoxy-beta-D-glucopyranosyl-(1→4)-beta-D-glucopyrano sid uronic acid. *Carbohydr.Res.* 1994, 258, 299.

187. Blatter, G.; Jacquinet, J.-C. The use of 2-deoxy-2-trichloroacetamido-D-glucopyranose derivatives in syntheses of hyaluronic acid-related tetra-, hexa-, and octa-saccharides having a methyl β-D -glucopyranosiduronic acid at the reducing end. *Carbohydr. Res.* 1996, 288, 109.

188. Bryan, K. S., Yeung, D., Hill, C., Janicka, M., Petillo, P. A. Synthesis of two hyaluronan trisaccharides. *Org. Lett.*, 2000, 2, 1279-1282.

189. Iyer, S. S., Rele, S. M., Baskarana, S., Chaikof, E. L. Design and synthesis of hyaluronan-mimetic gemini disaccharides. *Tetrahedron,* 2003, 59 631–638.

190. Rele, S. M., Iyera, S. S., Chaikof, E. L. Hyaluronan-based glycoclusters as probes for chemical glycobiology. *Tetrahedron Letters,* 2007, 48, 5055–5060.

191. Rena, Z. X., Yanga, Q., Pricea, K. N., Chena, T., Nygrena, C., Turnera, J. F. C., Baker, D. C. Synthesis of a C-linked hyaluronic acid disaccharide mimetic. *Carbohydr.Res*. 2007, 342, 1668–1679.

192. (a) Takanashi, S.; Hirasaka, Y.; Kawada, M. *J. Am. Chem. Soc.* 1962, *84*, 3029. (b) Jeanloz, R. W.; Flowers, H. M. *J. Am. Chem. Soc.* 1962, *84*, 3030. (c) Flowers, H. M.; Jeanloz, R. W. *Biochemistry* 1964, *3*, 123. (d) Walker-Nasir, E.; Jeanloz, R. W. *Carbohydr. Res.* 1979, *68*, 343. (e) Klaffke,W.; Warren, C. D.; Jeanloz, R. W. *Carbohydr. Res.* 1993, *244*, 171.

193. Slaghek, T. M.; Hypponen, T. K.; Ogawa, T.; Kamerling, J. P.;Vliegenthart, J. F. G. *Tetrahedron Lett.* **1993**, *34*, 7939.

194. (a) Slaghek, T.; Nakahara, Y.; Ogawa, T. *Tetrahedron Lett.* 1992, *33*, 4971. (b) Slaghek, T. M.; Nakahara, Y.; Ogawa, T.; Kamerling, J. P.;Vliegenthart, J. F. G. *Carbohydr. Res.* 1994, *255*, 61.

195. Carter, M. B.; Petillo, P. A.; Anderson, L.; Lerner, L. E. Carbohydr.Res. 1994, 258, 299.

196. Blatter, G.; Jacquinet, J.-C. *Carbohydr. Res.* 1996, *288*, 109.

197. de Bold AJ, Borenstein HB, Veress AT, Sonnenberg H. A rapid and potent natriuretic response to intravenous injection of atrial myocardial extract in rats. Life Sci 1981, 28:89–94.

198. Boerrigter G, Burnett JC Jr. Cardiorenal syndrome in decompensated heart failure: prognostic and therapeutic implications. Curr Heart Fail Rep 2004,

1:113–120.

199.   Chen HH, Burnett JC Jr. Clinical application of the natriuretic peptides in heart failure. Eur Heart J 2006, 8(Suppl E):E18–E25.

200.   Potter LR, Abbey-Hosch S, Dickey DM. Natriuretic peptides, their receptors, and cyclic guanosine monophosphatedependent signaling functions. Endocr Rev 2006, 27:47–72.

201.   Schweitz H, Vigne P, Moinier D, Frelin C, Lazdunski M. A new member of the natriuretic peptide family is present in the venom of the green mamba (Dendroaspis angusticeps). J Biol Chem 1992, 267:13928–13932.

202.   Schirger JA, Heublein DM, Chen HH, Lisy O, Jougasaki M, Wennberg PW et al. Presence of Dendroaspis natriuretic peptide-like immunoreactivity in human plasma and its increase during human heart failure. Mayo Clin Proc 1999, 74:126–130.

203.   Margulies KB, Burnett JC Jr. Visualizing the basis for paracrine natriuretic peptide signaling in human heart. Circ Res 2006, 99:113–115.

204.   Forssmann W, Meyer M, Forssmann K. The renal urodilatin system: clinical implications. Cardiovasc Res 2001, 51: 450–462.

205.   Burnett JC Jr, Costello-Boerrigter L, Boerrigter G. Alterations in the kidney in heart failure: the cardiorenal axis in the regulation of sodium homeostasis. In: Mann DL (ed) Heart failure: a companion to Braunwald's heart disease. Elsevier Inc,Philadelphia, 2004, pp 279–289.

206.   Suga S, Nakao K, Hosoda K, Mukoyama M, Ogawa Y, Shirakami G et al. Receptor selectivity of natriuretic peptide family, atrial natriuretic peptide, brain

natriuretic peptide, and C-type natriuretic peptide. Endocrinology 1992, 130:229–239.

207. Singh G, Kuc RE, Maguire JJ, Fidock M, Davenport AP. Novel snake venom ligand Dendroaspis natriuretic peptide is selective for natriuretic peptide receptor-A in human heart: downregulation of natriuretic peptide receptor-A in heart failure. Circ Res 2006, 99:183–190.

208. Burnett JC Jr, Kao PC, Hu DC, Heser DW, Heublein D, Granger JP et al. Atrial natriuretic peptide elevation in congestive heart failure in the human. Science 1986, 231:1145–1147

209. Mukoyama M, Nakao K, Hosoda K, Suga S, Saito Y, Ogawa Y et al. Brain natriuretic peptide as a novel cardiac hormone in humans. Evidence for an exquisite dual natriuretic peptide system, atrial natriuretic peptide and brain natriuretic peptide. J Clin Invest 1991, 87:1402–1412.

210. Sudoh T, Minamino N, Kangawa K, Matsuo H. C-type natriuretic peptide (CNP): a new member of natriuretic peptide family identified in porcine brain. Biochem Biophys Res Commun 1990, 168:863–870.

211. Stingo AJ, Clavell AL, Heublein DM, Wei CM, Pittelkow MR, Burnett JC Jr. Presence of C-type natriuretic peptide in cultured human endothelial cells and plasma. Am J Physiol 1992, 263:H1318–1321.

212. Del Ry S, Passino C, Emdin M, Giannessi D. C-type natriuretic peptide and heart failure. Pharmacol Res 2006, 54:326–333.

213. Garbers DL, Chrisman TD, Wiegn P, Katafuchi T, Albanesi JP, Bielinski V et al. Membrane guanylyl cyclase receptors: an update. Trends Endocrinol Metab

2006, 17:251–258.

214.   Ahluwalia A, MacAllister RJ, Hobbs AJ. Vascular actions of natriuretic peptides. Cyclic GMP-dependent and –independent mechanisms. Basic Res Cardiol 2004, 99:83–89.

215.   Koller KJ, Lowe DG, Bennett GL, Minamino N, Kangawa K, Matsuo H et al. Selective activation of the B natriuretic peptide receptor by C-type natriuretic peptide (CNP). Science 1991, 252:120–123.

216.   Wei CM, Aarhus LL, Miller VM, Burnett JC Jr. Action of C-type natriuretic peptide in isolated canine arteries and veins. Am J Physiol 1993, 264:H71–H73.

217.   Wennberg PW, Miller VM, Rabelink T, Burnett JC Jr. Further attenuation of endothelium-dependent relaxation imparted by natriuretic peptide receptor antagonism. Am J Physiol 1999, 277:H1618–H1621.

218.   Stingo AJ, Clavell AL, Aarhus LL, Burnett JC Jr. Cardiovascular and renal actions of C-type natriuretic peptide. Am J Physiol 1992, 262:H308–H312.

219.   Furuya M, Yoshida M, Hayashi Y, Ohnuma N, Minamino N, Kangawa K et al. C-type natriuretic peptide is a growth inhibitor of rat vascular smooth muscle cells. Biochem Biophys Res Commun 1991, 177:927–931.

220.   Cao L, Gardner DG. Natriuretic peptides inhibit DNA synthesis in cardiac fibroblasts. Hypertension 1995, 25:227–234.

221.   Tokudome T, Horio T, Soeki T, Mori K, Kishimoto I, Suga S-iet al. Inhibitory effect of C-type natriuretic peptide (CNP) on cultured cardiac myocyte hypertrophy: interference between CNP and endothelin-1 signaling pathways. Endocrinology 2004, 145:2131–2140.

222. Igaki T, Itoh H, Suga SI, Hama N, Ogawa Y, Komatsu Y et al. Effects of intravenously administered C-type natriuretic peptide in humans: comparison with atrial natriuretic peptide. Hypertens Res 1998, 21:7–13.

223. Hunt PJ, Richards AM, Espiner EA, Nicholls MG, Yandle TG. Bioactivity and metabolism of C-type natriuretic peptide in normal man. J Clin Endocrinol Metab 1994, 78:1428–1435.

224. Hobbs A, Foster P, Prescott C, Scotland R, Ahluwalia A. Natriuretic peptide receptor-C regulates coronary blood flow and prevents myocardial ischemia/reperfusion injury: novel cardioprotective role for endothelium-derived C-type natriuretic peptide. Circulation 2004, 110:1231–1235.

225. Scotland RS, Cohen M, Foster P, Lovell M, Mathur A, Ahluwalia A et al. C-type natriuretic peptide inhibits leukocyte recruitment and platelet-leukocyte interactions via suppression of P-selectin expression. Proc Natl Acad Sci USA 2005, 102:14452–14457.

226. Soeki T, Kishimoto I, Okumura H, Tokudome T, Horio T, Mori K et al. C-type natriuretic peptide, a novel antifibrotic and antihypertrophic agent, prevents cardiac remodeling after myocardial infarction. J Am Coll Cardiol 2005, 45:608–616.

227. Nazario B, Hu RM, Pedram A, Prins B, Levin ER. Atrial and brain natriuretic peptides stimulate the production and secretion of C-type natriuretic peptide from bovine aortic endothelial cells. J Clin Invest 1995, 95:1151–1157.

228. Widmaier, Eric P.; Hershel Raff, Kevin T. Strang. *Vander's Human Physiology, 11th Ed.*. McGraw-Hill. 2008, pp. 291, 509–10.

229. Potter LR, Yoder AR, Flora DR, Antos LK, Dickey DM. "Natriuretic peptides: their structures, receptors, physiologic functions and therapeutic applications". *Handb Exp Pharmacol* 2009, 191 (191): 341–66.

230. B-type natriuretic peptide: the level and the drug--partners in the diagnosis of congestive heart failure". *Congest Heart Fail* 10 (1 Suppl 1): 3–27.

231. Sudoh *et al.* 1990.

232. Hanga Agoston, Sameena Khan, Claudine G James, J Ryan Gillespie, Rosa Serra, Lee-Anne Stanton and Frank Beier, C-type natriuretic peptide regulates endochondral bone growth through p38 MAP kinase-dependent and −independent pathways, *BMC Developmental Biology* 2007, **7:**18

233. Karsenty G, Wagner EF: Reaching a genetic and molecular understanding of skeletal development. *Dev Cell* 2002 , 2:389-406.

234. Olsen BR, Reginato AM, Wang W: Bone development**.** *Annu Rev Cell Dev Biol* 2000 , 16:191-220.

235. Stanton LA, Underhill TM, Beier F: MAP kinases in chondrocyte differentiation. *Dev Biol* 2003 , 263:165-75.

236. Ballock RT, O'Keefe RJ: Physiology and pathophysiology of the growth plate. *Birth Defects Res Part C Embryo Today* 2003 , 69:123-43.

237. van der Eerden BCJ, Karperien M, Wit JM: Systemic and Local Regulation of the Growth Plate. *Endocr Rev* 2003 , 24:782-801.

238. Shum L, Coleman CM, Hatakeyama Y, Tuan RS: Morphogenesis and dysmorphogenesis of the appendicular skeleton. *Birth Defects Res Part C Embryo Today* 2003 , 69:102-22.

239.	Mundlos S, Olsen BR: Heritable diseases of the skeleton. Part II: Molecular insights into skeletal development-matrix components and their homeostasis. *Faseb J* 1997 , 11:227-33.

240.	Mundlos S, Olsen BR: Heritable diseases of the skeleton. Part I: Molecular insights into skeletal development-transcription factors and signaling pathways. *Faseb J* 1997 , 11:125-32.

241.	Zelzer E, Olsen BR: The genetic basis for skeletal diseases. *Nature* 2003 , 423:343-8.

242.	Chusho H, Tamura N, Ogawa Y, Yasoda A, Suda M, Miyazawa T, Nakamura K, Nakao K, Kurihara T, Komatsu Y, *et al*.: Dwarfism and early death in mice lacking C-type natriuretic peptide. *Proc Natl Acad Sci USA* 2001 , 98:4016-4021.

243.	Komatsu Y, Chusho H, Tamura N, Yasoda A, Miyazawa T, Suda M, Miura M, Ogawa Y, Nakao K: Significance of C-type natriuretic peptide (CNP) in endochondral ossification: analysis of CNP knockout mice. *J Bone Miner Metab* 2002 , 20:331-6.

244.	Mericq V, Uyeda JA, Barnes KM, De Luca F, Baron J: Regulation of fetal rat bone growth by C-type natriuretic peptide and cGMP. *Pediatr Res* 2000 , 47:189-93.

245.	Yasoda A, Ogawa Y, Suda M, Tamura N, Mori K, Sakuma Y, Chusho H, Shiota K, Tanaka K, Nakao K: Natriuretic peptide regulation of endochondral ossification. Evidence for possible roles of the C-type natriuretic peptide/guanylyl cyclase-B pathway**.** *J Biol Chem* 1998 , 273:11695-700.

246. Golembo, M.; Netayim, M.; Sitria, M. 2008, US Patent No.2008/0194682.

247. L.R. Potter, S. Abbey-Hosch, D.M. Dickey, Natriuretic peptides, their receptors, and cyclic guanosine monophosphate-dependent signaling functions, Endocr. Rev. 2006, 27, 47-72.

248. L.R. Potter, A.R. Yoder, D.R. Flora, L.K. Antos, D.M. Dickey, Natriuretic peptides: their structures, receptors, physiologic functions and therapeutic applications, Handb. Exp. Pharmacol.2009, 191, 341-366.

249. H. Schweitz, P. Vigne, D. Moinier, C. Frelin, M. Lazdunski, A new member of the natriuretic peptide family is present in the venom of the green mamba (Dendroaspis angusticeps), J. Biol.Chem. 1992, 267, 13928-13932.

250. R. Barbouche, N. Marrakchi, P. Mansuelle, M. Krifi, E. Fenouillet, H. Rochat, M. El Ayeb, Novel anti-platelet aggregation polypeptides from Vipera lebetina venom: isolation and characterization, FEBS Lett. 1996, 392, 6-10.

251. L.R. Potter, T. Hunter, Guanylyl cyclase-linked natriuretic peptide receptors: structure and regulation, J. Biol. Chem. 2001, 276, 6057-6060.

252. M. Silberbach, C.T. Roberts, Natriuretic peptide signalling: molecular and cellular pathways to growth regulation, Cell Signal. 2001, 13,221-231.

253. M.B. Anand-Srivastava, Natriuretic peptide receptor-C signaling and regulation, Peptides 2005, 26,1044-1059.

254. R.A. Rose, N. Hatano, S. Ohya, Y. Imaizumi, W.R. Giles, C-type natriuretic peptide activates a Page 17 of 39,17 non-selective cation current in acutely isolated rat cardiac fibroblasts via natriuretic peptide C receptor-mediated signalling. J. Physiol. 2007, 580, 255-274.

255.   R.A. Rose, W.R. Giles, Natriuretic peptide C receptor signalling in the heart and vasculature. J. Physiol. 2008, 586,353-366.

256.   P. Moffatt, G.P. Thomas, Osteocrin--beyond just another bone protein? Cell Mol. Life Sci. 2009, 66, 1135-1139.

257.   P. Moffatt, G.P. Thomas, K. Sellin, M. Bessette, F. Lafrenière, O. Akhouayri, R. St-Arnaud, C. Lanctôt, Osteocrin is a specific ligand of the natriuretic Peptide clearance receptor that modulates bone growth, J. Biol. Chem. 2007, 282, 36454-36462.

258.   H. Chusho, N. Tamura, Y. Ogawa, A. Yasoda, M. Suda, T. Miyazawa, K. Nakamura, K. Nakao, T. Kurihara, Y. Komatsu, H. Itoh, K. Tanaka, Y. Saito, M. Katsuki, K. Nakao, Dwarfism and early death in mice lacking C-type natriuretic peptide, Proc. Natl. Acad. Sci. U S A. 2001, 98, 4016-4021.

259.   C.Y.W. Lee, J.C. Burnett Natriuretic peptides and therapeutic applications, Heart Fail. Rev. 2007, 12, 131-142.

260.   D.G. Gardner, Natriuretic peptides: markers or modulators of cardiac hypertrophy? Trends Endocrinol. Metab. 2003, 14, 411-416.

261.   Y.H. Park, H.J. Park, B. Kim, E. Ha, K.H. Jung, S.H. Yoon, S.V. Yim, J. Chung, BNP as a marker of the heart failure in the treatment of imatinib mesylate, Cancer Lett. 2006, 243, 16-22.

262.   D.M. Dickey, J.C. Burnett, L.R. Potter, Novel bifunctional natriuretic peptides as potential therapeutics, J. Biol. Chem. 2008, 283, 35003-35009.

263. O. Lisy, B.K. Huntley, D.J. McCormick, P.A. Kurlansky, J.C. Burnett, Design, synthesis, and actions of a novel chimeric natriuretic peptide: CD-NP, J. Am. Coll Cardiol. 2008, 52, 60-68.

264. K. Inoue, K. Naruse, S. Yamagami, H. Mitani, N. Suzuki, Y. Takei, Four functionally distinct C-type natriuretic peptides found in fish reveal evolutionary history of the natriuretic peptide system, Proc. Natl. Acad. Sci. U S A. 2003, 100, 10079-10084.

265. B.C. Cunningham, D.G. Lowe, B. Li, B.D. Bennett, J.A. Wells, Production of an atrial natriuretic peptide variant that is specific for type A receptor, EMBO J. 1994, 13, 2508-2515.

266. J.R. Schoenfeld, P. Sehl, C. Quan, J.P. Burnier, D.G. Lowe, Agonist selectivity for three species of natriuretic peptide receptor-A, Mol. Pharmacol. 1995, 47, 172-180.

267. Candace, Y. W.; Lee, A.; Burnett, J. C., Jr. Heart Fail Rev 2007, 12, 131–142.

268. Gardner, D. G. Trends Endocrinol Metab 2003, 14, 411–416.

269. Golembo, M.; Netayim, M.; Sitria, M. 2008, US Patent No.2008/0194682.

270. Olney, R. C. Growth Horm IGF Res 2006, 16 (Suppl A),S6–S14.

271. Pejchalova, K.; Krejci, P.; Wilcox, W. R. Mol Genet Metab 2007, 92, 210–215.

272. Teixeira, C. C.; Agoston, H.; Beier, F. Dev Biol 2008, 319, 171– 178.

273. wei, C. M.; Kim, C. H.; Miller, V. M.; Burnett, J.C., Jr. J Clin Invest 1993, 92, 2048–2052.

274.   Potter, L. R.; Yoder, A. R.; Flora, D. R.; Antos, L. K.; Dickey, D. M. Handb Exp Pharmacol 2009, 191, 341–366.

275.   Moffatt, P.; Thomas, G. P. Cell Mol Life Sci 2009, 66, 1135–1139.

276.   Franceschi, R. T.; James, W. M.; Zerlauth, G. J Cell Physiol 1985, 123, 401–409.

277.   Rodan, S. B.; Imai, Y.; Thiede, M. A.,Wesolowski, G.; Thompson, D.; Bar-Shavit, Z.; Shull, S.; Mann, K.; Rodan, G. A. Cancer Res 1987, 47, 4961–4966.

278.   Revazova, E. S.; Solovev, Y. N.; Khizhnyakova, T. M. Bull Exp Biol Med 1988, 106, 471–472.

279.   Schedlich, L. J.; Muthukaruppan, A.; O'Han, M. K.; Baxter, R. C. Mol Endocrinol 2007, 21, 2378–2390.

280.   Nishida, Y.; Knudson, W.; Knudson, C. B.; Ishiguro, N. Exp Cell Res 2005, 307, 194–203.

281.   Takarada, M. Kokubyo Gakkai Zasshi 1996, 63, 375–386.

282.   Hosono, K.; Nishida, Y.; Knudson, W.; Knudson, C. B.; Naruse, T.; Suzuki, Y.; Ishiguro, N. Am J Pathol 2007, 171, 274–286.

283.   Franz-Odendaal, T.; Brian, K.; Hall, B. K.; Witten, P. E. Dev Dyn 2006, 235, 176–190.

284.   Suda, M.; Ogawa, Y.; Tanaka, K.; Yasoda, A.; Takigawa, T.; Uehira, M.; Nishimoto, H.; Itoh, H.; Saito, Y.; Shiota, K.; Nakao, K. Proc Natl Acad Sci USA 1998, 95, 2337–2342.

285.   Yasoda, A.; Komatsu, Y.; Chusho, H.; Miyazawa, T.; Ozasa, A.; Miura, M.; Kurihara, T.; Rogi, T.; Tanaka, S.;   Suda, M.; Tamura, N.; Ogawa, Y.; Nakao, K. Nat Med 2004, 10, 80–86.

286.   Mackie, E. J.; Ramsey, S. J Cell Sci 1996, 106, 1597–1604.

287.   Suda, M.; Komatsu, Y.; Tanaka, K.; Yasoda, A.; Sakuma, Y.; Tamura, N.; Ogawa, Y.; Nakao, K. Calcif Tissue Int 1999, 65, 472–478.

288.   Alan, T.; Tufan, A. C. J Cell Biochem 2008, 105, 227–235.

289.   Agui, T.; Yamada, T.; Legros, G.; Nakajima, T.; Clark, M.; Peschel, C.; Matsumoto, K. Endocrinology 1992, 130, 2487– 2494.

290.   Miller N, Williams GM, Brimble MA, Synthesis of fish antifreeze neoglycopeptides using microwave-assisted "click chemistry".Org Lett 2010, 12:1375–1376.

Poster , oral presentation and publications

Posters and oral presentation

1. Silanisation of Carbonate substituted Hydroxyapatite toward Covalent Biodecoration.

   ESB 2009, 7-11 September, Lausanne, Switzerland

2. Azidoalkyl and propargyl glycosides from unprotected monosaccahrides towords chemoselective ligation.

   15th Eueocarb, Vienna, Austria. July 19-24, 2009

3. Chemoselective ''Glycosylation'' of Biomaterials.

   15th Eueocarb, Vienna, Austria. July 19-24, 2009

4. Covalent Biofunctionalisation of hydroxyapatite scaffolds via plasma technology.

   ESB 2009, 7-11 September, Lausanne, Switzerland

5. Carbonated Hydroxyapatite Biofunctionalisation with Carbohydrates

   ESB 2009, 7-11 September, Lausanne, Switzerland.

6. Design of Smart Biomaterials,

   Italian-Spanish Joint Workshop, April 2010.

7. Hydroxyapatite functionalization by bioorganic molecules and its biological evaluation

   ICOS-18, Bergen-Norway, 1-6th Aug-2010

8. Hydroxyapatite three dimentional scaffolds:biofunctionalisation by plasma technology and biological evolution.

   IBS-2010, 14-18TH Sep 2010, Rimini-Italy

9. Biomolecules Synthesis And Functionalisation For Tissue Engineering Applications,

   CINMPIS Meeting, san bandetto del tronto-Italy, Sep- 2010.

Publications

1. C-type natriuretic peptide: structural studies, relevant sequence synthesis and preliminary biological evaluation in human osteosarcoma cell lines.
   Journal of Biopolymer: peptide science: 94, (2), 213-219, 2010

2. Ultrasonic assisted Fischer glycosylation: generating diversity for glycochemistry
   Journal of moleculer diversity,

3. Carbohydrate scaffolds in chemical genetic studies
   Journal of Biotechnology, 144, (3), 234-241, 2009.

4. Carbohydrate Mimetics and Scaffolds: Sweet Spots in Medicinal Chemistry.
   Future Medicinal Chemistry, 2010, Vol. 2, No. 4, Pages 587-599.

5. Hyaluronan: biological role, mimetics and applications in medicinal chemistry.
   Mini-Reviews in Medicinal Chemistry, manuscript submitted,

6. Molecular dynamics investigation of cyclic natriuretic peptides: dynamic properties reflect peptide activity.
   Journal of Molecular Graphics and Modelling 28 (2010) 834–841

7. Discovery and design of carbohydrate-based therapeutics
   Expert Opinion on Drug Discovery, Vol. 0, No. 0: Pages 1-17

8. Kdo: an essential monosaccharide for bacteria viability
   Nat. Prod. Rep., 2010, xx, 1–14.